TOWARD PERPETUAL WIRELESS NETWORKS: OPPORTUNISTIC LARGE ARRAYS WITH TRANSMISSION THRESHOLDS AND ENERGY HARVESTING

A Dissertation
Presented to
The Academic Faculty

by

Aravind Kailas

In Partial Fulfillment
of the Requirements for the Degree
Doctor of Philosophy in the
School of Electrical and Computer Engineering

Georgia Institute of Technology
August 2010

TOWARD PERPETUAL WIRELESS NETWORKS: OPPORTUNISTIC LARGE ARRAYS WITH TRANSMISSION THRESHOLDS AND ENERGY HARVESTING

Approved by:

Professor Mary Ann Ingram, Advisor
School of Electrical and Computer Engineering
Georgia Institute of Technology

Professor Doug Blough
School of Electrical and Computer Engineering
Georgia Institute of Technology

Professor Ye (Geoffrey) Li
School of Electrical and Computer Engineering
Georgia Institute of Technology

Professor Evans Harrell
School of Mathematics
Georgia Institute of Technology

Professor Raghupathy Sivakumar
School of Electrical and Computer Engineering
Georgia Institute of Technology

Date Approved: April 2010

DEDICATION

To my Mother and my Advisor.

ACKNOWLEDGEMENTS

I wish to express my deepest gratitude to Dr. Mary Ann Ingram for her tenacious support and faith in my abilities throughout the development of this doctoral dissertation. She has been an advisor, mentor, friend, confidante, and also a voice of reason, the voice that I have wanted to hear. I am thankful for her guidance, insightful coaching, and tremendous encouragement, more so when seeking an academic position. My journey through the Ph.D. program at Georgia Tech has been a memorable one and I couldn't ask for more in an advisor. It has been a real honor and privilege to work with you and to have been your Ph.D. Student. Thank You.

My special thanks go to the members of my thesis committee, Dr. Ye (Geoffrey) Li, Dr. Raghupathy Sivakumar, and Dr. Evans Harrell for their terrific support during my academic job hunt. I also express my appreciation to Dr. Doug Blough for being on my dissertation committee. Their enlightening suggestions have greatly improved my research and the quality of this dissertation. I also thank Dr. Ian Akyildiz, Dr. Xiaoli Ma, Dr. Justin Romberg, and Dr. Christopher Rozell for their guidance and encouragement during my senior years as a Ph.D. student, especially during my academic job hunt.

I appreciate the faith and funding of the National Science Foundation (NSF), the Electrical and Computer Engineering (ECE), and the Center for TeleInFrastruktur (CTIF) (during the summers of 2007 and 2008) in giving me the opportunity to pursue my doctoral research in an uninterrupted manner.

To Rev. Theron Stuart, go my thanks for being a thoughtful guardian, a well-wisher, and the best house-mate ever. I have enjoyed our discussions on diverse topics, and shall carry forward important life-lessons explained through his own personal

experiences. It has been a pleasure to have known him over the last three years. To David Clark, Ron Jeffers, Dr. Sandra MacMillan (and Bob), and Dr. Jesse Peel, go my thanks for their countless blessings and wishes during my stay in Atlanta.

I thank my awesome friends and colleagues (former/present) at the Smart Antenna Research Lab and Georgia Tech, Alper Akanser, Ali Behrooz, Dr. Kaushik Chowdhury, Kiruthika Devaraj, Patricia Dixon, Dr. Claudio Estevez, Syed Ali Hassan, Aaron Hatch, Jin Woo Jung, Amey Kaloti, Josep Montana, Jason Sherwin, and Lakshmi Thanayankizil, for their everlasting friendship, invigorating hours of procrastination, and moral support. Further, I thank all my friends outside Georgia Tech including Arvind Chandrasekaran, Kady Guo, Yogesh Jashnani, Kartik Krishnan, Smruti Patel, Shankar Raja, Venkatesh Ramaswamy, Shanthi Ramesh, Amit Shivale, Snigdha Singh, Tee Sivanadyan, Shankar Somasundaram, Shamik Valia, and so many others for always being there for me.

Last but not the least, to my parents and sister, go many special thanks for their perpetual love and affection. They have sacrificed several things so that I may pursue the best education possible and raised me in an intellectually stimulating environment. I don't have room in this dissertation to express my appreciation for them; however, they deserve every bit of credit for the continued success that I have enjoyed throughout my schooling and career. I am eternally indebted to them.

On a concluding note, the quote below is dedicated to the many people who have helped to inspire and encourage me in pursuing this degree, personally and/or professionally along the way. Thank You.

> "*There is no such thing as a 'self-made' man. We are made up of thousands of others. Everyone who has ever done a kind deed for us, or spoken one word of encouragement to us, has entered into the make-up of our character and of our thoughts.*"
>
> – George Matthew Adams

TABLE OF CONTENTS

LIST OF TABLES

LIST OF FIGURES

SUMMARY

Solving the key issue of sustainability of battery-powered sensors continues to attract significant research attention. The prevailing theme of this research is to address this concern using energy-efficient protocols based on a form of simple cooperative transmission (CT) called the opportunistic large arrays (OLAs), and intelligent exploitation of energy harvesting and hybrid energy storage systems (HESSs). The two key contributions of this research, namely, OLA with transmission threshold (OLA-T) and alternating OLA-T (A-OLA-T), offer an signal-to-noise ratio (SNR) advantage (i.e., benefits of diversity and array (power) gains) in a multi-path fading environment, thereby reducing transmit powers or extending range. Because these protocols do not address nodes individually, the network overhead remains constant for high density networks or nodes with mobility. During broadcasting across energy-constrained networks, while OLA-T saves energy by limiting node participation within a single broadcast, A-OLA-T optimizes over multiple broadcasts and drains the the nodes in an equitable fashion.

A major bottleneck for network sustainability is the ability of a rechargeable battery (RB) to store energy, which is limited by the number of charge-discharge cycles. Energy harvesting using a HESS that comprises a RB and a supercapacitor (SC) will minimize the RB usage, thereby preserving the charge-discharge cycles. Studying the HESS is important, rather than the SC-alone because while an SC with harvested energy may be sufficient for routine monitoring, if there is an alert, the RB could be used as necessary to support the heavier reporting requirements. Therefore, another key contribution of this research is the design and analysis of a novel routing metric called communications using HESS (CHESS), which extends the RB-life by relaying exclusively with SC energy.

CHAPTER I

INTRODUCTION

Wireless sensor networks (WSNs) consist of a large number of nodes with sensing and communication capabilities conveying information in a networked manner to a sink (the destination). WSNs have attracted considerable research interest for several years now. Their importance is being realized in the industry too, with some initial deployments (such as those by Crossbow Inc.) and several standardization activities (such as the IEEE 802.15.4 or the ZigBee standard). However, widespread deployment is still not a reality because several challenges remain that need to be addressed. Wireless sensor nodes have severe constraints in terms of their limited battery reserve, computational power, and storage capacity. These constraints correspondingly impact the kind of operations that can be supported by the network and limit the reliability, survivability, and lifetime of such networks. The large number of battery-operated sensors and random deployments render it impossible to deploy resource-hogging communication protocols or to frequently replace batteries. The expectation is that if reliable and maintenance-free wireless sensor networks could be designed, the scope of applications for WSNs would grow dramatically. Potential applications include monitoring the health of civil structures (e.g., bridges, office buildings, pipelines), environmental monitoring, and surveillance. It is in the context of these real-world challenges that *scalable opportunistic large array (OLA)-based protocols* and *energy harvesting* gain tremendous significance.

An opportunistic large array (OLA) is a large group of simple, inexpensive relays or forwarding nodes that cooperate without coordination between each other, but they naturally fire together in response to energy received from a single source or

another OLA. Each node has just one antenna. However, because the nodes are separated in space, they collectively form a 'virtual-multiple-input-multiple-output (MIMO) system,' thereby offering the benefits of diversity protection from multi-path fading and spectrum efficiency. OLA-based approaches have been shown theoretically to have significant advantages over conventional multi-hop networks in terms of total energy transmitted, lower node complexity, connectivity, and end-to-end delay (refer to Section 2.2.2).

The large-scale nature of the sensor network consisting of a large number of nodes in dense deployments, naturally encourages the use of distributed arrays of nodes. Further, the resource-constrained nature of sensor devices discourages the use of sophisticated and complicated capabilities such as smart antenna array processing on each node. Concurrent node transmissions (i.e., OLA-based transmissions) change the node membership (in every hop) and shape of the next OLA. This admits the possibility of adaptive topology control and maintenance of connectivity in the event of node failures. This improves the survivability of the network in the event of both node failures and node compromise. In OLA-based transmissions, this type of control is possible without individual node addressing. From all these arguments, it is clear that the use of OLAs for communication can make a widely deployed sensor network more robust and extend the network life.

The finite "cycle life" or the limited charge-discharge cycles limits the operation time of rechargeable batteries (RBs). Energy harvesting, often via solar cells or vibration harvesting, can be used as an alternative source of energy to supplement the primary source, in this case, the RB. Energy harvesting is the process of capturing minute amounts of energy from one or more ambient energy sources, accumulating them, and storing them for subsequent use. Energy harvesting devices efficiently and effectively capture, accumulate, and manage this energy and supply it in a form that can be used to perform a helpful task (such as routing packets). As wireless standards

begin to emerge for the industrial environment, and as more end-users launch industrial WSN applications, there are growing signs of progress on the energy harvesting front. While energy harvesting is a leading candidate to enable near-perpetual system operation, designing an efficient energy harvesting system that meets this requirement requires an in-depth understanding of several complex trade-offs. Moreover, the finite cycle life of an RB ultimately limits the lifetime of a network even if all nodes do ambient energy harvesting. One solution is to consider hybrid energy storage systems (HESSs) for combining two or more energy storage systems to get a superior energy source. HESSs comprising a RB and a supercapacitor (SC) are considered in the proposed research. SCs have a high efficiency (up to 97-98%), a high number of cycles (more than a half million compared to 200-1000 for RBs), and charge-recharge characteristics that favor storing and supplying power surges for short durations. Their high leakage, however, precludes their use for long-term energy storage. So, designing simple HESS *intelligence* that can leverage the complementary strengths of the two storage technologies and preserve RB cycle life is one of the goals of this doctoral research.

The overriding purpose of this research is to address sustainability, a key design issue for energy-constrained wireless networks. This is done in two different ways. First, simple, energy-efficient, cooperative-diversity-based protocols with 'user-defined' transmission thresholds, namely, OLA with transmission threshold (OLA-T) and alternating OLA-T (A-OLA-T) are proposed and analyzed. OLA-T saves energy by allowing only the nodes at the edge of the decoding range to relay, and it does this with almost no setup and no inter-node coordination (i.e., no medium access control (MAC)), making it a prime candidate for mobile networks. A-OLA-T is a variation of OLA-T that is more suitable for static networks. A-OLA-T balances the load of broadcasting by performing consecutive OLA-T broadcasts using mutually exclusive sets of nodes. Being OLA-based protocols, OLA-T and A-OLA-T offer benefits of

spatial diversity and a signal-to-noise ratio (SNR) advantage at the receiver. Thus, the transmit power per sensor is lowered, but the collective signal is strong enough and has enough diversity to enable its reception at a relatively long distance away by the sink node. Next, the doctoral research investigates extending node life and hence network life by "harvesting" ambient energy and reducing the dependence on the RB for routing. Using a very simple model for the SC, an integral part of a HESS, a novel routing metric to manage the energy transfer between the two storage devices in a HESS, namely, the RB and the SC is proposed and analyzed. Finally, it is envisioned that the lessons learned from this doctoral research will champion future research efforts for enabling perpetual operation without human intervention or servicing.

CHAPTER II

ORIGIN AND HISTORY OF THE PROBLEM

2.1 Cooperative Diversity

Cooperative transmission (CT) is an effective way for two or more single-antenna transmitters to achieve the benefits of an array transmitter by having two or more nodes cooperate to transmit the same message [1], [2]. Spatial diversity, which is a powerful mechanism to mitigate multi-path fading, is not available in single-antenna nodes. However in wireless ad hoc and sensor network applications, single-antenna nodes in proximity to each other can cooperatively transmit over independently faded channels to a common destination thereby obtaining the spatial diversity provided by a multi-antenna source. Spatial diversity provided by CT-based strategies enables dramatic reduction of the fade margins (i.e., the transmit powers) in a multi-path fading environment, thereby saving energy. In other words, by sharing information this way, the users can create a"virtual array" and achieve spatial array and diversity gain. Because of the diversity gain, all users can reduce their fade margins (i.e., their transmit powers) by as much as 12-15 dB, thereby reducing the energy consumed by each transmitter [2]. Because of the array gain (the simple summing of average powers from each antenna), the required transmission power for a link can be divided across multiple radios resulting in reduced energy consumption per radio.

The seminal work on CT for wireless networks studied the 'two-hop network' with only a source, a destination, and only one or more relays [1], [2]. In most of these works the relay node(s) is predetermined and is selected with the objective of determining the optimum rate and power allocation between the source and relay for various relative distances between the nodes. The aforementioned schemes assume

that the relay and source transmissions occur on orthogonal channels and require coordination among nodes. The orthogonality can be achieved using time division multiple-access (TDMA) [2] and distributed space-time repetition coding [3], [4]. Various other distributed coding schemes that avoid the repetition-coding scheme were also proposed in [5]–[7]; these schemes achieve coding gain at the cost of additional complexity. In [5], the source broadcasts a recursive code to both relay and destination, and a distributed turbo code is embedded in the relay channel, while in [6], [7], the authors investigate coded cooperation using Turbo codes, partitioning the codewords of each mobile and transmitting portions of each codeword through independent fading channels.

Several CT-based routing schemes have been proposed [1]–[8], but most of them treat a small number of nodes (e.g., source, destination, and one or more relays), and require significant inter-node coordination, which raises the network overhead and makes the performance sensitive to node mobility. For example, allocation of power to nodes [1], [8], allocation of orthogonal time slots to each of the transmitters [2], and path selection between two nodes using an appropriate metric (such as channel state information (CSI)) [8]–[12] have been proposed.

In contrast to the cooperative strategies proposed in [8]–[12], OLA-based routing schemes are suitable for large numbers of nodes [13]–[30]. The opportunistic large array (OLA) is a simple form of CT. An OLA is a group of nodes that behave without coordination between each other, but naturally fire at approximately the same time in response to energy received from a single source or another OLA [13]. All the transmissions within an OLA are repeats of the same waveform; therefore the signal received from an OLA has the same model as a multi-path channel. Small time offsets (because of different distances and computation times) and small frequency offsets (because each node has a different oscillator frequency) are like excess delays and Doppler shifts, respectively. As long as the receiver, such as a RAKE

receiver, can tolerate the effective delay and Doppler spreads of the received signal and extract the diversity, decoding can proceed normally. Even though many nodes may participate in an OLA transmission with diversity, total transmission energy can still be saved because all nodes can reduce their transmit powers dramatically and large fade margins are not needed. Even in non-fading channels, the array gain in an OLA transmission may be desirable for applications where there is a low maximum power per node constraint, resulting, for example, from severe cost or heat restrictions. It is noted that carrier sensing must be disabled for an OLA transmission, or else the OLA participants that provide the spatial diversity are suppressed. More recently, OLA transmission time synchronization with the root mean square transmit time delay spreads less than 100 ns have been demonstrated [31]. One simple, power amplifier-friendly way to achieve transmit diversity is to transmit on-off-shift keying (OOK) or frequency-shift keying (FSK) on orthogonal carriers, with a simple energy detectors in the receiver [31].

2.2 Broadcasting in Wireless Networks

In wireless sensor networks (WSNs), the goals of energy efficiency of the battery-powered wireless terminals and long network life pervade all aspects of the system design. Broadcasting is a significant operation to support numerous applications. For example, broadcasting is used in the dissemination of location-specific information, mobile multimedia data to clients [32], code updates and maintenance [33], route discovery, signaling and data forwarding operations, and queries in WSNs [34]. One of the key contributions of this doctoral work is to propose simple broadcast algorithms that ensure that all nodes in a network contribute efficiently and equally to broadcasts.

In the remainder of this section, broadcasting algorithms in energy-constained networks relevant to this research are reviewed. Flooding, one of the earliest broadcast protocols for multi-hop transmissions, where all nodes relay the received message, is

energy inefficient and unreliable, as it leads to severe contention, collision and redundancy, a situation referred to as *broadcast storm* [35]. Many broadcast strategies have been proposed to avoid the broadcast storm and save energy during the broadcast.

Minimum energy routing protocols identify the path through the network that consumes the least energy [36]. Over a period of time, persistent use of such protocols can cause a significant disparity between the 'energy-depleted' and 'energy-rich' nodes of the network, leading to network partitioning [36]. In contrast, energy-aware and harvesting-aware algorithms route packets so that the nodes are drained equitably, and the time to network partition increases.

2.2.1 Non-Cooperative Broadcasting Algorithms

Energy-aware broadcast algorithms can be broadly classified into cooperative and non-cooperative algorithms. First, some of the non-cooperative broadcast algorithms relevant to this research work are reviewed. These can be further classified as requiring either global or localized topology control [36]. Among the global topology control types are the broadcast tree-based algorithms such as the broadcast incremental power (BIP) algorithm [37], the directed minimum spanning tree (DMST) algorithm [38], the minimum longest edge (MLE) [39], and more recently, the energy-aware broadcast algorithms that solve a lexicographic problem [40]. A spanning tree is a minimal graph structure that is rooted at the source node and supports network connectivity. By designing optimal spanning trees, one can minimize the number of nodes participating in the network. Additionally, there are the probability-based algorithms that rely on basic network topology understanding to determine the probability that a node will re-broadcast [41]. Other examples use multipoint relaying (MPR) to reduce the number of redundant re-transmissions during network broadcast [42]. Algorithms such as [42] (and the works referenced within) assume some neighbor knowledge to select these MPRs in a mobile wireless environment. In contrast to these algorithms,

the proposed broadcast algorithms do not address nodes individually and the nodes do not require their geographical location for energy-efficient broadcasting.

Among the broadcast algorithms that do not require global topology information, but use local information to decide on packet forwarding, are the border retransmission protocol (BRP) [43], relative neighborhood graph (RNG)-based algorithm [44], cone-based topology control (CBTC) algorithms [45], the local minimum spanning tree (LMST) algorithm [46], and the Irrigation protocol [47]. The BRP is a probabilistic protocol that privileges the retransmission by nodes located at the radio border of the transmitter [43]. Border nodes are identified through single-hop exchanges of "Hello" messages and hence this scheme requires no location or signal strength information. In the RNG relay subset protocol [44], only a subset of nodes relay the message from the source. Pairs of nodes are assumed to be able to evaluate their relative distance with integration of a positioning system or a signal strength measure. Since both [43] and [44] require neighbor information, these protocols will not scale well with node density. Even though such spanning tree algorithms are very energy efficient, most of them require centralized control to determine the optimum tree, which is not practical in highly dense and/or mobile deployments. In all these algorithms, some network overhead is needed to set up an overlay infrastructure, or determine the neighbor set based on location information of one-hop neighbors, and this overhead grows excessively with node density. In contrast, the network overhead of the proposed protocols is constant with increasing network density.

2.2.2 OLA-based Cooperative Broadcasting Algorithms

The first OLA-based broadcasting scheme [13] is what will be referred to in this dissertation as 'Basic OLA.' In a Basic OLA broadcast, the first OLA comprises all the nodes that can decode the transmission from the originating node; then the first OLA transmits and all nodes that can decode that transmission form the second

OLA, and so forth. There are no collisions resulting from a single broadcast because OLA nodes relay exactly the same packet; this means that a relay cannot impress any of its own information, such as its address, on the packet. The resulting OLAs form concentric rings around the originating node. A fundamental distinction between broadcast trees and OLA broadcasting is as follows. Ideally, in a broadcast tree, a node receives the signal the first time from just one transmitter. In other words, the relays are chosen so that there are no collisions. OLA transmission is just the opposite; a receiver is *supposed* to receive the signal simultaneously from multiple transmitters. In [13] it was shown that a Basic OLA broadcast yielded an energy savings of about 5 dB compared to the BIP algorithm. More recently, in [16], the authors compared the power efficiency of OLA-based cooperative broadcasting relative to non-cooperative broadcasting, both with optimal power allocation, and showed that the former saved at least 60% of the radiated power.

2.3 Environmentally-Powered Sensor Networks

A new observation related to energy-aware routing is that electronic devices can "harvest" energy from the environment. Harvesting ambient energy, such as solar, heat, vibration energy, etc., is a way to extend battery life. However, even rechargeable batteries (RBs) have finite lifetimes because they have a limited "cycle life," which is the number of charge-discharge cycles before the capacity falls below 80% of its initial rated capacity [48], [49]. The hybrid energy storage system (HESS), in which a supercapacitor (SC) protects the battery from current spikes, is another strategy for battery-life extension.

The SC and RB differ greatly in terms of their leakage and cycle life characteristics. The following key characteristics of RBs and SCs form the motivation and basis for the proposed research.

- An RB is characterized by its capacity (typically given in mAh), its leakage, and

its "cycle life," An RB, depending on is type (e.g., nickel metal hydride (NiMH) or lithium ion polymer) can have cycle life ranging from hundreds to thousands of cycles [50], [51]. The cycle life is what ultimately limits the lifetime of a wireless network that depends on RBs even if all nodes do energy harvesting. However, the existing literature on harvesting-aware routing does not consider this limitation.

- An SC is also characterized by its capacity, leakage, and cycle life, but the values of SC parameters are different from the RB values. For example, an SC cycle life is typically in the millions of cycles [52]. On the other hand, SC leakage is much higher than RB leakage and depends highly on the residual energy [53].

- Shallow discharging, that is, limiting the battery discharge to 25% or less of the capacity, preserves capacity and increases the number of cycles; this is true for all battery chemistries. The number of cycles yielded by a battery goes up exponentially by the reduction of the depth of discharge [55], [56].

The earliest works that considered energy harvesting considered simple schemes of routing packets via the energy harvesting nodes [57]. More recently, [58] proposed a cost metric that takes into account the nodes' residual energy, harvesting rate, and energy requirement for routing the packet. In [59], the authors analyzed the requirements for "energy neutral" WSN operation. By characterizing the nominal energy harvesting rate and its maximum deviation and by characterizing the nominal energy consumption rate and its maximum deviation, [59] determined bounds on the nominal consumption, the required battery capacity, and the required starting battery stored energy. Consumption rate is adapted by changing the duty cycle or the transmit power of the nodes [59]. For the "field monitoring" application, [59] maximizes the rate at which the field may be sampled under a constraint on transmit power and for given solar energy profiles. The transmit power constraint implies

a constraint on data rate. For the "event monitoring" application, [59] minimizes latency under a constraint on duty cycle. Neither [58] nor [59] considered cycle life or hybrid energy harvesting. Additionally, wireless sensors having only the SC or a HESS have been investigated and designed in [60]–[62]. Researchers have investigated the performance improvement in the RB when the SC was used. The SC delivered a current pulse for the required time, minimized the voltage droop [60], and reduced the internal losses in the battery [61], all of which increased the lifetime of the RB. In [62], the authors proposed and implemented a multi-stage energy buffering system consisting of an SC and an RB, which limited the use of the RB to emergencies to increase the lifetime of the network. Studying the HESS is important, rather than the SC-alone because, while an SC with the harvested energy may be sufficient for routine monitoring; if there is an alert, the RB will be necessary to support the heavier reporting requirements.

CHAPTER III

ANALYTICAL FRAMEWORK

This chapter describes the framework used to analyze novel OLA-based protocols, namely the OLA with transmission threshold (OLA-T) and the alternating OLA-T (A-OLA-T), and to derive performance bounds and conditions for sustained operation. The disc- and strip-shaped cooperative routes (networks) correspond to the largest and smallest ratios of nodes (or areas) used up during a successful broadcast, respectively, and in the following chapters, OLA-T and A-OLA-T are analyzed for these two scenarios. Analyzing these cooperative diversity-based protocols for these two contrasting and extreme network topologies will then set the performance bounds for arbitrary-shaped routes or networks.

3.1 Two-Dimensional Disc

Half-duplex nodes are assumed. For the purpose of analysis, the nodes are assumed to be distributed uniformly and randomly over a continuous area with average density ρ. The originating node is assumed to be a point source at the center of the given network area. It is assumed that a node can decode and forward a message without error when its received signal-to-noise ratio (SNR) is greater than or equal to a modulation-dependent threshold [18]. The assumption of unit noise variance transforms the SNR threshold to a received power criterion, which is denoted as the decoding threshold τ_l. It should be noted that the decoding threshold τ_l is not explicitly used in real receiver operations. A real receiver always just tries to decode a message. If no errors are detected, then it is assumed that the receiver power must have exceeded τ_l.

In contrast, the two key contributions of this research, namely, the OLA-T and A-OLA-T, use a "user-defined" transmission threshold that is explicitly compared to

an estimate of the received SNR. The basic principles of OLA-T and A-OLA-T are introduced in Sections 4.2 and 5, respectively. This additional criterion for relaying limits the number of nodes in each hop because a node would relay only if its received SNR is *less* than τ_u. So the thresholds, τ_l and τ_u, define a range of received powers that correspond to the "significant" boundary nodes, which form the OLA. While each boundary node in OLA-T must transmit a somewhat higher power, compared to Basic OLA, there is still an overall transmit energy savings with OLA-T because of the favorable location of the boundary nodes. The relative transmission threshold (RTT) is defined as $\mathcal{R} = \frac{\tau_u}{\tau_l}$.

For simplicity, the *deterministic model* [18] is assumed, which means that the power received at a node is the sum of the powers from each of the node transmissions. This implies that signals received from different nodes are orthogonal. The orthogonality can be approximated, for example, with direct sequence spread spectrum (DSSS) modulation, RAKE receivers, and by allowing transmitting nodes to delay their transmission by a random number of chips [63].

Continuing to follow [18], a non-fading environment and a path loss exponent of 2 are assumed. The path loss function in Cartesian coordinates is given by $l(x, y) = (x^2 + y^2)^{-1}$, where (x, y) are the normalized coordinates at the receiver. As in [18], distance d is normalized by a reference distance, d_0. Let power P_0 be the received power at d_0. As in [18], the aggregate path loss from a circular disc of radius r_0 at an arbitrary distance $p > d_0$ from the source is given by

$$f(r_0, p) = \int_0^{r_0} \int_0^{2\pi} l(p - r\cos\theta, r\sin\theta) r dr d\theta = \pi \ln \frac{p^2}{|p^2 - r_0^2|}. \quad (1)$$

Let the normalized source and relay transmit powers be denoted by P_s and P_r, respectively, and the relay transmit power per unit area be denoted by $\overline{P_r} = \rho P_r$. The normalization is such that P_s and P_r are actually the SNRs at a receiver d_0 away from the transmitter [22]. It is assumed that the network has a continuum of nodes, which means that the node density ρ becomes very large ($\rho \to \infty$), while $\overline{P_r}$ is kept

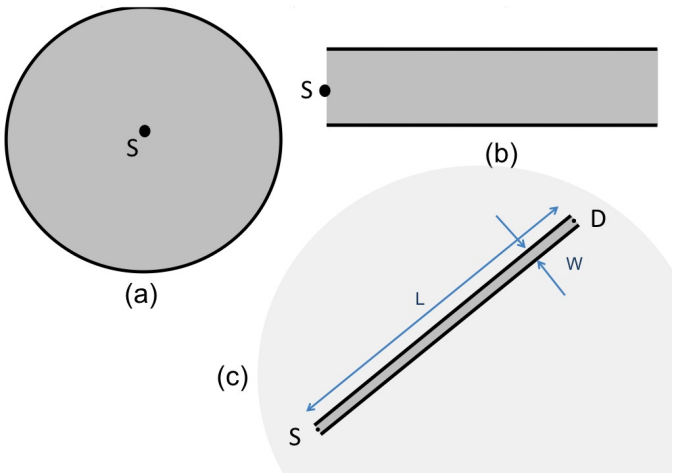

Figure 1: (a) Two-dimensional disc, (b) Two-dimensional strip, and (c) Strip-shaped unicast route. The gray areas denote the nodes in the network.

fixed. Figure 1(a) illustrates such a network topology, in which every point on the two-dimensional disc is a relay. 'S' in Figure 1(a) denotes the *point source*. Using (1), the received power at a distance p from the source, P_p is given by $P_p = \overline{P_r}\pi \ln \frac{p^2}{|p^2 - r_0^2|}$.

Last, the decoding ratio (DR) is defined as $\mathcal{D} = \tau_l / \overline{P_r}$, named as such because it can be shown to be the ratio of the receiver sensitivity (i.e., minimum power for decoding at a given data rate) to the power received from a single relay at the 'distance to the nearest neighbor,' $d_{nn} = 1/\sqrt{\rho}$. If ρ is a perfect square, the d_{nn} would be the distance between the nearest neighbors if the nodes were arranged in a uniform square grid. However, $\mathcal{D}$ relates to the node degree, $\mathcal{K}$, which is the average number of nodes in the decoding range of a transmitter, as $\mathcal{K} = \frac{\pi}{\mathcal{D}}$. The results are parameterized by $\mathcal{R}$ and node degree, $\mathcal{K}$, given by $\mathcal{K} = \pi \overline{P_r}/\tau_l$ for any finite node density[26].

3.2 Demystifying the Normalization of Parameters

The results given so far have been in terms of normalized units. This section presents some examples of un-normalized values for these variables to give an idea of what power levels and node densities can achieve the various values of $\mathcal{K}$ and FES. The decoding ratio, $\mathcal{D}$, was previously defined as $\tau_l / \overline{P_r}$, where τ_l is the required SNR for

Table 1: Examples of un-normalized variables for a two-dimensional disc

Example	P_t (dBm)	Node Density (nodes/area)	RX sens. (dBm)	d_{nn} (m)	$\mathcal{K}$
1	-56.00	2.65 nodes/m^2	-90.00	0.61	2
2	-56.00	2.65 nodes/m^2	-94.77	0.61	7
3	-34.95	1 node/16 m^2	-90.00	4.00	7
4	-43.98	1 node/4 m^2	-90.00	2.00	4
5	-20.97	9 nodes/3.60 km^2	-90.00	20.00	7

decoding, P_r is the normalized relay transmit power, and ρ is the node density in number of nodes per area, where area is normalized by the square of the reference distance, d_0^2. Expanded in terms of un-normalized variables, $\mathcal{D}$ can be rewritten as

$$\mathcal{D} = \frac{\left(\frac{\text{Receiver Sensitivity in mW}}{\sigma_n^2}\right)}{\left[\frac{P_t G_t G_r}{\sigma_n^2}\left(\frac{\lambda}{4\pi d_0}\right)^2\right]\left[\frac{(\#\text{ nodes})d_0^2}{\text{Area in m}^2}\right]}, \tag{2}$$

where P_t is the relay transmit power in mW, G_t and G_r are the transmit and receive antenna gains, σ_n^2 is the thermal noise power, λ is the wavelength in meters, and d_0 is the reference distance in meters. Suppose that the radio frequency is 2.4 GHz ($\lambda = 0.125$ m), and the antennas are isotropic ($G_t = G_r = 1$). Alternatively, (2) can be rewritten in terms of $\mathcal{K}$ as

$$\mathcal{K} = \frac{\left[\frac{P_t G_t G_r}{\sigma_n^2}\left(\frac{\lambda}{4\pi d_0}\right)^2\right]\left[\frac{(\#\text{ nodes})d_0^2}{\text{Area in m}^2}\right]}{\left(\frac{\text{Receiver Sensitivity in mW}}{\sigma_n^2}\right)}, \tag{3}$$

which can be simplified to

$$\mathcal{K} = \frac{\left[P_t \text{ in mW}\right]\left[\frac{(\#\text{ nodes})}{\text{Area in m}^2}\right]}{\left(\text{Receiver Sensitivity in mW}\right)10^4}. \tag{4}$$

Table 1 shows five different examples of un-normalized variables and their resulting d_{nn} and $\mathcal{K}$ values. It is observed that $\mathcal{K} = 7$ can be obtained in Examples 2, 3, and 5, ranging from high density (2.65 nodes/m^2) to low density (9 nodes/3.60 km^2). it

Table 2: Examples of un-normalized variables for a two-dimensional strip

Example	P_r (dBm)	Node Density (nodes/area)	RX sens. (dBm)	$\mathcal{K}$	$\mathcal{R}$ (dB)
1	-48.00	3 nodes/m^2	-90.00	12.56	1.2
2	-48.00	18 nodes/m^2	-94.77	2	2.5
3	-56.00	10 node/m^2	-90.00	7.85	2.26
4	-20.97	2.5 nodes/km^2	-90.00	7	1
5	-20.97	2.5 nodes/km^2	-90.00	7	1

is also observed that the high density cases, Examples 1 and 2, correspond to very low transmit powers.

3.3 Two-Dimensional Strip

The notation and assumptions of [22] are adopted, some of which were used earlier in [17]. Half-duplex nodes are assumed to be distributed randomly and uniformly over a continuous strip defined by $\mathbb{S} = \{(x, y) : |y| \leq \frac{W}{2},\ 0 \leq x \leq L\}$ with average node density ρ, width W, and length L. The originating source (assumed to be a point source) and the destination are assumed to be at the opposite ends of the network strip. An OLA-based protocol may be viewed as a broadcast strategy if the entire network has a strip shape, or it may be viewed as a unicast strategy if there is a set of pre-designated cooperators along a conventional multi-hop route, which is refered to as a cooperative route. Figures 1(b) and (c) illustrate such this network topology, where the gray-shaded regions denote the nodes along the cooperative route (network). In the figure, 'S' and 'D' denote the *Source* and the *Destination*, respectively. All the other system parameters of interest such as node degree, $\mathcal{K}$ and $\mathcal{R}$, to name a couple, are the same as that of a two-dimensional disc that is described in Section 3.1. Here too, the results are parameterized in terms of $\mathcal{R}$ and $\mathcal{K}$, and columns 2–5 of Table 2 give some example values of our key parameters.

CHAPTER IV

ENHANCING THE ENERGY-EFFICIENCY OF A SINGLE BROADCAST

The energy efficiency of OLAs can be improved by preventing the nodes whose transmissions have a negligible effect on the formation of the next OLA from participating in the relaying. By definition, a node is near the forward boundary if it can only barely decode the message. The state of *barely decoding* can be determined in practice by measuring the average length of the error vector (the distance between the received and detected points in signal space), conditioned on a successful cyclic redundancy check (CRC) check. On the other hand, a node that receives much more power than is necessary for decoding is more likely to be near the source of the message. The OLA with a transmission threshold (OLA-T) method is simply Basic OLA with the additional transmission criterion that the node's received SNR must be less than a specified *transmission threshold*, τ_u.

OLA-T is distinct from cooperative medium access control (MAC) protocols that use thresholds on SNR or on other figures of merit as a basis for relay participation [2], [64]–[68]. The main differences are that the MAC protocols (i) rely on feedback from the destination in a link, from which potential relays learn the quality of their link to the destination, (ii) the protocols require that the relays contend for the channel (several authors have proposed a priority-based contention window size to favor the preferred relays [70], [69]), and finally, (iii) multiple relays are recruited to form a 'relay set'. In contrast, OLA-T is a purely feed-forward approach, and there is no contention among relays, because in any particular hop, the relays transmit together, synchronously. The paper by [68] uses an SNR threshold on only the source-relay

signal. However, [68] assumes no decoding error detection at the relay (e.g. CRC check) and requires that a relays SNR must be higher than the threshold, while the proposed OLA-T does the opposite on both points; furthermore [68] analyzes the error probability of a single link whereas the requirements for successful transmission over an unlimited number of hops is analyzed in this dissertation. Another distinction is that, while the cooperative route (i.e., the strip of candidate relays) may have been originally defined based on a sequence of single-input-single-output (SISO) links in a conventional non-CT (i.e., "primary") route, the SISO links are no longer respected after the cooperative route has been formed; instead the OLAs are formed on-the-fly, simply based on each node's ability to decode and its measurement of the SNR of the previous-hop signal. The conditions derived for OLA-T, which depend on node degree and the transmission threshold, ensure that the OLAs will keep propagating down the cooperative route.

The concept and analysis of OLA-T are original contributions of this doctoral research work. Initially, we analyze and derive performance bounds for OLA-T during broadcasting over disc-shaped networks, and then consider strip-shaped networks (in Section 4.3). The dual threshold cooperative broadcast (DTBC), which is the same as OLA-T, was introduced in [16] as a way to save even more energy compared to the Basic OLA broadcast, by allowing a node to join an OLA only if its received signal power is less than a given threshold. However the DTBC concept was not analyzed in [16]. This doctoral work also extends the concept to allow the thresholds to vary from OLA to OLA. OLA with variable threshold (OLA-VT) can be optimized to minimize total energy in a broadcast. OLA-VT can also be used to control OLA sizes, thereby enabling certain other protocols, such as the OLA concentric routing algorithm (OLACRA), which does upstream routing in WSNs [26]. OLA-T and OLA-VT can both be shown to be suboptimal trivial schedules [16], with the virtues of simple implementation and good performance.

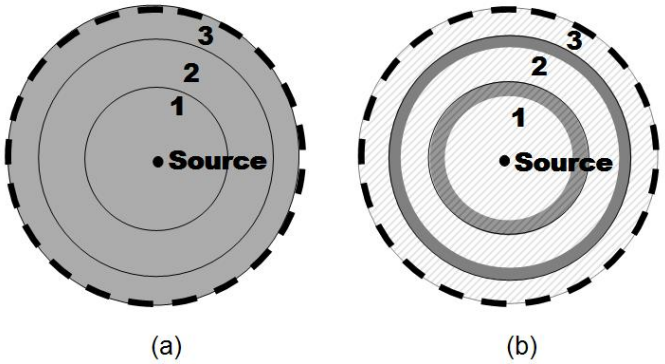

Figure 2: (a) Broadcast using Basic OLA, (b) Broadcast using OLA with transmission threshold (OLA-T). Only nodes in the gray areas relay.

4.1 Basic OLA

First, successful Basic OLA broadcasting [14] is reviewed. In a Basic OLA broadcast [14], a node relays immediately if it can decode and if it has not relayed before. The aim is to succeed in broadcasting the message over the whole network. The source node transmits a message and the group of neighboring nodes that receive and decode the message form Decoding Level 1 (DL_1), which is the disk enclosed by the smallest circle in Fig. 2(a). Next, each node in DL_1 transmits the message. These transmitting nodes in DL_1 constitute the first OLA. Next, nodes outside DL_1 receive the superposition of relayed copies of the message. Nodes in this group that can decode the message constitute DL_2, which is represented as the ring between DL_1 and the next bigger concentric circle in Fig. 2(a). All the nodes in a decoding level form an OLA, which in turn generates the next decoding level. From [18], the necessary and sufficient condition for the relayed signal to propagate in a sustained manner by concentric OLAs is given by

$$2 \geq \exp\left(\frac{1}{\mathcal{K}}\right). \tag{5}$$

Figure 2(a) illustrates this phenomenon for a given network area (defined in Fig. 2 by the dashed line).

4.2 OLA with Transmission Threshold (OLA-T)

Figure 2(b) illustrates a scenario where successful broadcasting over the network is achieved using OLA-T. The gray strips in Fig. 2(b) represent OLAs within each decoding level. Unlike the approach depicted in Fig. 2(a), the nodes that compose an OLA are only a subset of the nodes in a decoding level.

Before the analysis of OLA-T, it is important to point out that the transmission threshold, τ_u, is only one of the ways to achieve energy savings. For example, it is also possible to save on energy by varying the relay transmission power, P_r, of the sensors (depending on their level) across the network. OLA-T can be thought of as an extreme quantization of variable power allocation and therefore will not be as power efficient as an optimal continuous power allocation. However, OLA-T has the advantage of essentially no network overhead, making it potentially applicable to highly mobile networks.

Although OLA-T saves energy compared to Basic OLA in a single broadcast, the nodes selected by OLA-T for relaying will drain their batteries quickly because the same nodes are always selected for a fixed source in a static network. In this case, OLA-T would cause a network partition even earlier than Basic OLA because the relays use a slightly higher transmit power. However, the opposite will be true if the source location varies randomly or if the nodes move about randomly. Even for a fixed source and a static network, network lifetime can be extended relative to Basic OLA by modifying OLA-T to use mutually exclusive sets of nodes on consecutive broadcasts. This new technique, which is called alternating OLA-T (A-OLA-T) (refer to Section 5) builds on the results reported for OLA-T.

Finally, in order to decode, a node in an OLA-T network receives energy from just one decoding level. Multiple levels are not ganged to form a very thick OLA as in [16], nor are OLA transmissions at different times from different decoding levels combined as in [15]. Instead, the emphasis of OLA-T is on forming thin, widely

separated OLAs.

4.2.1 OLA-T Broadcast for Constant Transmission Thresholds

In this section, the OLA boundaries are determined as functions of the decoding level k, for the case when the transmission threshold (and hence the RTT) is constant over the network. The case of variable RTT is treated in Section 4.2.3. For the constant RTT, the OLA boundaries can be found recursively using

$$\overline{P_r}\left[f(r_{o,k}, r_{j,k+1}) - f(r_{i,k}, r_{j,k+1})\right] = \tau,\ j \in \{o, i\}, \tag{6}$$

where $r_{o,k}$ and $r_{i,k}$ are the outer and inner boundary radii for the k-th OLA ring, respectively. The parameter τ takes the value τ_l (or τ_u) when computing outer (or inner) boundary radii for each OLA ring. Applying (1) yields $\frac{\tau}{\overline{P_r}} = \pi \ln \frac{|r_{j,k+1}^2 - r_{i,k}^2|}{|r_{j,k+1}^2 - r_{o,k}^2|}$. Using the initial conditions $r_{o,1} = \sqrt{\frac{P_s}{\tau_l}}$ and $r_{i,1} = \sqrt{\frac{P_s}{\tau_u}}$, recursive formulae for the k-th OLA are given by

$$r_{o,k}^2 = \frac{\beta(\tau_l) r_{o,k-1}^2 - r_{i,k-1}^2}{\beta(\tau_l) - 1},\ r_{i,k}^2 = \frac{\beta(\tau_u) r_{o,k-1}^2 - r_{i,k-1}^2}{\beta(\tau_u) - 1}, \tag{7}$$

where $\beta(\tau) = \exp\left[\tau/(\pi\overline{P_r})\right]$. Further, the closed-form expressions for the OLA-T radii have been derived by slightly modifying the continuum approach in [18] and can be found in Appendix A.

The radii given by (46) have been plotted in Fig. 3 on a logarithmic scale, as functions of the OLA index. The low, moderate, and high values of RTT in dB are 0.79, 1.55, and 3.42, respectively. Where network broadcast is achieved, the radii grow in an unbounded fashion, with a rate that increases with level index, k. It was observed that for some values of RTT, such as $\mathcal{R} = 1.55$ dB, the radii increased at a sub-linear rate with respect to k, up to a certain point, and then the increases were faster than linear for all higher k (that were tested).

It is learned that if $\mathcal{K}$ and $\mathcal{R}$ are constant throughout the network, they must satisfy a necessary and sufficient condition to achieve infinite network broadcast (refer

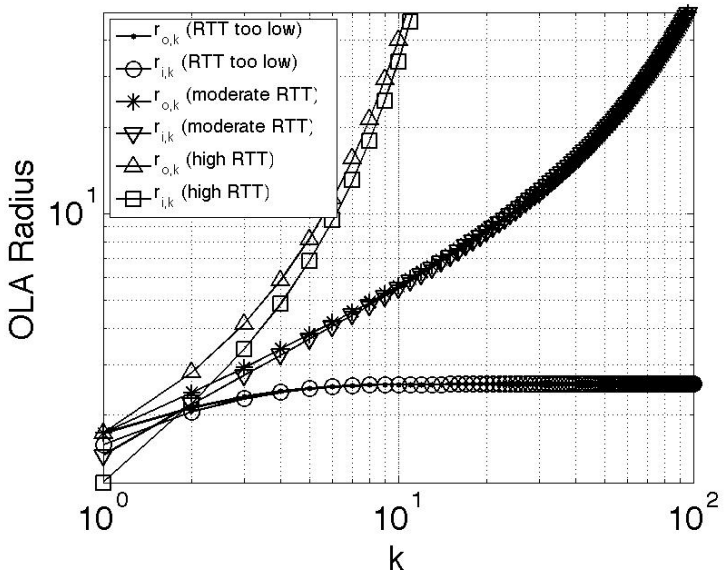

Figure 3: Outer radii, $r_{o,k}$, and the inner radii, $r_{i,k}$, versus OLA index, k.

to Appendix B for the derivation),

$$2 \;\geq\; \exp\left(\frac{1}{\mathcal{K}}\right) + \exp\left(\frac{-\mathcal{R}}{\mathcal{K}}\right). \tag{8}$$

It can be inferred that when $\mathcal{R} \to \infty$, OLA-T becomes Basic OLA, and (8) becomes

$$2 \geq \exp\left(\frac{1}{\mathcal{K}}\right) \Rightarrow \mathcal{K} \geq \frac{1}{\ln 2},$$

which is the condition for successful Basic OLA broadcast [18]. From (8), it is observed that $\mathcal{K}$ must approach infinity as $\mathcal{R} \to 1$ (i.e., as $\tau_u \to \tau_l$), in order to maintain successful broadcast. Finally, (8) can be rewritten in terms of a lower bound for $\mathcal{R}$ as follows:

$$\mathcal{R}_{\text{lower bound}} = -\mathcal{K} \ln\left[2 - \exp\left(\frac{1}{\mathcal{K}}\right)\right]. \tag{9}$$

Figure 4 shows the lower bound on RTT, $\mathcal{R}_{\text{lower bound}}$, in dB, versus the node degree, $\mathcal{K}$. It is observed that as $\mathcal{K}$ increases, the 'SNR window' decreases. For example, for $\mathcal{K} = 1$, the minimum transmission threshold is about 1.8 dB higher than the decoding threshold. It can also be inferred that theoretically, it is possible for OLA-T to achieve infinite network broadcast with an infinitesimally small $\mathcal{R}_{\text{lower bound}}$

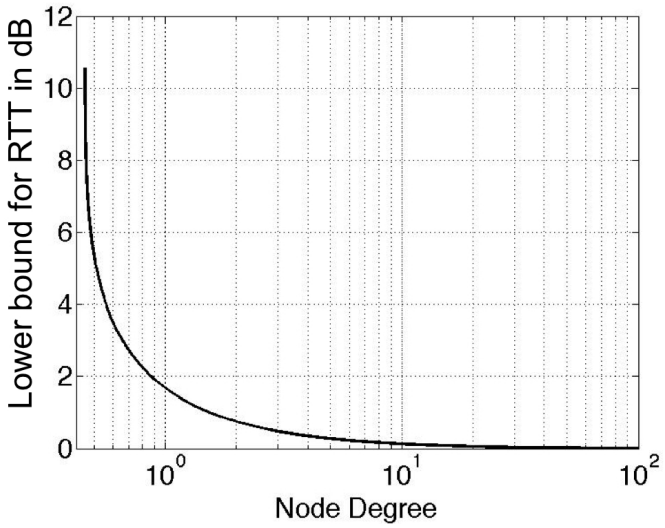

Figure 4: Lower bound on RTT, $\mathcal{R}_{\text{lower bound}}$, in dB, versus node degree, $\mathcal{K}$.

and very high $\mathcal{K}$. However, a very small $\mathcal{R}_{\text{lower bound}}$ may not be very effective if the precision in the estimate of the SNR is not good enough.

4.2.2 Energy Analysis for Broadcasting

In this section, the total radiated energy during a successful OLA-T broadcast is compared to that of a successful Basic OLA broadcast. This is done in two steps. First, expressions are derived for fraction of energy saved by OLA-T relative to Basic OLA considering only the transmit energy for the two protocols. Subsequently, this analysis is extended to also include the received energy to get closed-form expressions for the whole fraction of energy saved by OLA-T relative to Basic OLA in a single broadcast.

As $\mathcal{R} \to \infty$ (or $\tau_u \to \infty$), the OLA-T OLAs grow in thickness until they become the same as the Basic OLA decoding levels [18]. On the other hand, as $\mathcal{R} \to 1$, one would expect the transmitting strips to start thinning out. In other words, the inner and outer radii for each OLA become close and the OLA areas decrease. Because as $\mathcal{R} \to 1$, the favorably located "border nodes" play an increasingly dominant role, the thinner OLAs are more energy efficient, as will be shown below.

Continuing with the same notations, the outer and inner boundary radii for the k-th OLA ring are denoted as $r_{o,k}$ and $r_{i,k}$, respectively. The radiated energy consumed by OLA-T in the first L levels for a continuum case is mathematically expressed, in energy units, as

$$E_{\text{rad(OT)}} = \overline{P_r}_{\text{(OT,min)}} T_s \sum_{k=1}^{L} \pi (r_{o,k}^2 - r_{i,k}^2), \tag{10}$$

where T_s is the length of the message in time units and $\overline{P_r}_{\text{(OT,min)}}$ is the lowest value of $\overline{P_r}$ that would guarantee successful broadcast using OLA-T. The energy consumed by Basic OLA is given by

$$E_{\text{rad(O)}} = \overline{P_r}_{\text{(O,min)}} T_s \pi r_{o,L}^2, \tag{11}$$

where $\overline{P_r}_{\text{(O,min)}}$ is the lowest value of $\overline{P_r}$ that would guarantee successful broadcast using Basic OLA. Because of the continuum assumption, the fraction of transmission energy saved (FES) for OLA-T relative to Basic OLA can be expressed in terms of relative areas as

$$\begin{aligned} \text{FES} &= 1 - \frac{E_{\text{rad(OT)}}}{E_{\text{rad(O)}}}, \\ &= 1 - \frac{\overline{P_r}_{\text{(OT,min)}} \sum_{k=1}^{L} \left(r_{o,k}^2 - r_{i,k}^2\right)}{\overline{P_r}_{\text{(O,min)}} r_{o,L}^2}. \end{aligned} \tag{12}$$

Next, the numerator and denominator of the ratio are multiplied by π/τ_l, and substitute the minimum node degrees, $\mathcal{K}_{\text{(OT,min)}} = \frac{\pi \overline{P_r}_{\text{(OT,min)}}}{\tau_l}$ and $\mathcal{K}_{\text{(O,min)}} = \frac{\pi \overline{P_r}_{\text{(O,min)}}}{\tau_l}$ are substituted to get

$$\text{FES} = 1 - \frac{\mathcal{K}_{\text{(OT,min)}} \sum_{k=1}^{L} \left(r_{o,k}^2 - r_{i,k}^2\right)}{\mathcal{K}_{\text{(O,min)}} r_{o,L}^2}. \tag{13}$$

Next, $\mathcal{K}_{\text{(O,min)}}$ is substituted by $1/\ln 2$ and can be rewritten (13) as

$$\text{FES} = 1 - \frac{\mathcal{K}_{\text{(OT,min)}} \ln 2 \sum_{k=1}^{L} \left(r_{o,k}^2 - r_{i,k}^2\right)}{r_{o,L}^2}. \tag{14}$$

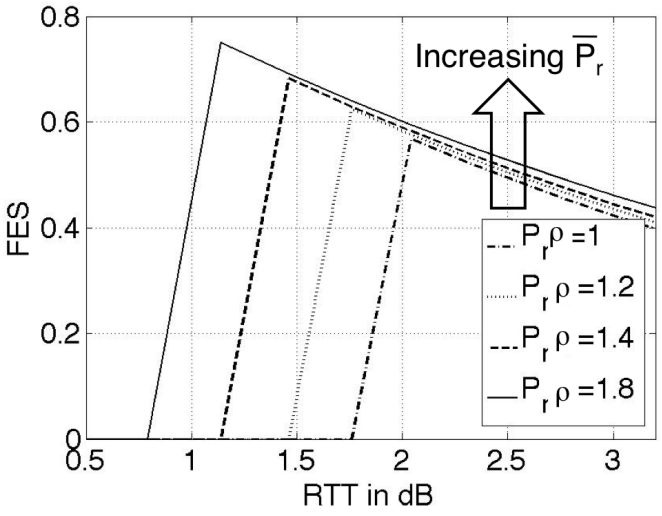

Figure 5: FES versus $\mathcal{R}$, in dB, for different $\overline{P_r}$.

In WSNs, the radiated energy does not always dominate the total energy budget. Let the total circuit-consumed energy ($\mathrm{E_{cir}}$) consumed by the network be proportional to $E_{\mathrm{rad(O)}}$: $\mathrm{E_{cir}} = \alpha E_{\mathrm{rad(O)}}$. Then, the whole-energy fraction of energy saved (WFES) can be defined as follows:

$$\begin{aligned} \mathrm{WFES} &= 1 - \left(\frac{E_{\mathrm{rad(OT)}} + \mathrm{E_{cir}}}{E_{\mathrm{rad(O)}} + \mathrm{E_{cir}}}\right), \\ &= \left(\frac{1}{1+\alpha}\right)\left(1 - \frac{E_{\mathrm{rad(OT)}}}{E_{\mathrm{rad(O)}}}\right), \\ &= \frac{\mathrm{FES}}{1+\alpha}. \end{aligned} \tag{15}$$

If the transmit energy consumptions ($\alpha = 0$) for Basic OLA and OLA-T are compared for the same $\mathcal{K}$ (same relay power density, $\overline{P_r}$), it can be shown that OLA-T saves over 50% of the energy consumed by Basic OLA [20]. Fig. 5 shows the FES versus $\mathcal{R}$, in dB, for different $\overline{P_r}$. FES is computed for a set of $\mathcal{R}$ for a fixed number of levels (10 in this case), and for different choices of $\overline{P_r}$. If the OLAs fail to propagate (i.e., if broadcast is not achieved), then fraction of areas is set to zero. The "cliff" in the curves indicates that excessively small values of e cause broadcast failure. The choice for $\mathcal{R}$ that yields the maximum FES value happens to be the one that just barely achieves network flooding. Fig. 5 also shows that higher FES for the

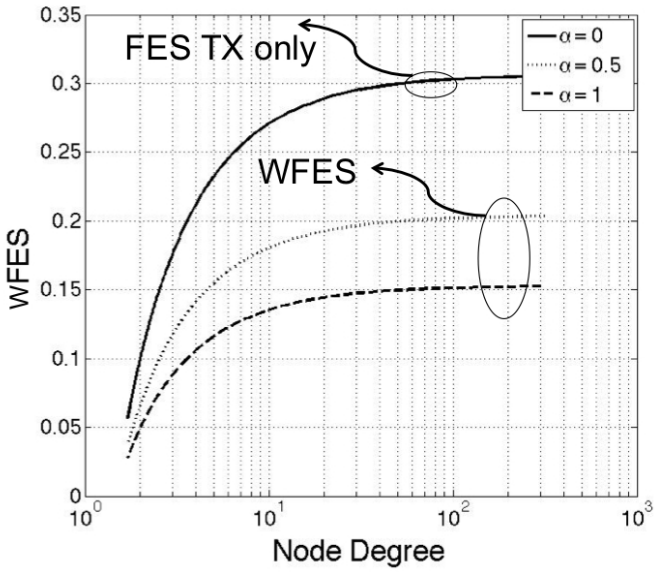

Figure 6: Variation of WFES with the minimum OLA-T node degree, $\mathcal{K}_{(\mathrm{OT,min})}$ for a network with 1000 levels.

sensor network can be achieved if the sensors transmit with more power. However, this comes at the price of the sensor battery-life, and hence could be application specific. Increasing the value of $\overline{P_r}$ also improves the network flooding by OLA-T at lower values of $\mathcal{R}$, which did not achieve broadcast. Thus, there is a tradeoff existing between the choice of e and the FES that can be achieved for a given relay power.

However, as indicated in (5) and (8), Basic OLA can achieve successful broadcast at a lower $\mathcal{K}$ than OLA-T [18]. Hence, these two protocols should be compared for a fixed value of τ_l (i.e., data rate) such that each is in its minimum energy configuration (lowest $\mathcal{K}$).

Figure 6 shows WFES versus minimum node degree, $\mathcal{K}_{(\mathrm{OT,min})}$ (on a logarithmic scale), for a disc-shaped network with 1000 levels for different values of α. For example, for $\alpha = 0$, at $\mathcal{K}_{(\mathrm{OT,min})} = 10$, FES is about 0.28. This means that at their respective lowest energy levels at $\mathcal{K}_{(\mathrm{OT,min})} = 10$, OLA-T saves about 28% of the radiated energy used by Basic OLA. On the other hand, when both the circuit and transmit energies are equal or $\alpha = 1$, and $\mathcal{K}_{(\mathrm{OT,min})} = 10$, the WFES is about 0.14,

Table 3: Currents and powers for different radios

Parameter	CC1021	CC2420	XE1205	nRF2401	nRF905
$I_{\text{tx}}^{\text{max}}$	25.1 mA	17.4 mA	62 mA	13 mA	30 mA
$I_{\text{tx}}^{\text{min}}$	14.5 mA	8.5 mA	25 mA	8.8 mA	9 mA
I_{rx}	19.9 mA	19.7 mA	14 mA	19 mA	12.5 mA
$P_{\text{rad}}^{\text{max}}$	5 dBm	0 dBm	15 dBm	0 dBm	10 dBm
$P_{\text{rad}}^{\text{min}}$	-20 dBm	-25 dBm	0 dBm	-20 dBm	-10 dBm

meaning that OLA-T saves about 14% of the total energy consumed during broadcast relative to Basic OLA, both protocols operating in their minimum power configurations. It is noted that WFES increases with $\mathcal{K}_{(\text{OT,min})}$ and attains a maximum of about 32%. This is because high values of $\mathcal{K}_{(\text{OT,min})}$ imply very slender OLA strips, which reduces the overall energy consumption in the network during broadcast.

For example, if the circuit-consumed energy in a relaying node is the same as its radiated energy, then $\alpha = 1$. When $\alpha = 0$, then only the radiated energy is considered (i.e., WFES = FES), and when $\alpha \neq 0$, the circuit energy is some fraction of the radiated energy. Table 3 gives the permissible currents and powers for three currently available radios, CC1021 [82], CC2420 [83], XE1205 [81], and the Nordic devices, nRF2401 [84] and nRF905 [85]. We acknowledge that none of these radios support OLA transmission because they do not provide diversity reception. However, we still consider them because we think their characteristics would be similar to OLA-supporting radios, and also because they show how the differences between radios affect the results. For example, for the XE1205, we have $\alpha \approx 0.22$, and for the nRF905, we have $\alpha \approx 0.4$ [72].

4.2.3 OLA-T Broadcast with Variable Transmission Threshold

The OLA-based cooperative transmission techniques presented thus far involve just a single *fixed* $\mathcal{R}$ for the whole wireless system. A shortcoming of this technique is that the radii growth is polynomial and the OLA rings keep growing bigger, expending

more energy than is needed, to cover a given network area. This strongly motivates the investigation of the potential energy savings by letting each level have a different $\mathcal{R}$. The resulting broadcast protocol is referred to as OLA with variable threshold (OLA-VT).

The Genetic Algorithm is adopted to determine the sequence of $\{\mathcal{R}_k\}$ that yields the minimum OLA-T energy per broadcast, for a given τ_l, $\overline{P_r}$, and fixed number of decoding levels. Two different constraints are considered. For each constraint, the radii are computed for the optimized $\{\mathcal{R}_k\}$, and the FES is computed, assuming Basic OLA is in its minimum energy configuration. Fig. 3 suggests that a criterion for successful broadcast is the eventual upward concavity of the curve. To capture this, the k-th double difference (DD) is defined as $DD_k = (r_{o,k+2} - r_{o,k+1}) - (r_{o,k+1} - r_{o,k})$. Constraint Type 1 is that $DD_k > 0$ for $k \geq 4$; the total number of levels or hops is fixed, but no constraint is made on the physical size of the network. Constraint Type 2, on the other hand, fixes the number of levels *and* the physical size of the network. The key difference is that Constraint Type 2 requires that the outer radius of the last decoding level be greater than the specified network radius.

Figure 7 plots the FES as a function of network radius. Constraint Type 1 is evaluated for a maximum of 20 levels (dashed lines), and Constraint Type 2 is evaluated for 10 levels (dotted lines) and 20 levels (dash-dotted lines). Both Constraint Type 2 cases fix the network radius to be 25 distance units. As an example, for the 20-level case, the Constraint Type 2 algorithm minimizes broadcast energy with the constraint that $r_{o,20} > 25$. The fixed $\mathcal{R}$ case (solid line) is included for reference and requires 150 levels to reach a radius of 25. All OLA-T and -VT examples share the same $\mathcal{K}$ of ≈ 4, and $P_s/\overline{P_r}$ of 4.31 dB. The fixed $\mathcal{R}$ case uses the $\mathcal{R}_{\text{lower bound}}$ of 1.56 dB. The points on each curve are the FES values calculated for each radius in the sequence $\{r_{o,1}, r_{i,2}, r_{o,2}, r_{i,3}, \ldots\}$. Since the FES is a function of whole levels and not partial levels, the FES for $r_{i,k}$ is just defined to be equal to the FES for $r_{o,k-1}$; this

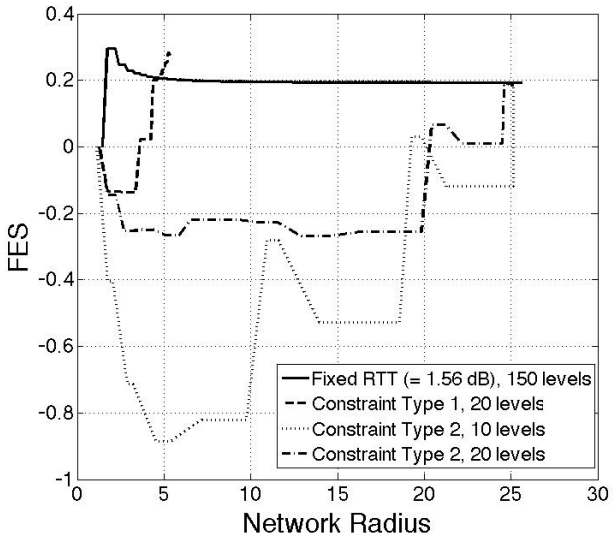

Figure 7: FES comparisons for variable $\mathcal{R}_k$ versus fixed $\mathcal{R}$

enables us to identify OLA widths as the widths of the flat parts of the curve. The first non-zero point represents the FES at $r_{o,1}$, since the FES at $r_{i,1}$ is zero. Even though the constraints involve a fixed number of levels or physical network size, the FES value at a particular radius, r, indicates the FES as though the network were truncated to have radius r. For example, after 2 OLAs (i.e., at the right edge of the second plateau), the constant $\mathcal{R}$ curve indicates an FES of about 0.25 at a radius of about 3. This means that a network of radius 3 that uses the fixed $\mathcal{R}$ of 1.56 dB to form two OLAs will achieve 25% energy savings over the minimum energy Basic OLA for a network of radius 3.

It is noted that the "network radius" in Fig. 7 is normalized by the reference distance. This means that if $d_0 = 1$ m, a network with a normalized radius of 5 has an un-normalized radius of 5 m. On the other hand, if $d_0 = 100$ m, the same normalized network radius represents an un-normalized radius of 500 m. When d_0 increases in (2) to maintain the same normalized relay transmit power, the un-normalized transmit power must increase by a factor of d_0^2, and to maintain the same normalized density, the un-normalized density must decrease by d_0^2. In other words, if d_0 increases by

a factor of 10, then the FES can be conserved by having the nodes spread out so that inter-node un-normalized distances increase by a factor of 10 and having the un-normalized relay transmit power increase by a factor of 100.

First, the Constraint Type 1 curve is compared to the fixed $\mathcal{R}$ curve. It is observed that the fixed $\mathcal{R}$ curve starts high and then decays down to about 0.2. The Constraint Type 1 curve, on the other hand, drops to negative FES values and then climbs to a final value of about 0.3. That the final value of 0.3 is higher than the FES of the fixed $\mathcal{R}$ curve for the same network radius of approximately 5 is evidence that variable $\mathcal{R}$ can be more energy efficient than fixed $\mathcal{R}$. The FES is negative because the $\overline{P_r}$ for OLA-T is larger than the $\overline{P_r}$ for Basic OLA, while the first few OLAs of OLA-T are allowed to be large and are comparable to the first few OLAs of Basic OLA in size. The step sizes or hop distances for the fixed $\mathcal{R}$ curve decrease smoothly with network radius, while the step sizes for the Constraint Type 1 curve are on the same order for the first four levels, until the FES reaches 0.2, and then the step sizes decrease significantly. Relatively small step sizes should be OK as long as the density is high enough so that the OLA ring is several d_{nn} thick.

Constraint Type 2 curves drop to much lower FES values and eventually climb back up to about 0.2. At first glance, it may seem that the variable $\mathcal{R}$ case does no better than the constant $\mathcal{R}$ case, until one considers that the variable $\mathcal{R}$ case reaches the same FES in only 10 or 20 steps, while constant $\mathcal{R}$ requires 150 steps. A d_0 of 10 m, for example, would result in a Constraint Type 2 network of radius 250 m, with OLA sizes that would be reasonable for ρ on the order of 1 node/4 m^2, as in Example 4 in Table 1.

4.3 OLA-T for Strip-Shaped Networks

In the previous sections, the performance of OLA-T has been studied for disc-shaped networks. In this section, we propose a method to systematically set the transmission

threshold and design the OLAs for two-dimensional strip-shaped networks. Theoretical bounds and conditions for achieving sustained OLA propagation and reducing the total energy consumption in the network using OLA-T have been derived in the following section. These results would also apply to arbitrarily shaped networks that have node participation limited to strip-shaped collections.

Strip-shaped networks might be deployed on structures that are strip-shaped, for example, dense distributions of wireless strain gages may be deployed on bridges in the structural health monitoring application [86]. Alternatively, a strip may occur as a "cooperative route," within a larger, dense multi-hop network. A cooperative route is a set of nodes that are candidates for cooperation between a source and a destination; the set is many hops long and multiple nodes wide, and may be constructed based on a conventional multi-hop route [87], [88], or by using other means, such as the OLA-ROAD protocol [26], [27], which does not require an existing conventional route. Our work assumes that the strip-shaped candidate set already exists, and provides a simple and systematic way for the cooperators along such routes to be selected. "Basic OLA" for the strip network was studied in [17], and in this section, that work is extended to include a *user-defined* transmission threshold, which is a mechanism to limit node participation and save energy.

Figure 8(c) represents the propagation of a packet along a strip network using OLA-T. The source node, S, initiates the packet transmission and all the nodes in the vicinity of the source node that can decode the packet form the *first* Decoding Level, $\mathbb{D}_1$. The nodes in $\mathbb{D}_1$ that satisfy the transmission threshold constitute the "OLA-1" nodes or the first OLA, and are denoted by $\mathbb{S}_1$ in Fig. 8(c). Mathematically, $\mathbb{S}_1 = \{(x, y) \in \mathbb{S} : \tau_l \leq \int\int P_s \; l(x, y)dxdy \leq \tau_u\}$.

Next, the set of nodes in the vicinity of OLA 1 that decode the packet, but have not previously decoded the same packet, form the *second* Decoding Level, $\mathbb{D}_2$. Again, *only* the nodes in $\mathbb{D}_2$ that satisfy the transmission threshold constitute the "OLA-2"

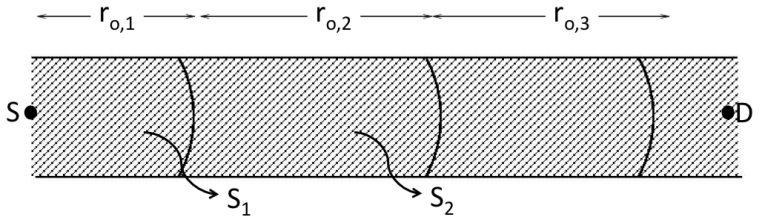

(a) Basic OLA.

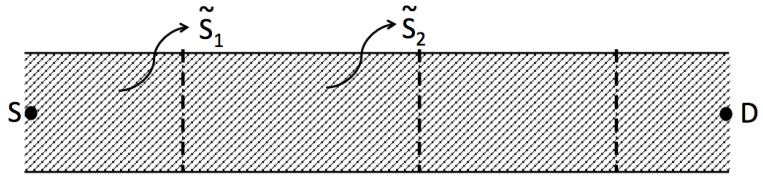

(b) Approximating OLAs with straight lines.

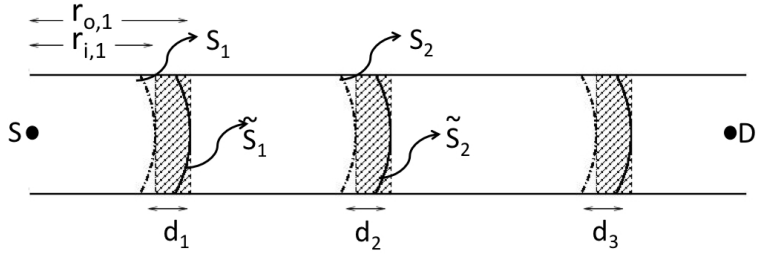

(c) OLA-T.

Figure 8: Propagation along a network strip using Basic OLA and OLA-T with a *straight line* approximation.

Table 4: Asymptotic parameters for the examples in Table 2

Example	W	$r_{o,\infty}$	d_∞	% error in asymptotic areas
1	10 m	49.6 m	2.89 m	1.12
2	2 m	14.50 m	2.45 m	2.15
3	5 m	38.70 m	2.77 m	1.58
4	10 km	54.92 km	4.32 km	6.76
5	3 km	54.92 km	4.32 km	2.04

nodes, denoted by $\mathbb{S}_2$ in Fig. 8(c). Mathematically, OLA-2 nodes are given by

$$\mathbb{S}_2 = \{(x,y) \in \mathbb{S} \backslash \mathbb{D}_1 : \tau_l \leq \overline{P_r} \int\int_{\mathbb{S}_1} l(x-x', y-y') dx' dy' \leq \tau_u\}.$$

In general, the OLA-k nodes are given by

$$\mathbb{S}_k = \{(x,y) \in \mathbb{S} \backslash \bigcup_{i=1}^{k-1} \mathbb{D}_i : \tau_l \leq \overline{P_r} \int\int_{\mathbb{S}_{k-1}} l(x-x', y-y') dx' dy' \leq \tau_u\}. \quad (16)$$

4.3.1 Rectangular Approximation

It is assumed that the width of the strip, W, the hop distance, $r_{o,k}$, and the OLA lengths, d_k, of the k-th hop, are such that the 'curved' decoding ranges (the regions between the solid and dash-dotted lines) $\mathbb{S}_k$ can be approximated by the 'shaded' rectangles $\tilde{\mathbb{S}}_k$ shown in Fig. 8(c). Table 4 lists the asymptotic values of the hop distance and OLA lengths that correspond to hop index $>> 1$ or steady state for the examples in Table 2. It can be seen that the straight-line approximation results in low approximation errors in Examples 1, 2, 3, and 5, while Examples 4 and 5 show that a smaller W yields a better approximation. It is also observed that the high density cases, Examples 1, 2, and 3, correspond to very low transmit powers.

With this approximation, the boundaries for the k-th OLA can be derived for the OLA-T protocol. The inner and outer boundaries that define the OLA-1 nodes are $r_{i,1}$ and $r_{o,1}$, respectively, as shown in Fig. 8(c). Using the definition of the path loss functions defined previously, $r_{i,1} = \sqrt{\frac{P_s}{\tau_u}}$ and $r_{o,1} = \sqrt{\frac{P_s}{\tau_l}}$. $\tilde{\mathbb{S}}_1$ is the first OLA with

boundary conditions given by $\sqrt{\frac{P_s}{\tau_u}} \leq x \leq \sqrt{\frac{P_s}{\tau_l}}$ and $|y| \leq \frac{W}{2}$. The length of the first OLA is denoted as d_1, given by $d_1 = r_{o,1} - r_{i,1} = \sqrt{\frac{P_s}{\tau_l}} - \sqrt{\frac{P_s}{\tau_u}}$.

In order to approximate the curved inner and outer boundaries for $\mathbb{S}_2$ by straight lines, $r_{i,2}$ and $r_{o,2}$ are chosen to satisfy

$$\overline{P_r} \int\int_{\tilde{\mathbb{S}}_1} l(x - [r_{i,1} + d_1 + r_{\Omega,2}], y) dx dy = \tau_\Gamma, \tag{17}$$

where $\Gamma = u$ when $\Omega = i$ and $\Gamma = l$ when $\Omega = o$.

We observe from (17), and Fig. 8(c), that $r_{i,2}$ and $r_{o,2}$ are both defined relative to $r_{o,1}$. By substituting the definition for $l(x, y)$ and making the limits explicit, we can write,

$$\int_{-W/2}^{W/2} \int_{r_{o,2}}^{r_{o,2}+d_1} \frac{\overline{P_r}}{x^2 + y^2} dx dy = \int_{r_{o,2}}^{r_{o,2}+d_1} \frac{2\overline{P_r}}{x} \arctan\left(\frac{W}{2x}\right) dx = \tau_l.$$

Similarly, $\int_{r_{i,2}}^{r_{i,2}+d_1} \frac{2\overline{P_r}}{x} \arctan\left(\frac{W}{2x}\right) dx = \tau_u$. So, $\tilde{\mathbb{S}}_2$ is the second OLA with a length $d_2 = r_{o,2} - r_{i,2}$. In this way, the subsequent OLA lengths $d_3, d_4, \ldots$ can be found iteratively $d_k = r_{o,k} - r_{i,k} = h_o(d_{k-1}) - h_i(d_{k-1})$, where the functions $h_\Omega(d_{k-1})$ for $d_{k-1} > 0$, $\Omega \in \{i, o\}$ are defined as the unique solutions of

$$\int_{h_\Omega(d_{k-1})}^{h_\Omega(d_{k-1})+d_{k-1}} \frac{2\overline{P_r}}{u} \arctan\left(\frac{W}{2u}\right) du = \tau_\Gamma, \tag{18}$$

where $\Gamma = u$ when $\Omega = i$ and $\Gamma = l$ when $\Omega = o$. We denote $h_o(\cdot) - h_i(\cdot) = g(\cdot)$. So, $d_{k+1} = g(d_k)$. The following properties for $g(\cdot)$ have been proved in Appendix C.

1. $\lim_{d \to 0} g(d) = 0$.

2. The function g is monotonically increasing.

3. The function g is concave downward.

4. The tangent at zero, $g'(0)$, is given by

$$g'(0) \;=\; h_o^{'}(0) - h_i^{'}(0) = \frac{1}{\exp\left(\frac{1}{\mathcal{K}}\right) - 1} - \frac{1}{\exp\left(\frac{\mathcal{R}}{\mathcal{K}}\right) - 1}. \tag{19}$$

5. When $g'(0) > 1$, then g has a unique positive fixed point $g(d) = d$. When $g'(0) < 1$, the only fixed point of g is at $d = 0$.

4.3.2 Sufficient and Necessary Conditions for Infinite OLA Propagation along a Two-Dimensional Strip

Infinite propagation of the packet is determined by how the sum $\sum_k d_k$ grows with k. When this sum *is unbounded*, the OLAs (and hence, the packet) will propagate forever keeping the link between the source and destination intact irrespective of the distance between these points. However, if the sum is *finite*, then the packet does not reach the destination when the source and destination are too far apart.

We shall prove that $g'(0) < 1$ implies that the transmissions die out and only a finite portion of the network is reached, i.e., $\lim_{k\to\infty} d_k = 0 \Rightarrow \sum_k d_k < \infty$. Since g is concave downward, the tangent to the curve at $d_k = 0$ stays above, i.e., $g(d_k) \leq g'(0)d_k,\ \forall d_k \geq 0$.By Mathematical Induction, we establish $d_{k+1} \leq (g'(0))^k d_1$. Assume $d_k \leq (g'(0))^{k-1} d_1$. So,

$$d_{k+1} = g(d_k) \leq g'(0)d_k \leq (g'(0))^k d_1,$$

and it follows that

$$\sum_k d_k \leq d_1 \sum_k (g'(0))^k = d_1 \frac{1}{1-g'(0)} = d_1 \left[\frac{\exp\left(\frac{1+\mathcal{R}}{\mathcal{K}}\right) - \exp\left(\frac{1}{\mathcal{K}}\right) - \exp\left(\frac{\mathcal{R}}{\mathcal{K}}\right) + 1}{\exp\left(\frac{1+\mathcal{R}}{\mathcal{K}}\right) - 2\exp\left(\frac{\mathcal{R}}{\mathcal{K}}\right) + 1} \right] < \infty.$$

Since the series is summable, $d_k \to 0$ as $k \to \infty$.

Next, we prove that $g'(0) > 1$ implies that the transmission step sizes (OLA lengths) reaching a steady value. The convergence of one-dimensional dynamical system can be established by the so-called "staircase diagram" [89] in case there is monotone convergence to a fixed point as shown in Fig. 9. Since g is monotonically increasing and concave, when the system starts from an initial condition (d_1 in Fig. 9), which is below the fixed point of g, then d_k increases monotonically towards the attractor or the fixed point. The convergence of the trajectory to a fixed point (defined as the point where the function g and the line $g(d_k) = d_k$ intersect) is determined by the value of the slope, i.e., $|g'(d_k)|$. If $|g'(d_k)| < 1$ at $g(d_k) = d_k$, then the iterate d_k

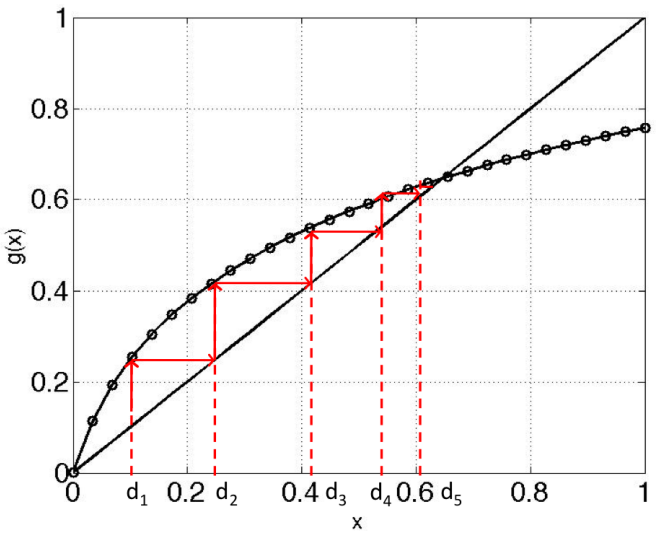

Figure 9: $g(x)$ versus x for $g'(0) > 1$.

converges to the fixed point. In the example shown in Fig. 9, it takes 5 iterations to reach the fixed point.

So, the propagation of the packet along the strip network can be predicted by computing the slope of the *concave* function g at zero [17]. In particular, properties (4) and (5) of $g(\cdot)$ imply analytical expressions for the two extreme cases: Transmissions reach a steady state when $g'(0) > 1$ and die out when $g'(0) < 1$. Equivalently, transmissions reach a steady state when $2 > \exp\left(\frac{1}{\mathcal{K}}\right) + \exp\left(\frac{-\mathcal{R}}{\mathcal{K}}\right)$. We observe that when $\mathcal{R} \to \infty$, $\exp\left(-\mathcal{R}/\mathcal{K}\right) \to 0$, OLA-T becomes Basic OLA, and the above equations become the conditions in [17]. Finally, the condition for sustained propagation can be rewritten in terms of a lower bound for $\mathcal{R}$ as follows,

$$\mathcal{R}_{\text{lower bound}} = -\mathcal{K} \ln \left[2 - \exp\left(\frac{1}{\mathcal{K}}\right) \right]. \tag{20}$$

So, $\mathcal{R} < \mathcal{R}_{\text{lower bound}}$ results in very thin OLAs (fewer nodes) that are too weak to sustain infinite propagation and eventually die out. We observe that (20) is the same lower bound as for the infinite disc network in 4.2.1. This is not surprising since a similar condition for sustained broadcast held for both the disc and strip networks using Basic OLA [14], [17].

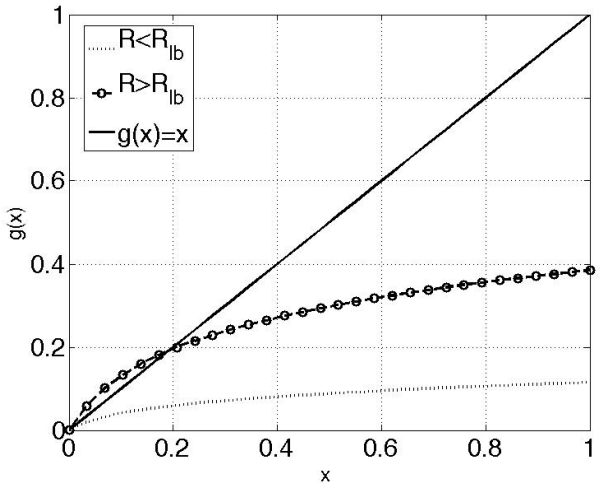

Figure 10: $g(x)$ versus x for the three cases; $g'(0) < 1$ and $g'(0) > 1$.

Figure 10 shows the two extreme cases of $g'(x)$, depending on the value of the slope at $x = 0$. To generate these results, a node degree, $\mathcal{K} = \pi$ was assumed, which resulted in $\mathcal{R}_{\text{lower bound}} = 1.476$ or 1.68 dB. Violation of the lower bound should correspond to $g'(0) < 1$. To check this, $\mathcal{R}$ was chosen to be 1.3 (1.13 dB) and 3 (4.77 dB), for the cases, $g'(0) < 1$ and $g'(0) > 1$, respectively. $g'(0) < 1 \Rightarrow \mathcal{R} < \mathcal{R}_{\text{lower bound}}$ case is denoted by the dotted curve in Fig. 10. The other extreme is when $g'(0) > 1 \Rightarrow \mathcal{R} > \mathcal{R}_{\text{lower bound}}$, and this is represented by the dash-circle curve in Fig. 10. A fixed-point attractor away from zero at about $x = 2$ can be observed for the dash-circle curve, ensuring that the transmissions don't die out.

4.3.3 Energy Evaluation of OLA-T for Strip-Shaped Routes

Analogous to the disc-shaped networks, we use the fraction of *radiated* energy saved (FES) as the metric for comparing the energy-efficiency of OLA-T relative to Basic OLA. Under the continuum assumption, the total energy consumption is simply the area of the rectangular OLAs. The FES for the strip network is computed as follows. The radiated energy consumed by OLA-T in the first N levels is mathematically

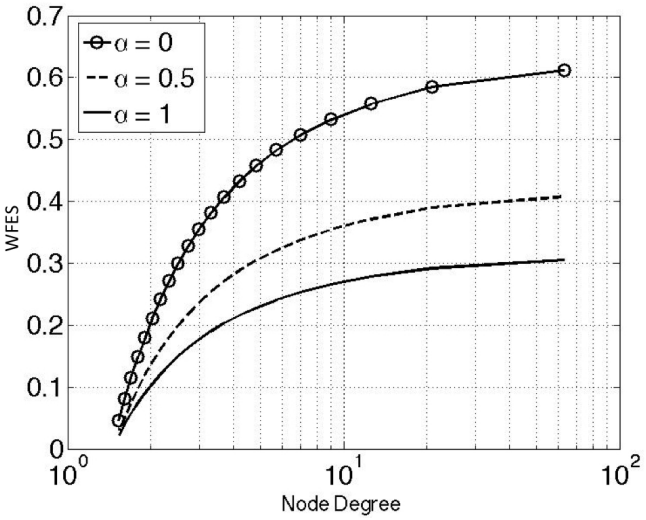

Figure 11: Variation of WFES with the minimum node degree, $\mathcal{K}_{(\mathrm{OT,min})}$.

expressed as

$$E_{\mathrm{rad(OT)}} = \overline{P_r}_{(\mathrm{OT,min})} T_s W \sum_{k=1}^{N} d_k,$$

where $\overline{P_r}_{(\mathrm{OT,min})}$ is the lowest value of $\overline{P_r}$ that would guarantee successful broadcast using OLA-T and T_s is the length of the packet in time units. The energy consumed by Basic OLA is

$$E_{\mathrm{rad(O)}} = \overline{P_r}_{(\mathrm{O,min})} T_s W r_{\mathrm{strip}},$$

where $r_{\mathrm{strip}} = \sum_{k=1}^{N} r_{o,k}$, and $\overline{P_r}_{(\mathrm{O,min})}$ is the lowest value of $\overline{P_r}$ that would guarantee successful broadcast using Basic OLA. So, FES can be expressed as:

$$\begin{aligned} \mathrm{FES} &= 1 - \frac{E_{\mathrm{rad(OT)}}}{E_{\mathrm{rad(O)}}}, \\ &= 1 - \frac{\mathcal{K}_{(\mathrm{OT,min})} \ln 2 \sum_{k=1}^{N} d_k}{r_{\mathrm{strip}}}, \end{aligned}$$

where $\mathcal{K}_{(\mathrm{OT,min})}$ is the node degree for OLA-T to guarantee successful broadcast when operating in its minimum power configuration. As derived in Section 4.2.2, $WFES = \frac{\mathrm{FES}}{1+\alpha}$ and $0 \leq \alpha \leq 1$.

Figure 11 shows WFES versus node degree, $\mathcal{K}_{(\mathrm{OT,min})}$ (on a logarithmic scale) for

a strip network for different values of α and $N = 30$. For example, for $\alpha = 0$, at $\mathcal{K}_{(\mathrm{OT,min})} = 10$, FES is about 0.55. This means that at their respective lowest energy levels at $\mathcal{K}_{(\mathrm{OT,min})} = 10$, OLA-T saves about 55% of the radiated energy used by Basic OLA. On the other hand, when both the circuit and transmit energies are equal or $\alpha = 1$, and $\mathcal{K}_{(\mathrm{OT,min})} = 10$, the WFES is about 0.28, meaning that OLA-T saves about 28% of the total energy consumed during broadcast relative to Basic OLA, both protocols operating in their minimum power configurations. It is noted that WFES increases with $\mathcal{K}_{(\mathrm{OT,min})}$ and attains a maximum of about 62%.

4.4 OLA-T for a Disc Compared to a Strip

Interestingly, the WFES in a strip network is *almost twice* that of the WFES for a disc network from [22]. Intuitively, the reason is that the OLA part of the Decoding Level 1 is a significantly larger portion of the whole for the disc compared to the strip. The analytical reasoning for this is presented below. Consider the WFES for just the *first* OLA for both networks, because the first level dominates in the comparison. Let $r_{i,1}$ and $r_{o,1}$ be the inner and outer boundaries for the first OLA, respectively, and let $d_1 = r_{o,1} - r_{i,1}$. We note that the values of these parameters are equal for disc and strip networks (see Section III.A). $\mathrm{WFES}_{\mathrm{strip}} = \left(1 - \frac{d_1}{r_{o,1}}\right)\left(\frac{1}{1+\alpha}\right)$, and $\mathrm{WFES}_{\mathrm{disc}} = \left(1 - \frac{r_{o,1}^2 - r_{i,1}^2}{r_{o,1}^2}\right)\left(\frac{1}{1+\alpha}\right)$. Observe that

$$\mathrm{WFES}_{\mathrm{disc}} = \left(1 - \frac{d_1}{r_{o,1}} \underbrace{\frac{(r_{o,1} + r_{i,1})}{r_{o,1}}}_{>1}\right)\left(\frac{1}{1+\alpha}\right) < \mathrm{WFES}_{\mathrm{strip}}.$$

To summarize, OLA-T and its variants extend Basic OLA [13]–[14] through the introduction of the "transmission threshold," and have been proposed and analyzed for broadcasting over wireless networks. A node that successfully decodes the message (e.g., by passing a cyclic redundancy check (CRC)), compares its received SNR to this threshold and relays only if its SNR is *less* than the threshold; the nodes that relay are

in the best position to participate in the next OLA transmission. By self-scheduling their transmissions using the thresholds, nodes can save significant energy.

When compared to Basic OLA, OLA-T saves up to 32% of the transmitted energy by limiting the number of nodes in each OLA. OLA with variable threshold (OLA-VT), described in Section 4.2.3, saves additional energy with no overhead and no central control through optimization of the threshold for each decoding level. For fixed-size networks, OLA-VT simplifies boundary-matching. OLA-T protocol along strip-shaped routes (networks) was found to save as much as 62% of the transmitted energy relative to Basic OLA, when both protocols operated in their lowest power configurations. The physical interpretation is that restricting the *energy-spilling* to just the relay nodes in the direction of the destination makes the broadcasting along strips more energy-efficient.

Lastly, it is remarked that Basic OLA transmission has been proposed for unicast transmission because of its lack of overhead [71]. For radios that consume substantial energy when receiving and decoding, Basic OLA might not be advantageous for unicast, since every node receives and decodes. However, in the context of unicast, OLA-T, a node doesn't need to decode the data if it is not a relay and not the destination. If the energy spent determining that a node should relay can be made extremely small, then OLA-T might be an attractive unicast scheme.

CHAPTER V

EXTENDING NETWORK LIFETIME FOR A FIXED SOURCE AND STATIC NETWORK

OLA-T is an energy-efficient cooperative broadcast strategy relative to Basic OLA. However, for a fixed source such as the fusion node in a WSN, and for a static network, OLA-T causes the same subset of nodes to participate in all broadcasts. Therefore, participating nodes in OLA-T will eventually die ("death" happens when the batteries die), causing significant areas of the network to lose their sensing function and partitions to form. It is noted that a network of randomly moving nodes will not have this problem, as eventually all nodes spend some time in the "OLA area," thereby sharing the broadcasting burden. If network life is defined to be the length of time before the first node dies, and the broadcasts are assumed to be the only transmissions, then it follows that for a static network, OLA-T has no advantage over Basic OLA in terms of lifetime even though it consumes less total transmit energy in a single broadcast, especially when $\mathcal{K}$ is the same. So, a variant of OLA-T called the alternating OLA-T (A-OLA-T) that improves the network lifetime compared to Basic OLA and OLA-T is proposed. The concept and analysis of A-OLA-T are original contributions of this doctoral research work.

The idea of A-OLA-T is that the nodes that do not participate in one broadcast make up the OLAs in the next broadcast. To ensure that the sets of OLAs during each broadcast are mutually exclusive, the OLA boundaries should not change during the two broadcasts. Fig. 12 illustrates the concept. The gray areas on the left of Fig. 12 are the OLAs in the first broadcast, while the gray areas on the right are the OLAs in the second broadcast. Ideally, these two sets of OLAs have no nodes in common

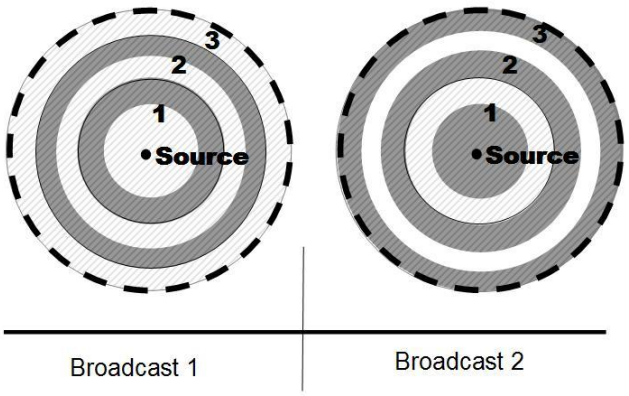

Figure 12: The gray strips represent the transmitting nodes (that form the OLA), which alternate during each broadcast.

and their union includes all nodes. A-OLA-T can be extended to have three or more sets of OLAs that have no nodes in common, such that the union includes all the nodes in the network. Under the continuum assumption, more sets will increase the network life because border nodes play an increasingly dominant role. However, with finite node density, the practical limit in the number of sets is expected to be low.

5.1 A-OLA-T for Disc-shaped Networks

Like in the case of OLA-T, A-OLA-T has also been analyzed separately for disc- and strip-shaped cooperative routes (network shapes), which correspond to the largest and smallest ratios of nodes (or areas) used up during a single network broadcast. First, we analyze the two-set A-OLA-T for disc-shaped networks, followed by the m alternating sets, and then consider strip-shaped networks in Section .

5.1.1 Two Alternating Sets (Two-Set A-OLA-T)

The basic concept of A-OLA-T is that an arbitrary number of broadcasts could be grouped under the continuum assumption; however, with finite node density, smaller group sizes are expected to be the best to ensure that the OLAs are populated with a sufficient number of nodes. So in this section, just two groups are considered and are called *Broadcast 1* and *Broadcast 2*.

Figures 13(a) and (b) contain illustrations of successful and unsuccessful A-OLA-T broadcasts, respectively. These figures show how to ensure that both broadcasts are sustaining. The upper parts of both drawings correspond to Broadcast 1, and the outer and inner OLA radii for the k-th OLA ring are labeled $r_{o,k}$ and $r_{i,k}$, respectively. The lower parts of both drawings correspond to Broadcast 2, and the outer and inner OLA radii for the k-th OLA ring are relabeled $v_{o,k}$ and $v_{i,k}$, respectively. The initial conditions for the second broadcast are $v_{i,1} = 0$, and $v_{o,1} = \sqrt{\frac{P_s}{\tau_u}}$, where $v_{o,1}$ was fixed in Broadcast 1. In Fig. 13(a), the first OLA during Broadcast 1 is denoted by *OLA 1,1* and is defined by the radii pair, $r_{i,1}$ and $r_{o,1}$. On the other hand, the first OLA during Broadcast 2 is denoted by by *OLA 1,2* and is the circular disk of radius $v_{o,1}$. Let $\widetilde{v}_{o,2}$ be the decoding range of *OLA 1,2* during Broadcast 2. The key idea is that $\widetilde{v}_{o,2}$ must be greater than $r_{i,2}$. In Fig. 13(a), this inequality is satisfied, while in Fig. 13(b), it is not. More generally, the network designer just needs to check that the decoding range, $\widetilde{v}_{o,k+1}$, of the k-th OLA in Broadcast 2 is always greater than $r_{i,k+1}$, for all k. Alternatively, the received power at $r_{i,k+1}$ can be computed and confirmed that it is greater than the minimum. Using $v_{o,k} = r_{i,k}$ and $v_{i,k} = r_{o,k-1}$, it is easy to see that

$$\overline{P_r}\left[f(r_{i,k}, r_{i,k+1}) - f(r_{o,k-1}, r_{i,k+1})\right] \geq \tau_l. \tag{21}$$

Intuitively, as $\mathcal{R}$ becomes very large, the OLAs during Broadcast 1 would become larger and the OLAs of Broadcast 2 would become relatively smaller, as shown in Fig. 13(b). As a result, the sets of nodes that did not transmit during Broadcast 1 (or the OLAs during Broadcast 2) eventually become so small that their decoding range (for *OLA 1,2*, this is indicated by the dashed line in Fig. 13(b)) cannot reach the next Broadcast 2 OLA to sustain propagation, i.e., $\widetilde{v}_{o,2} < v_{i,2}$. In other words, for a very high value of $\mathcal{R}$, the k-th OLA in Broadcast 2 may be so weak that no nodes between $v_{i,k+1}$ and $v_{o,k+1}$ can decode the signal. When this happens, OLA formations die off during Broadcast 2 and A-OLA-T fails to achieve network broadcast. Thus,

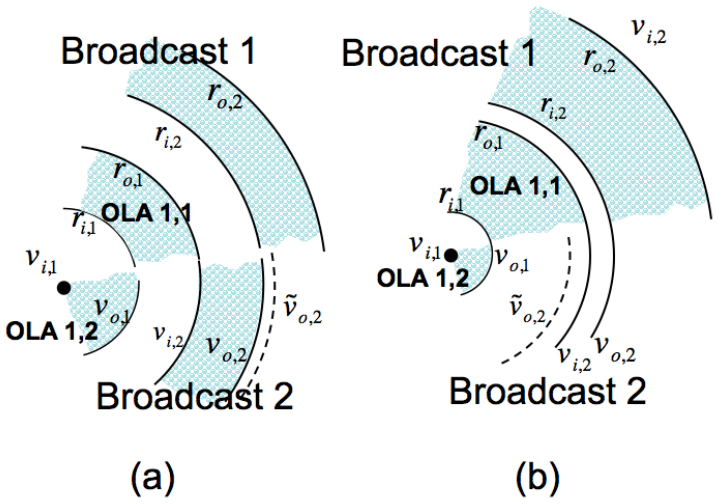

Figure 13: Illustration of the A-OLA-T Algorithm with (a) admissible $\mathcal{R}$, (b) inadmissible $\mathcal{R}$.

it makes sense for $\mathcal{R}$ to have an upper bound.

After substituting (7) into (21), and simplifying, the condition in (21) can be rewritten to show the explicit dependence on the Broadcast 1 radii:

$$0 \quad \leq \quad \frac{\beta(\tau_l) r_{i,k}^2 - r_{o,k-1}^2 - (\beta(\tau_l) - 1)\, r_{i,k+1}^2}{\beta(\tau_l) - 1}. \tag{22}$$

Substituting the expressions for $r_{o,k}$ and $r_{i,k}$ from (46)–(49) into (22) and collecting the A_1 and A_2 terms yields

$$A_1^{k-1}\Omega - A_2^{k-1}\Pi \geq 0. \tag{23}$$

where

$$\Omega = \Big(\alpha(\tau_l) + 1\Big)\zeta_1 - \alpha(\tau_l)\eta_1 A_1^{-1} - \zeta_1 A_1, \text{ and} \tag{24}$$

$$\Pi = \Big(\alpha(\tau_l) + 1\Big)\zeta_2 - \alpha(\tau_l)\eta_2 A_2^{-1} - \zeta_2 A_2.$$

Using $A_2 = 1$ and the expressions for η_2 and ζ_2, $\Pi = \zeta_2 - \eta_2 = 0$, which, when applied to (23) along with $A_1 > 0$, the inequality in (23) may be simplified to $\Omega \geq 0$. While not obvious from $\Omega \geq 0$, this inequality implies an upper bound on $\mathcal{R}$. The derivation of the closed-form expression for the upper bound on $\mathcal{R}$ can be found in Appendix

D, and is given by

$$\mathcal{R}_{\text{disc,upper bound}} = \frac{\mathcal{K}}{2} \ln \left\{ \exp\left(\frac{1}{\mathcal{K}}\right) + 1 + \sqrt{\left[\exp\left(\frac{1}{\mathcal{K}}\right) + 1\right]^2 - 4} \right\}. \quad (25)$$

It is remarked that it is not necessary to assume the same $\mathcal{R}$ for both broadcasts or even for different levels within a single broadcast [22]. With the flexibility of level-dependent transmission thresholds ($\tau_{u,k}$ or $\mathcal{R}_k$), a designer may be able to make the decoding ranges in Broadcast 2 match up exactly with the boundaries in Broadcast 1 and thereby save more transmit energy.

5.1.2 Factor of Life Extension

Figure 14 is a plot of the upper and lower bounds for relative transmission threshold, $\mathcal{R}$, in dB, for A-OLA-T, as a function of the node degree, $\mathcal{K}$. First, it is observed that as $\mathcal{K}$ increases, the difference between the upper and lower bounds increases. As an example, for a small increase in $\mathcal{K}$ from 2 to 4, the range of $\mathcal{R}$ increases from $[0.8, 4.2]$ to $[0.4, 5.6]$. This has two reasons. Increasing $\mathcal{R}$ could be done by increasing the $\overline{P_r}$, which enables Broadcast 1 to be successful with more slender OLAs. This corresponds to a decrease of the lower bound. Fatter Broadcast 2 OLAs more easily reach across the next pair of boundaries and so this increases the upper bound. Next, decreasing τ_l also increases $\mathcal{K}$. Decreasing τ_l decreases the lower bound, because a lower value of τ_l corresponds to a lower SNR requirement at the receiving node, and so in order to meet this power requirement, the OLAs can afford to have fewer nodes during Broadcast 1. OLAs during Broadcast 1 become thinner but more powerful, and the OLAs during Broadcast 2 grow thicker. This is implied by an increase in the upper bound.

Also, it is observed from Fig. 14 that the upper and lower bounds converge as $\mathcal{K}$ decreases. This also implies a lower bound on $\mathcal{K}$ for A-OLA-T, $\mathcal{K}_{(\text{A,min})} = \frac{\pi \overline{P_r}_{(\text{A,min})}}{\tau_l}$, where $\overline{P_r}_{(\text{A,min})}$ is the minimum value of $\overline{P_r}$ for a given τ_l. It was not possible to obtain an exact value of $\mathcal{K}_{(\text{A,min})}$; however, using numerical analysis it was found that

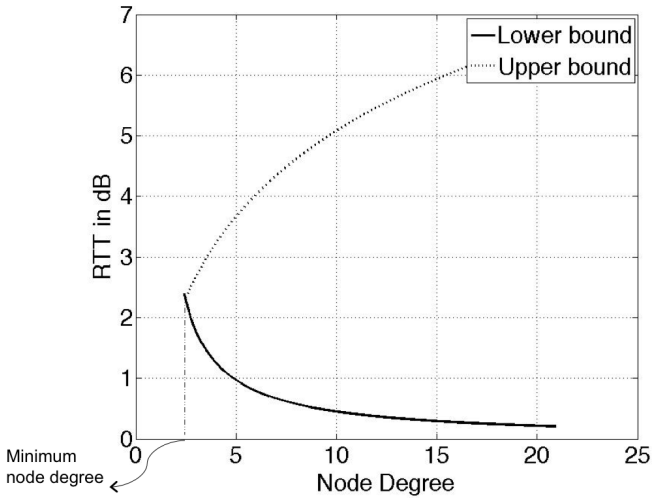

Figure 14: Relative transmission threshold, $\mathcal{R}$, in dB, versus node degree for A-OLA-T, $\mathcal{K}$. The $\mathcal{K}$ corresponding to the intersection of the two curves is the $\mathcal{K}_{(\mathrm{A,min})}$.

$\mathcal{K}_{(\mathrm{A,min})} = 2.45$. It is noted from (5) that $\mathcal{K}$ has a smaller lower bound for Basic OLA, $\mathcal{K}_{(\mathrm{O,min})} = (\pi \ln(2))^{-1} = 1.44$. For $\mathcal{K} < \mathcal{K}_{(\mathrm{A,min})}$, network broadcast fails for A-OLA-T because the OLAs die out during Broadcast 2. For A-OLA-T, from the definition of $\mathcal{K}_{(\mathrm{A,min})}$, $\overline{P_r}_{(\mathrm{A,min})} \simeq 0.78\tau_l$. From (5), the minimum $\overline{P_r}$ for Basic OLA, denoted by $\overline{P_r}_{(\mathrm{O,min})}$, is given by $0.46\tau_l$. It is observed that A-OLA-T requires less than double the power of Basic OLA because it uses border nodes.

Next, the "broadcast life" extension of A-OLA-T compared to Basic OLA is computed. Broadcast life here means the lifetime of the network if only broadcasts were transmitted. If A-OLA-T and Basic OLA use the same $\overline{P_r}$, then A-OLA-T doubles the network life compared to Basic OLA. However, this is not a fair comparison since Basic OLA can achieve successful broadcast at a lower $\overline{P_r}$. Realizing that every broadcast in A-OLA-T is essentially an OLA-T broadcast, the factor of life extension (FLE) may be defined as

$$\mathrm{FLE} = \frac{1}{1 - \mathrm{FES}}, \tag{26}$$

where FES denotes the fraction of energy saved by OLA-T relative to Basic OLA in a single broadcast (from Section 4.2.2). FLE can be evaluated for any powers that

satisfy $\overline{P_{r(\mathrm{A})}} \geq 0.25\tau_l$ and $\overline{P_{r(\mathrm{O})}} \geq 0.15\tau_l$, for A-OLA-T and Basic OLA, respectively. However, upon substituting the minimum powers, (26) becomes

$$\widehat{\mathrm{FLE}} = \frac{1}{1 - \widehat{\mathrm{FES}}}, \tag{27}$$

where $\widehat{\mathrm{FLE}}$ and $\widehat{\mathrm{FES}}$ denote the FLE and FES, respectively, when both protocols operate in their minimum power configurations. The minimum powers for Basic OLA and A-OLA-T correspond to the minimum node degrees, $\mathcal{K}_{(\mathrm{O,min})}$ and $\mathcal{K}_{(\mathrm{A,min})}$, respectively. From Fig. 6, $\widehat{\mathrm{FES}} = 0.145$ at $\mathcal{K}_{(\mathrm{A,min})} = 2.45$, resulting in $\widehat{\mathrm{FLE}} \approx 1.17$. This means that A-OLA-T with two alternating sets can extend network life by a factor of 1.17 relative to Basic OLA when both protocols are optimized.

5.1.3 Equal Area Property

Let the 'Ratio of Areas' be the ratio of the total area of the Broadcast 1 OLAs to the total area of the network, and be given by

$$\tilde{\Psi} = \frac{\sum_{k=1}^{L} \left(r_{o,k}^2 - r_{i,k}^2\right)}{r_{o,L}^2}, \tag{28}$$

where $r_{o,k}$ and $r_{i,k}$ denote the outer and inner boundary radii, respectively, for the k-th OLA ring formed during the Broadcast 1, and L is the number of OLAs in the OLA-T network. In [24], it was shown that for the $m = 2$ case, $\tilde{\Psi} = 1/2$ when $\mathcal{K} = \mathcal{K}_{(\mathrm{A,min})}$. This implies that the respective accumulated areas of the two sets of OLAs during Broadcasts 1 and 2 are equal.

To summarize, for the two-set A-OLA-T, Broadcast 1 fixes the radii for Broadcast 2. The trick then is to choose transmission thresholds to ensure that the detection boundaries in Broadcast 2 exceed (or match up) with transmission threshold boundaries in Broadcast 1. In [24], it was established that there exists a minimum value of $\mathcal{K}$, denoted by $\mathcal{K}_{(\mathrm{A,min})}$, and when $\mathcal{K} < \mathcal{K}_{(\mathrm{A,min})}$, network broadcast fails for A-OLA-T because the OLAs die out during Broadcast 2. $\mathcal{K}_{(\mathrm{A,min})}$ implies a minimum value of

$\overline{P_r}$ for a given τ_l, denoted by $\overline{P_{r(\mathrm{A,min})}}$. Compared to Basic OLA, A-OLA-T with two sets extends the network longevity by a factor of 1.17 when both OLA-based protocols operate in their minimum power configuration [24]. This work may be useful for future very large and very fine-grained monitoring applications, of the type that may be enabled by sensor nodes that do energy harvesting.

5.1.4 m Alternating Sets (m-Set A-OLA-T, $m > 2$)

In this section, it is shown that using m alternating sets of OLAs ($m > 2$) extends the life of the network even more than for $m = 2$. To show this, we conjecture that the Equal Area Property applies to the $m > 2$ case. Assuming that the conjecture is true implies that $\tilde{\Psi} = \frac{1}{m}$ for all broadcast sets, when the system is in its lowest energy configuration, i.e., when $\mathcal{K} = \mathcal{K}_{(\mathrm{A,min})}$. We confirm the assumption numerically in the next section. Based on the assumption, we are able to derive an expression for $\mathcal{K}_{(\mathrm{A,min})}$, which in turn, allows us to quantify the relative transmit energy consumption of m-set A-OLA-T to Basic OLA. The derivation of $\mathcal{K}_{(\mathrm{A,min})}$ is sketched here and the details are in the appendices.

Figure 15 illustrates the A-OLA-T concept with 3 alternating sets of OLAs. Each broadcast is an OLA-T broadcast. The gray areas in the left of Fig. 15, are the OLAs in "Broadcast 1," while the gray areas in the center and on the right, are the OLAs in "Broadcast 2," and "Broadcast 3," respectively. Ideally these three sets of OLAs have no nodes in common and their union includes all nodes. In Fig. 15, the sets of OLAs during Broadcasts 1, 2, and 3 comprise $\mathrm{OLA}_{1,1}$ and $\mathrm{OLA}_{2,1}$, $\mathrm{OLA}_{1,2}$ and $\mathrm{OLA}_{2,2}$, and $\mathrm{OLA}_{1,3}$ and $\mathrm{OLA}_{2,3}$, respectively; these sets do not have any common nodes and their union includes all the nodes in the network. This increases the network longevity for broadcast applications because each node participates once in every three broadcasts, and therefore the load is shared equally.

We use the closed-form expressions for OLA-T ring radii from [22] to put $\tilde{\Psi}$ for

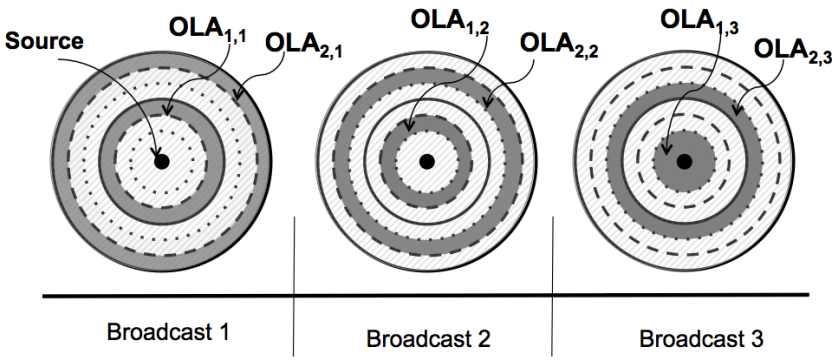

Figure 15: A-OLA-T with 3 alternating mutually exclusive sets of OLAs.

Broadcast 1 solely in terms of $\mathcal{R}$ and $\mathcal{K}$. Then setting $\tilde{\Psi} = \frac{1}{m}$ allows an expression for $\mathcal{R}$ in terms of $\mathcal{K}$ and m. Next, assuming the lowest energy configuration means that $\mathcal{R}$ must be equal to its lower bound (in [22], the upper and lower bounds on $\mathcal{R}$ meet at the minimum energy configuration for $m = 2$). Solving this equality for $\mathcal{K}$ yields the expression

$$\mathcal{K}_{(\mathrm{A,min})} = \left[\ln\left(\frac{m+1}{m}\right) \right]^{-1}. \tag{29}$$

In fact, it can be proved that $\mathcal{K}_{(\mathrm{A,min})} \approx \frac{2m^2}{2m-1}$ to the second order, and $\mathcal{K}_{(\mathrm{A,min})} \to m$ as $m \to \infty$. A disc-shaped network achieves the maximum FES per broadcast as $\mathcal{K}_{(\mathrm{A,min})} \to \infty$ (because the OLAs become thinner), and from Fig. 6, $\widehat{\mathrm{FES}} \approx 0.32$. Substituting this value in (27), we get $\widehat{\mathrm{FLE}} = 1.47$. Hence, A-OLA-T with m alternating sets, $m \to \infty$, offers a maximum life extension factor of 1.47 relative to Basic OLA when both protocols are optimized.

5.1.5 Numerical Results for m-Set A-OLA-T

For the two-set A-OLA-T in [24], the asymptotic convergence of the ratio of the differences in the radii of the mutually exclusive sets of OLAs to 1 meant that the ratio of the accumulated areas of the mutually exclusive sets of OLAs was exactly 1. This implied that the ratio of the accumulated areas for a 'single' broadcast to the total area of the network, $\tilde{\Psi}$ was exactly 1/2 for both broadcasts.

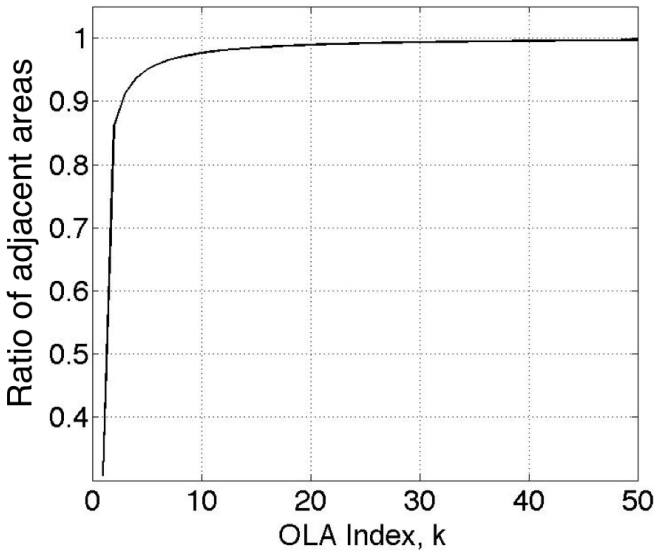

Figure 16: Ratio of adjacent areas versus OLA index, k for $m = 3$.

For an m-A-OLA-T, it was conjectured that $\tilde{\Psi}$ would be $1/m$ for all m broadcasts. This conjecture is verified numerically for $m = 3$ in Fig. 16. Figure 16 is a plot of the ratio of adjacent areas versus k for the three successive broadcasts. As seen in the figure, convergence of ratio of areas to ≈ 1 shows that the widths of adjacent OLAs from Broadcast 1, 2, and 3 become equal. This also implies that the ratio of the accumulated areas for a 'single' broadcast to the total area of the network, $\tilde{\Psi}$, is 0.3333 for all the three mutually exclusive broadcasts.

Next, we establish the network lifetime extensions using m-A-OLA-T. Figure 17 is a plot of the FLE versus the number of alternating sets, m, on a logarithmic scale. We observe that as m increases, the FLE increases (solid line), and for a large number of alternating sets, it reaches its asymptotic value (shown by dashed line) of around 1.47. This means that m-set A-OLA-T can extend the network life by a maximum factor of about 1.47 when both protocols are optimized. When $m = 2$, $\widehat{\text{FLE}} = 1.17$, which is consistent with the findings for the two-set A-OLA-T.

Finally, it remains to check if infinite network broadcast can be achieved when the m-set A-OLA-T is operating in the minimum power configuration, i.e., at $\mathcal{K} =$

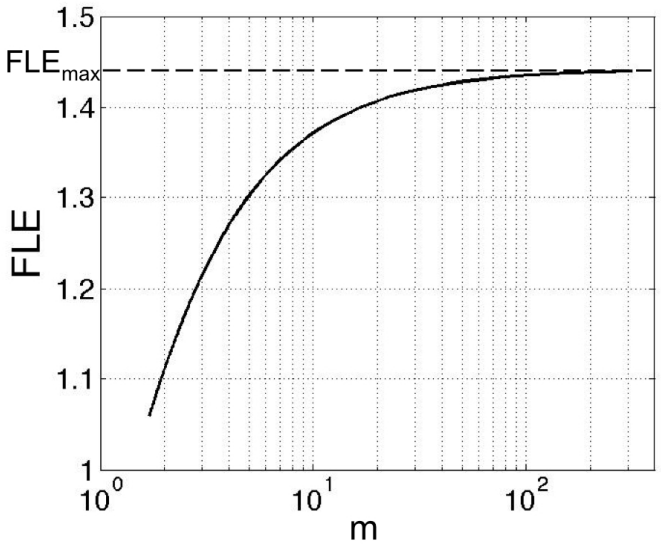

Figure 17: FLE as a function of the number of alternating sets, m.

$\mathcal{K}_{(\mathrm{A,min})}$, which is given by (29). For our example, we use Matlab simulations and choose $m = 3$. Let $v_{o,k}$ and $v_{i,k}$, denote the outer and inner boundary radii for the k-th OLA ring formed during the Broadcast 2, respectively. If $u_{o,k}$ and $u_{i,k}$, denote the outer and inner boundary radii, respectively, for the k-th OLA ring formed during the Broadcast 3, and if $\tilde{u}_{o,k+1}$ represents the decoding range of the $(k+1)$-st OLA, then $\tilde{u}_{o,k+1} \geq v_{i,k+1}$ must hold to guarantee infinite network broadcast. The inner and outer boundaries have been simulated using the closed form expressions given by (46). It is remarked that even though the continuum assumptions of [22] are used for these simulations, it has been shown in [22] using Monte-Carlo simulations that the continuum and deterministic assumptions can be approximated well by networks of finite density with Rayleigh fading channels. We test infinite network broadcast numerically at $\mathcal{K}_{(\mathrm{A,min})}$. The shaded background in Fig. 18 is a plot of the 3-set A-OLA-T normalized radii at $\mathcal{K}_{(\mathrm{A,min})}$ for the 999-th and 1000-th levels as a function of normalized distance. The white circle in the foreground is a magnified version of the region enclosed by the smaller dotted circle. The normalized Source power, P_s was chosen to be 5 and from Appendix F, $\mathcal{K}_{(\mathrm{A,min})} = \pi/0.9038$. We now explain the plot

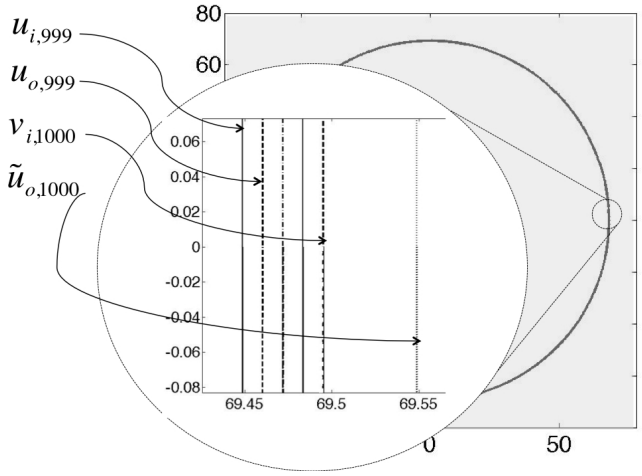

Figure 18: 3-set A-OLA-T radii growth in the minimum power case. The 999-th and 1000-th levels are shown in the figure.

in the foreground. Continuing to follow the notations from the previous paragraph, Broadcast 3 boundary radii for the 999-th level, $u_{i,999}$ and $u_{o,999}$, are represented by the solid and dashed lines, respectively. The dashed line (second from the right) is the Broadcast 2 inner boundary radii for the 1000-th level, $v_{i,1000}$. The right-most dotted line represents the decoding range of the 1000-th OLA, $\tilde{u}_{o,1000}$. From Fig. 18, we observe that $\tilde{u}_{o,1000} > v_{i,1000}$, and so this is indicative of infinite network broadcast at $\mathcal{K}_{(\mathrm{A,min})}$. It was observed that for $\mathcal{K} < \mathcal{K}_{(\mathrm{A,min})}$, Broadcast 3 OLAs die out.

5.2 A-OLA-T for Strip-Shaped Networks

In the previous sections, the performance of A-OLA-T has been studied for disc-shaped Networks. In this section, we propose a method to systematically set the transmission threshold and design the OLAs for two-dimensional strip-shaped networks. Theoretical bounds and conditions for achieving sustained OLA propagation and extending network longevity using A-OLA-T have been derived in the following sections. These results would also apply to arbitrarily shaped networks that have node participation limited to strip-shaped collections.

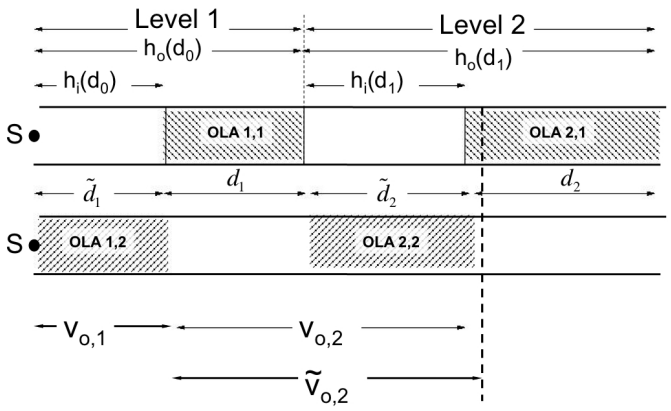

Figure 19: Illustration of the A-OLA-T with admissible $\mathcal{R}$.

5.2.1 Performance of Two-Set A-OLA-T

From Section 4.3.2, we know that the necessary and sufficient condition to achieve infinite network broadcast with a constant transmission threshold is the inequality,

$$2 \;\geq\; \exp\left(\frac{1}{\mathcal{K}}\right) + \exp\left(\frac{-\mathcal{R}}{\mathcal{K}}\right), \tag{30}$$

which takes the form of the following lower bound for $\mathcal{R}$

$$\mathcal{R}_{\text{lower bound}} = -\mathcal{K} \ln\left[2 - \exp\left(\frac{1}{\mathcal{K}}\right)\right].$$

Since the boundaries don't change, we will follow the approach described in Section 5.1.1 to derive a necessary and sufficient condition for Broadcast 2 to also be successful. The sufficient condition for Broadcast 1 to be successful takes the form of a lower bound on $\mathcal{R}$. An $\mathcal{R}$ that satisfies this bound fixes the boundaries. The condition for Broadcast 2 then gives an upper bound on $\mathcal{R}$. During Broadcast 2, the set of nodes that transmitted during Broadcast 1 will not transmit and the nodes that did not participate during the the first broadcast will transmit. From Section 5.1.1, it is clear that an upper bound for $\mathcal{R}$ exists. In the remainder of this section, only the basic framework that is used to derive the upper bound for $\mathcal{R}$ is formulated, while the complete analysis can be found in Appendix G.

Figures 19 and 20 illustrate how it is possible to design OLAs for Broadcasts 1 and 2, to ensure that their propagation is sustained. Let S be the originating node.

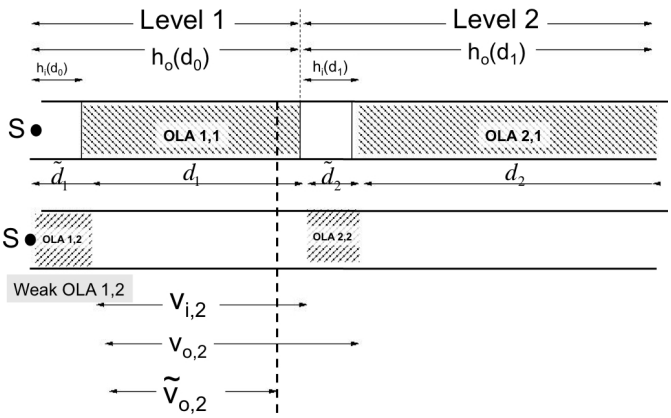

Figure 20: Illustration of the A-OLA-T with inadmissible $\mathcal{R}$.

The upper parts of both drawings correspond to Broadcast 1 and the boundaries are labeled as $\{h_o(d_k)\}$ and $\{h_i(d_k)\}$. The lower parts of both drawings correspond to Broadcast 2. In Fig. 19 the OLA radii are relabeled $\{v_{o,k}\}$ and $\{v_{i,k}\}$, to denote the outer and inner boundary sequences, respectively for the k-th OLA formed during the Broadcast 2. The initial conditions for the second broadcast are $v_{i,1} = 0$, and $v_{o,1} = h_i(d_0) = \sqrt{\frac{P_s}{\tau_u}}$. In the upper part of Fig. 19, the first OLA during Broadcast 1 is denoted by *OLA 1,1* and is defined by the boundary pair, $h_i(d_0)$ and $h_o(d_0)$. On the other hand, the first OLA during Broadcast 2 is denoted by *OLA 1,2* and rectangular block of length $v_{o,1}$. Let $\widetilde{v}_{o,2}$ be the decoding range of *OLA 1,2* during Broadcast 2. The key idea is that $\widetilde{v}_{o,2}$ must be greater than $d_1 + h_i(d_1)$. In Fig. 19, this inequality is satisfied, while in Fig. 20, it is not. More generally, the network designer just needs to check that the decoding range, $\widetilde{v}_{o,k+1}$, of the k-th OLA in Broadcast 2 is always greater than $d_k + h_i(d_k)$, for all k. Alternatively, we can compute the received power at $h_i(d_k)$ and confirm that it is greater than the minimum. Mathematically, we express this as

$$v_{o,k+1} \geq d_k + h_i(d_k) \Rightarrow h_o(\widetilde{d_k}) \geq d_k + h_i(d_k). \tag{31}$$

The derivation of the closed-form expression for the upper bound on $\mathcal{R}$ can be

found in Appendix G, and is given by

$$\mathcal{R}_{\text{strip,upper bound}} = \mathcal{K} \ln \left[2 \exp \left(\frac{1}{\mathcal{K}} \right) - 1 \right], \tag{32}$$

and it can be seen that $\mathcal{R}_{\text{strip,upper bound}} \leq \mathcal{R}_{\text{disc,upper bound}} \; \forall \; \mathcal{K}$. Intuitively, the area of a strip is smaller than that of a disc implying fewer nodes (and hence weaker OLAs) under the continuum assumption, which explains the aforementioned inequality.

As in the case of disc-shaped networks (Section 5.1.2), the upper and lower bounds for the relative transmission threshold, $\mathcal{R}$, were plotted as a function of the node degree, $\mathcal{K}$. It was observed that the upper and lower bounds converged as $\mathcal{K}$ decreased; the $\mathcal{K}$ corresponding to the intersection of the two curves being the $\mathcal{K}_{(\text{A,min})}$. Using numerical analysis it was found that $\mathcal{K}_{(\text{A,min})} \approx 2.45$, the exact same value obtained for disc-shaped networks, and this results in the same minimum value of $\overline{P_r}$ for a successful A-OLA-T broadcast, $\overline{P_{r\,(\text{A,min})}}$. However, the factor of life extension (FLE) offered by A-OLA-T relative to Basic OLA is ≈ 1.41, i.e., 20.51% more than that in a disc-shaped network. Because areas do matter in each individual broadcast, whatever differences exist between disk and strip, in terms of OLA-T savings over Basic OLA, are also seen for A-OLA-T.

5.2.2 Performance of m-Set A-OLA-T ($m > 2$)

To analyze the performance of the A-OLA-T with m alternating sets for a strip-shaped route (network), we adopt an approach similar to the one described in Section 5.1.4. During OLA propagation, it is observed that after a transient period, a "steady state" is attained in which the OLA lengths (or step sizes) become uniform, i.e., independent of the index, k. In other words, the lengths of adjacent OLAs from successive broadcasts become equal and the ratio of areas converge to ≈ 1. This phenomenon is illustrated in Figs. 21(a) and (b).

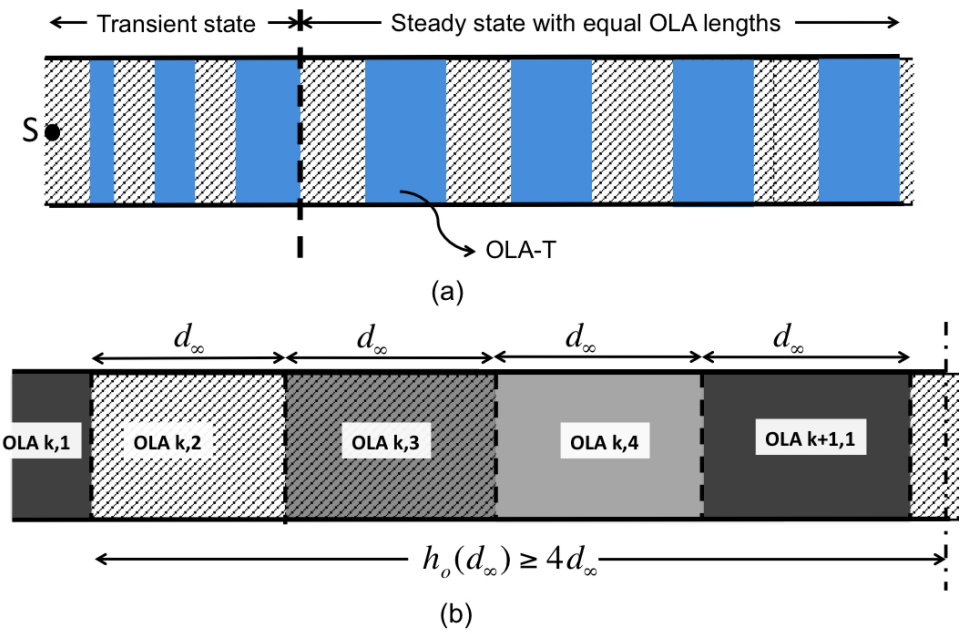

Figure 21: (a) Transient and steady state behaviors of OLA propagation, (b) steady state OLA propagation for $m = 4$.

Because the OLAs are rectangular shaped, the ratio of the total area of the Broadcast 1 OLAs to the total area of the network (for the first N levels) is given by

$$\tilde{\Psi} = \frac{\sum_{k=1}^{N} d_k}{r_{\text{strip}}}, \tag{33}$$

where d_k are the OLA lengths, $r_{\text{strip}} = \sum_{k=1}^{N} h_o(d_k)$, and $h_o(d_k)$ being the outer boundary of the k-th OLA. Numerically, it can be shown that for the $m = 2$ case, $\tilde{\Psi} = 1/2$ when $\mathcal{K} = \mathcal{K}_{(\text{A,min})}$. This implies that the respective accumulated areas of the two sets of OLAs during Broadcasts 1 and 2 are equal. For an m-A-OLA-T, it was conjectured that $\tilde{\Psi}$ would be $1/m$ for all m broadcasts, and this conjecture is verified numerically for $m = 4$.

To derive the closed-form expression of the minimum node degree, $\mathcal{K}_{(\text{A,min})}$ that guarantees successful m-set A-OLA-T broadcast, we proceed as follows. Figure 21(b) shows the steady state OLA propagation when alternating between four mutually exclusive sets of cooperating nodes. The k-th OLA during the Broadcast m is denoted

by *OLA k,m*. During Broadcast 1, the network designer just needs to check that the decoding range of the k-th rectangular OLA is at least greater than $4d_\infty$ to ensure enough nodes in the $(k+1)$-st OLA for sustaining OLA propagation. More generally, assuming steady state OLA propagation, it is claimed that satisfying $h_o(d_\infty) \geq md_\infty$ will guarantee a successful A-OLA-T broadcast, i.e., exercise mutually exclusive sets of nodes during successive broadcasts.

The optimum m-set A-OLA-T broadcast is achieved when the aforementioned condition becomes an equality, i.e., at the minimum node degree, $\mathcal{K}_{(\mathrm{A,min})}$. A closed-form expression for $\mathcal{K}_{(\mathrm{A,min})}$ is derived as follows: Consider $h_o(d_\infty) = md_\infty$. Taking derivatives on both sides with respect to d_∞, we get $h_o^{'}(d_\infty) = m \; \forall \; d_\infty$. In particular,

$$\begin{aligned} h_o^{'}(0) &= m, \\ \Rightarrow \frac{1}{\exp\left(\frac{1}{\mathcal{K}_{(\mathrm{A,min})}}\right) - 1} &= m. \end{aligned}$$

Further simplifications result in $\mathcal{K}_{(\mathrm{A,min})} = \left[\ln\left(\frac{m+1}{m}\right)\right]^{-1}$, the same as that for a disc-shaped network (given by (29)), but a maximum life extension factor of ≈ 2.78, i.e., 89.2% more compared to a disc-shaped network.

5.2.3 Limiting OLA lengths, d_∞

Figure 22 is a plot of h versus the OLA length, d, for different values of m when the m-set A-OLA-T is operating in its minimum power configuration. The value on the abscissa corresponding to the intersection point of the line, $h(d) = md$ with the curve $h(d)$ is the limiting OLA length (or step size), i.e., when the OLA propagations have attained their steady state. It can be observed that with increasing m, the limiting OLA length decreases. When m is increased from 2 to 3, the limiting OLA length, d_∞ decreases from ≈ 0.3 to 0.2 units. This is because as the number of alternating sets increases, the OLA-T strips become narrower resulting in steady state OLAs of shorter lengths. It is remarked that Fig. 22 is plotted at the minimum permissible

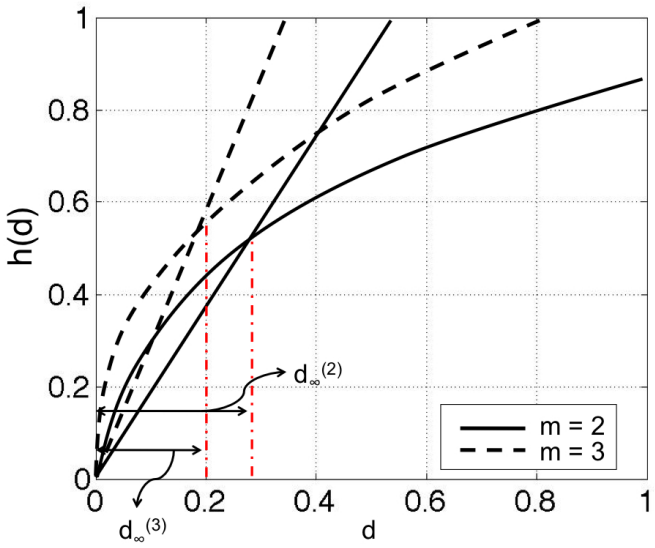

Figure 22: Numerical evaluation of the limiting OLA lengths for different m at the minimum node degree, $\mathcal{K}_{(\mathrm{A,min})}$. The cases when $m = 2$ and 3 are shown in this plot.

node degree, $\mathcal{K}_{(\mathrm{A,min})}$ for the different values of m. It was also observed (not shown here) that operating A-OLA-T at higher node degrees increased the limiting OLA lengths, lowered the lifetime extension relative to Basic OLA.

It is not possible to obtain a closed-form expression for the limiting OLA length, d_∞. Using the results from [17], we are able provide an upper bound for d_∞, and the derivation is as follows:

$$\begin{aligned} r_{o,\infty} + d_\infty &\leq \frac{W\mathcal{K}}{\pi}, \\ r_{i,\infty} + d_\infty &\leq \frac{W\mathcal{K}}{\pi\mathcal{R}} \Rightarrow r_{i,\infty} \leq \frac{W\mathcal{K}}{\pi\mathcal{R}} \text{ (since } d_\infty \geq 0). \end{aligned}$$

As a result, we have

$$\begin{aligned} (r_{o,\infty} + d_\infty) - r_{i,\infty} &\leq \frac{W\mathcal{K}}{\pi} - r_{i,\infty}, \\ \Rightarrow 2d_\infty &\leq \frac{W\mathcal{K}}{\pi} - r_{i,\infty} \ \forall \ r_{i,\infty}, \\ \Rightarrow 2d_\infty &\leq \mathrm{LUB}\left[\frac{W\mathcal{K}}{\pi} - r_{i,\infty}\right], \end{aligned}$$

where LUB is the least upper bound.

$$\mathrm{LUB}\left[\frac{W\mathcal{K}}{\pi} - r_{i,\infty}\right] = \frac{W\mathcal{K}}{\pi} - \frac{W\mathcal{K}}{\pi\mathcal{R}}.$$

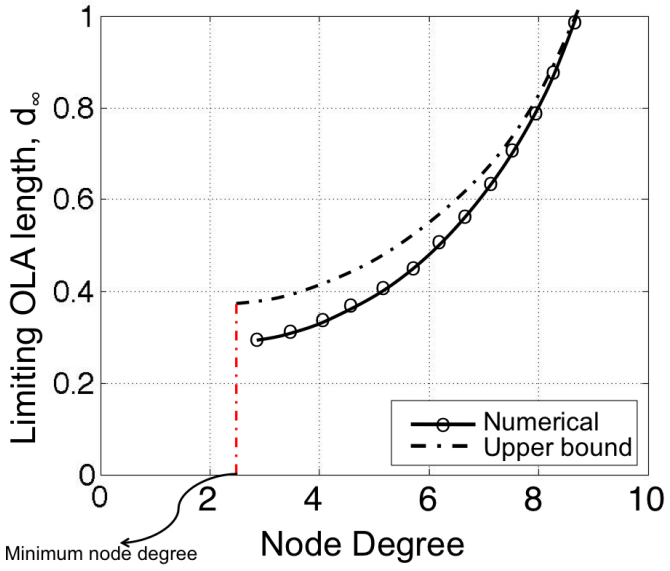

Figure 23: The limiting OLA length, d_∞, versus node degree, $\mathcal{K}$.

So, $d_\infty \leq \frac{W\mathcal{K}}{2\pi} - \frac{W\mathcal{K}}{2\pi\mathcal{R}}$. It can be seen that the upper bound for $d_\infty \rightarrow$ upper bound for $r_{o,\infty}$ (as in [17]) when $\mathcal{R} \rightarrow \infty$. Figure 23 shows a comparison of the analytical bound with the numerical d_∞. The value of m was chosen to be 2. It is seen from the figure that the upper bound becomes very tight at high node degrees away from the minimum node degree.

In summary, the alternating broadcast scheme, A-OLA-T (described in Section 5), is a modified version of OLA-T that optimizes multiple, consecutive OLA-T broadcasts, so that different sets of nodes relay in each broadcast and eventually all nodes relay the same number of times. Since A-OLA-T drains the batteries efficiently and uniformly across the network, it is most appropriate for static networks. Unlike OLA-T and other OLA-based schemes, A-OLA-T optimizes groups of broadcasts instead of a single broadcast. The transmission threshold is used to minimize the OLA sizes while maintaining mutually exclusive sets of OLAs on consecutive broadcasts. It is shown that the maximum life extension factor using A-OLA-T with two sets was 1.17 relative to the Basic OLA when both protocols are operated in their minimum energy configurations. Further, when two-set A-OLA-T is compared to OLA-T, the

Table 5: $\mathcal{R}$ for Basic OLA, OLA-T, and A-OLA-T with two alternating sets, at a fixed $\mathcal{K}$.

Protocol	$\mathcal{R}$
Basic OLA	∞
OLA-T	$\mathcal{R}_{\text{lower bound}} \leq \mathcal{R}$
A-OLA-T with 2 alternating sets	$\mathcal{R}_{\text{lower bound}} \leq \mathcal{R} \leq \mathcal{R}_{\text{disc,upper bound}}$

battery-life of the nodes is doubled. A-OLA-T with m sets, $m >> 1$ extended the network life by a maximum 147% relative to the Basic OLA when both protocols are operated in their minimum energy configurations. Broadcasting using strip-shaped networks increased the maximum factor of life extension to 2.78.

5.3 Operating Points of OLA-Based Broadcast Protocols

In this section, a comparison of the different operating points (such as $\mathcal{K}$ and $\mathcal{R}$) for the OLA broadcast protocols, namely, OLA-T and A-OLA-T for a path loss exponent of 2 are presented.

First, the relation between the relative transmission threshold, $\mathcal{R}$ for a fixed admissible node degree , $\mathcal{K}$ for Basic OLA, OLA-T, and A-OLA-T is presented. Table 5 compares the ranges of the $\mathcal{R}$, for the OLA-based protocols that guarantee successful network broadcast for a fixed $\mathcal{K}$. Since Basic OLA does not use any transmission threshold, $\mathcal{R} = \infty$. While $\mathcal{R}$ for OLA-T is lower-bounded, for A-OLA-T, there are lower and upper bounds on $\mathcal{R}$ for guaranteed broadcast success. Small "operating windows" of $\mathcal{R}$ may not be very desirable because of limited precision in the estimate of the SNR.

Table 6 quantifies the minimum node degree, $\mathcal{K}$, for Basic OLA, OLA-T and A-OLA-T, for $\mathcal{R} = 2.5$ dB. It can be observed that as the number of sets of the broadcast protocol increases, the maximum $\mathcal{K}$ required to ensure successful broadcast increases. Among these three protocols, Basic OLA has the lowest node degree (can achieve successful broadcast with fewer nodes), and A-OLA-T has the highest node degree.

Table 6: The minimum node degree, $\mathcal{K}_{\min}$, for Basic OLA, OLA-T, and A-OLA-T at $\mathcal{R} = 2.5$ dB.

Protocol	$\mathcal{K}_{\min}$
Basic OLA	1.4
OLA-T	2.1
A-OLA-T with 2 alternating sets	2.5
A-OLA-T with 5 alternating sets	5.5
A-OLA-T with 10 alternating sets	10.5
A-OLA-T with 100 alternating sets	100.5

Another way to interpret this trend is as follows. The same received power criterion (the decoding threshold, τ_l) assumption for all the protocols implies that the minimum $\overline{P_r}$ for the nodes in the network is highest for A-OLA-T and the lowest for Basic OLA. This is because fewer nodes participate during each broadcast cycle; these "border nodes" use a slightly higher P_r to ensure the OLA formations don't die down. Among the different versions of A-OLA-T, it is observed that as the number of alternating sets, m, increases, the node degree increases. As m increases, the cooperating area becomes smaller, which makes the OLAs thinner, which in turn, increases the $\overline{P_r}$ for the network.

OLA-T's only memory requirements are the threshold value and the identifier of the last packet broadcasted. A-OLA-T adds to this only the memory of the number of broadcasts received since the broadcast relayed. These broadcast schemes share the properties of no centralized control, no individual node addressing, no inter-node coordination, no reliance on node location knowledge, and no dependence on density, given that the density is at least sufficient to support OLA transmission. The extensions of Basic OLA offer advantages of transmit energy efficiency and network longevity relative to Basic OLA, but they come with a price. The introduction of additional system parameters increases the implementation/hardware "complexity" and power requirements compared to Basic OLA.

5.4 Practical Issues Associated with OLA-Based Broadcast Protocols

Other than a preliminary treatment of finite density networks in Chapter 3 (Tables 1 and 2) and in Section 4.3.1 (Table 4), the analysis in this dissertation has assumed a continuum of nodes and that all nodes transmit orthogonal signals, neither of which is true in practice. However, results based on these assumptions have been shown to be closely approximated with high densities and limited orthogonality in fading channels [22], [18]; in [22], several examples of un-normalized variables (i.e.,relay powers in dBm, densities in number of nodes per m^2, etc) are given that are consistent with the high density assumption.

Nevertheless, finite density might mean that higher than minimum powers will be needed to ensure successful broadcast for both Basic OLA and A-OLA-T. The additional power needed might be called the "density margin," and is a subject of ongoing research. Finite density and multi-path fading will limit the number of sets that could be used by A-OLA-T to some relatively low number.

Another practical issue is that radiated energy is not the only energy consumed by a relay. There is usually "base" of energy required by the electronics [90], and sometimes, the energy required by the receiver electronics exceeds that of the transmitter electronics [90]. Since radiated and circuit-consumed energies are added in a "total energy" model of a node, then, the fraction of energy saved (FES) and factor of life extension (FLE) will be lower in comparison to Basic OLA than what has been derived analytically, since both protocols would have the same circuit-consumed energies.

CHAPTER VI

OLA-BASED PROTOCOLS FOR HIGHER PATH LOSS EXPONENTS

6.1 Motivation

Several researchers have been investigating sensor networks in very lossy communication media, such as body area networks (BANs) and indoor sensor networks [73]–[77]. The electromagnetic waves are attenuated considerably, or stated otherwise, the radio signals experience high path loss. For example, in the case of BANs, the path loss along and inside the human body either using narrowband radio signals or Ultra-wideband (UWB) have been investigated, and the observations have been that the value of the path loss exponent, γ varies greatly. It was found that $\gamma = 3$ for the line of sight (LOS) propagation along and external to the human body [78], [79]. In [80], it was found that $\gamma = 7$ for non-line of sight (NLOS) situations for propagations external, and going around the human body. Thus, the path loss for such sensor networks is a lot different from the free space propagation exponent (i.e., $\gamma = 2$). Because of these losses, cooperative diversity-based approaches become advantageous and sometimes an absolute requirement to boost the energy-efficiency of the system. The high path loss impacts the energy consumption. A cooperative approach can decrease energy consumption in such harsh conditions because the transmission effort is spread over the whole network.

The OLA-based protocols described thus far, namely, OLA-T, A-OLA-T, and their variants, have been analyzed using a deterministic path loss model with a path loss exponent of 2. When the path loss exponent increases, one might expect the border

nodes of OLA-T to dominate the OLA transmission energy even more, thereby widening the gap in energy consumption between Basic OLA and OLA-T. This strongly motivates investigation of the energy-efficient "transmission threshold-based" OLA-based protocols in environments with higher (> 2) path loss exponents. Only OLA-T for disc-shaped networks are considered in this chapter.

6.2 Performance Evaluation at Higher Path Loss Exponents

Continuing to follow the approach in Section 4.2.2, we compare the total radiated energy during a successful OLA-T broadcast to that of a successful Basic OLA broadcast when both protocols are operating in their minimum power configurations.The fraction of energy saved (FES) defined in (13) can be re-written as:

$$\text{FES} = 1 - (\text{ratio of areas}) \times (\text{ratio of minimum node degrees}). \tag{34}$$

However, the minimum node degrees for Basic OLA and OLA-T given by (5) and (9), respectively, hold only for $\gamma = 2$, and need to be evaluated for higher path loss exponents. Also, the radii definitions for computing the ratio of areas also depend on γ. Thus, both the ratios in (34) depend on γ, implying that FES depends on γ.

Under the deterministic path loss model, the concentric ring structure of the OLA propagation is still preserved. So, the parameters of interest can be obtained by iteratively solving the aggregate path loss function given by (1) in Chapter 3 for τ_l (and τ_u for OLA-T). For an arbitrary choice of γ, the aggregate path loss function is given by:

$$f(r_0, p) = \int_0^{r_0} \int_0^{2\pi} [(p - r\cos\theta)^2 + r\sin\theta^2]^{-\gamma/2}, \tag{35}$$

where $\gamma > 2$. As there are no closed-form solutions for (35), it is computed numerically.

In order to evaluate FES under the path loss model assumption for higher values of γ ($\gamma > 2$), we proceed as follows. First, the minimum node degree, $\mathcal{K}_{\text{O,min}}$, for

infinite broadcast using Basic OLA is obtained for a disc-shaped network under the continuum assumption. Using Monte-Carlo simulations, we verify these results for random network realizations with finite node densities. Next, the minimum node degree, $\mathcal{K}_{\mathrm{OT,min}}$, which guarantees infinite network broadcast when using OLA-T is obtained for higher path loss exponents. We consider $\gamma = 3$ and 4. For each γ, the OLA boundaries are computed by solving (35) numerically for Basic OLA and OLA-T, both operating in their minimum power configurations. Using these results, the FES achieved by OLA-T relative to Basic OLA for each γ is obtained. The results along with the details of the simulations are presented in the following sections.

6.3 Simulation Details

For the continuum case, 1000 radii definitions (levels) were computed iteratively for different values of γ to test for infinite broadcast. We considered $\gamma = 2, 3$, and 4, and a range of values for the node degree, $\mathcal{K}$. The source power, P_s was chosen to be 3 and the decoding threshold, τ_l was 1. The minimum node degrees for Basic OLA and OLA-T, $\mathcal{K}_{\mathrm{O,min}}$ and $\mathcal{K}_{\mathrm{OT,min}}$, respectively, corresponded to the values of $\mathcal{K}$ at which the radii stopped increasing, i.e., only a finite portion of the network was reached. Additionally, for OLA-T, each $\mathcal{K}_{\mathrm{OT,min}}$ corresponded to a lower bound on RTT, $\mathcal{R}_{\text{lower bound}}$.

The Monte-Carlo simulations assumed 2000 nodes to be uniformly and randomly distributed on a disc of radius 20 distance units with the source node located at the center. A successful broadcast was when 99% of the nodes in the network could decode the message. The Monte-Carlo results were obtained from a simulation of 400 random network realizations. Normalized values were used in each case. The source and relay powers were chosen to be 3 and 0.5, respectively. The decoding threshold, τ_l, and the reference distance, d_0 were assumed to be unity. Nodes in the first level used an $\mathcal{R} = 5.44$ in dB, for all the trials.

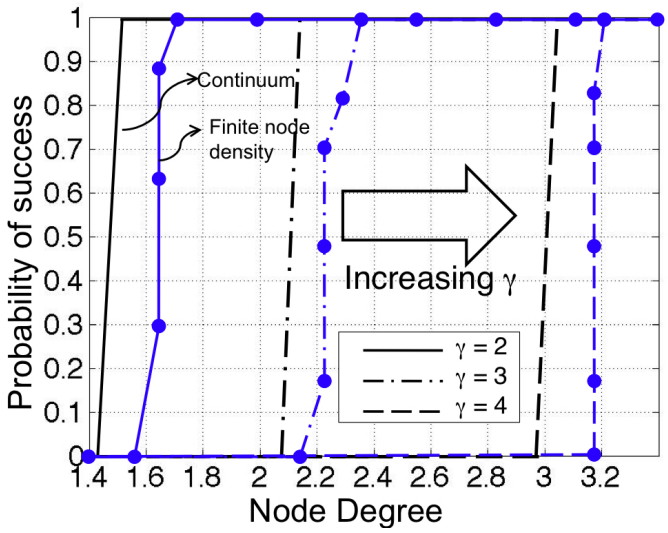

Figure 24: Probability of successful broadcast (PSB) for Basic OLA for different path loss exponents, γ. The blue and black curves represent the finite node density and continuum cases, respectively.

6.4 Results and Discussion

6.4.1 Minimum Node Degree for Basic OLA, $\mathcal{K}_{\mathrm{O,min}}$

Figure 24 is a plot of the PSB as a function of node degree for different path loss exponents, γ, for Basic OLA. We consider $\gamma = 2, 3$, and 4. The plot shows the simulation to obtain the minimum node degree, $\mathcal{K}_{\mathrm{O,min}}$, for a non-coherent OLA-based cooperative broadcast. $\mathcal{K}_{\mathrm{O,min}}$ is also evaluated for different network density cases, namely the continuum ($\rho \to \infty$) and the finite density. The results for the continuum case are discussed first. The horizontal axis is node degree and the vertical axis is the probability of a successful broadcast. The step function that represents the continuum assumption is plotted for each γ. It can be observed that as the path loss exponent, γ, increases from 2 to 4, $\mathcal{K}_{\mathrm{O,min}}$ increases from 1.44 to ≈ 3 (black curves). It is noted that the $\mathcal{K}_{\mathrm{O,min}}$ for $\gamma = 2$ obtained numerically is consistent with (5). In order to validate the numerical results for the continuum case, we considered random networks with finite node densities to obtain the $\mathcal{K}_{\mathrm{O,min}}$ for different γ. As expected, the minimum node degree required for a successful broadcast is slightly higher for

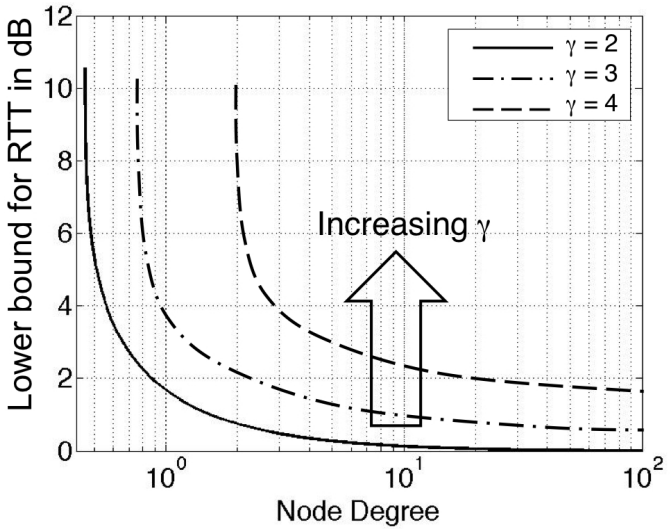

Figure 25: Lower bound on RTT, $\mathcal{R}_{\text{lower bound}}$, in dB, versus node degree, $\mathcal{K}$, for different path loss exponents, γ, for OLA-T.

the finite node density case, and when γ increases from 2 to 4, $\mathcal{K}_{\text{O,min}}$ increases from ≈ 1.6 to ≈ 3.2 for the finite node density case (blue curves). It is noted that the $\mathcal{K}_{\text{O,min}}$ for $\gamma = 2$ obtained numerically is very close to the theoretical value using (5). Lastly, the minimum node degrees to ensure infinite network broadcast for the two node density cases are within 10% of each other, thereby validating the continuum assumption and adding confidence to the numerically obtained results.

6.4.2 Numerical Lower Bounds on RTT, $\mathcal{R}_{\text{lower bound}}$, for OLA-T

Figure 25 shows the lower bound on RTT, $\mathcal{R}_{\text{lower bound}}$, in dB, versus the the node degree for different path loss exponents, $\gamma = 2, 3$, and 4, for OLA-T. These results are for the continuum case only. It can be observed that for a given node degree, the $\mathcal{R}_{\text{lower bound}}$ increases as γ increases from 2 to 4. For example, for $\mathcal{K} = 10$, the minimum transmission threshold is ≈ 0.1 dB for path loss exponent 2 (solid line). However, the min transmission threshold is ≈ 1 dB (dash-dotted line) and ≈ 2.2 dB (dashed line) for $\gamma = 3$ and 4, respectively. So the value of $\mathcal{R}$ for sustained OLA propagations when $\gamma = 2$ is insufficient when $\gamma > 2$. Alternatively, this implies that higher node degrees are required for operating OLA-T in its minimum power

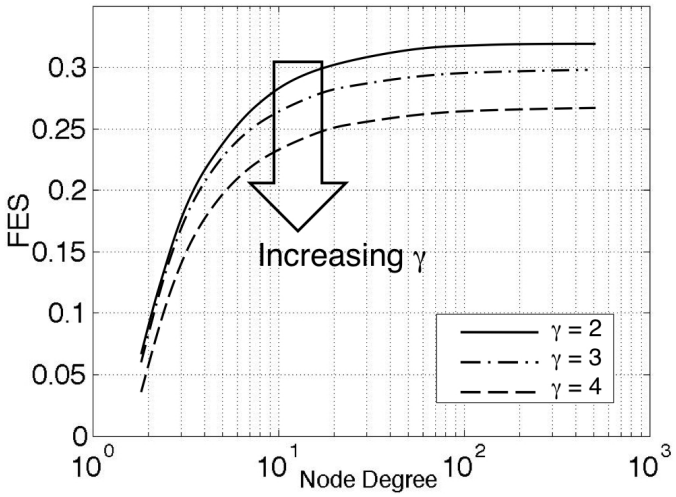

Figure 26: Variation of FES with the minimum OLA-T node degree, $\mathcal{K}_{(\mathrm{OT,min})}$, for a disc-shaped network with 1000 levels for different path loss exponents.

configuration as γ increases. For example, compared to $\gamma = 2$, there is a 20% increase in the required node degree for infinite network broadcast when $\gamma = 4$. It is also remarked that operating at $\mathcal{R}_{\text{lower bound}}$ may not be very effective if the precision in the estimate of the SNR is not good enough. All these factors increase the thickness of the OLAs in each hop/energy consumption of OLA-T at higher path loss exponents, thereby affecting the FES.

6.4.3 Fraction of Energy Saved

Figure 26 shows FES versus minimum node degree, $\mathcal{K}_{(\mathrm{OT,min})}$ (on a logarithmic scale), for a disc-shaped network with 1000 levels for different values of γ. For example, when $\gamma = 2$ (solid line), at $\mathcal{K}_{(\mathrm{OT,min})} = 10$, FES is about 0.28. This means that at their respective lowest energy levels at $\mathcal{K}_{(\mathrm{OT,min})} = 10$, OLA-T saves about 28% of the transmitted energy consumed by Basic OLA. On the other hand, for $\mathcal{K}_{(\mathrm{OT,min})} = 10$ and $\gamma = 4$ (dashed line), the FES is about 0.24, meaning that OLA-T saves about 24% of the total transmitted energy during broadcast relative to Basic OLA, both protocols operating in their minimum power configurations. It is noted that FES increases with $\mathcal{K}_{(\mathrm{OT,min})}$ and attains a maximum of about 30% (for $\gamma = 3$) and about

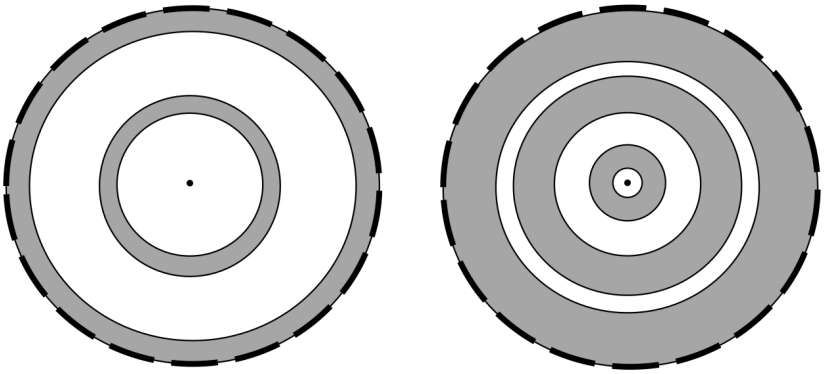

(a) $\gamma = 2$. (b) $\gamma = 4$.

Figure 27: Successful minimum power OLA-T broadcasts under deterministic path loss models with different exponents, γ. The gray strips denote the set of nodes that participated during network broadcast.

26% (for $\gamma = 4$).

Further, when the whole fraction of energy saved (WFES) given by (15) (in Section 4.2.2) is computed, the energy savings resulting from OLA-T relative to Basic OLA diminish further. For example, when both the circuit and transmit energies are equal, OLA-T offers a maximum energy savings of 15% (for $\gamma = 3$) and 13% (for $\gamma = 4$).

Figures 27(a) and 27(b) illustrate successful OLA-T broadcasts for different path loss exponents, $\gamma = 2$ and 4, respectively, when operating in their minimum power configurations. The node degree in the network, $\mathcal{K}$ was chosen to be 5, which resulted in $\mathcal{R}_{\text{lower bound}} \approx 0.2$ and 3 dB, for $\gamma = 2$ and 4, respectively. The gray strips denote the set of nodes that participated in the network broadcast. It can be observed that increasing γ from 2 to 4 results in a larger number of hops to cover the network and slightly thicker OLAs implying an increase in the ratio of areas used. This is responsible for the drop in FES by OLA-T relative to Basic OLA when operating at high path loss exponents. To summarize, OLA-T is still an energy-efficient alternative compared to Basic OLA for network broadcast, but offers lower energy savings while operating at a higher path loss ($\gamma > 2$). This implies that for very lossy channels

($\gamma > 4$), the energy savings would diminish considerably, and the performance of OLA-T would approach that of Basic OLA during network broadcast.

CHAPTER VII

COMMUNICATION USING HYBRID ENERGY STORAGE SYSTEMS (CHESS)

Network life may also be extended by tapping energy from ambient sources such as the sun, vibration, pressure, etc., through small devices referred to as energy harvesters. The state of the art in harvesting-aware routing seeks to maintain "energy-neutral" operation, and ignores that rechargeable batteries (RBs) have finite cycle lives. However, the life of the network is limited by the cycle-life of its storage devices, where cycle life is the number of charge-discharge cycles before the storage device fails to hold the charge.

Two energy storage media, the RB and the supercapacitor (SC), have dramatically different cycle lives, with the RB having lives on the order of a few 1000s and SC having lives on the order of millions. While hybrid combinations of RB and SC are used today so that the SC can protect the RB from supplying large, short pulses of current, in the proposed thesis, this type of hybrid energy storage system (HESS) will be used differently. Therefore, another key contribution of this thesis is the analysis of a novel communications using HESS (CHESS) routing metric, which causes routing and MAC protocols to prefer nodes that can relay exclusively with SC energy, thereby prolonging the cycle life of the RB. To enable CHESS analysis, the development of a novel simple model of the harvester-HESS set is proposed in this research. Finally, OLA broadcasting will be explored for use on HESS nodes.

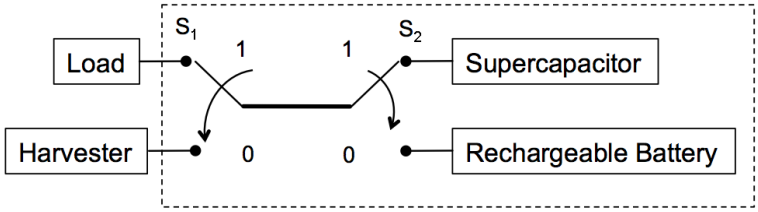

Figure 28: Simplified block diagram of the switched hybrid energy storage system.

7.1 HESS Model

A simplified block diagram of the HESS is shown in Fig. 28. The switches, S_1 and S_2, respectively represent our assumptions that a node cannot harvest energy and transmit a packet at the same time, and that the SC is never connected to the RB. This latter assumption distinguishes our model from other "hybrid" system models that always have a connection between the SC and the RB [91]. Also, we assume that the RB is not connected to the harvesting source until the RB has discharged down to the specified depth of discharge. This collection of assumptions enable us to use a simplified cycle life model [55], [56]. As in [58], we assume that the node is dead if the battery exceeds its cycle life.

A node that is selected to relay sets Switch S_1 to the "1" or "Load" state. Unselected nodes set Switch S_1 to the "0" or "harvesting" state. The RB is recharged when its residual energy falls below a pre-set threshold $(1-D)u_{\mathrm{RB}}$, where D is "depth of discharge" (DoD), and u_{RB} is the maximum capacity of the RB. For example, if we never want to use more than 30% of the energy of the RB within a single discharge cycle, then $D = 0.3$; to determine the cycle life from the graph of [50], express DoD as a percentage, e.g., $D \times 100\% = 30\%$. If the RB energy is above the threshold, then the SC is charged using the harvested energy, which corresponds to Switch S_2, being set to "1." If the RB has discharged below $(1-D)u_{\mathrm{RB}}$, then the node will not accept any more route requests until the RB has been fully recharged.

Next, we describe our update equations that model HESS leaking, charging, and

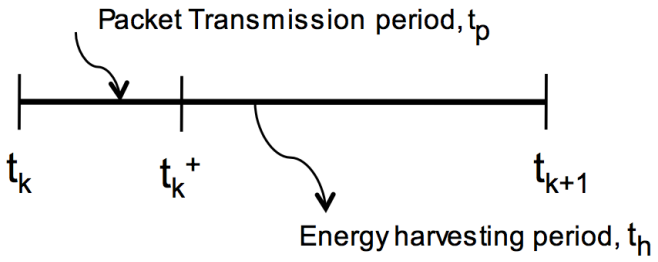

Figure 29: Representation of a time slot.

loading. The CHESS cost function will be described in the next section. We assume that each node knows its energy level (battery reserve) and has an accurate short-term energy replenishment schedule. We also assume that the reduction in energy after fulfilling a packet route request is instantaneous, as the rate of energy replenishment is much slower than the energy used for transmitting a packet [58].

It is assumed that the source transmits equal-length packets periodically. Let t_k denote the arrival time of the k-th packet request at a node. t_k defines the beginning of the k-th time slot, which is illustrated in Fig. 29. If the the routing algorithm selects the node, the node relays the packet. The period of activity comprising route selection and relaying of the packet, and during which the node does not harvest energy, is assumed to be t_p seconds long. We define $t_k^+ = t_k + t_p$. The node harvests energy during the remainder of the time slot, which is t_h seconds long. It follows that $t_{k+1} = t_k^+ + t_h$.

Next, the models of residual energy on the RB and SC are described. The following events are defined:

$$\begin{aligned}
\texttt{SC-ABLE} &= \{\widehat{E}_{\mathrm{SC}}(n, t_k) - l(j)E(n, R(j)) > 0\}, \\
\texttt{RB-ABLE} &= \{\widehat{E}_{\mathrm{RB}}(n, t_k) - (1 - D)u_{\mathrm{RB}} \\
&\quad -l(j)E(n, R(j)) > 0\}, \\
\texttt{RB-RECHARGE} &= \{\widehat{E}_{\mathrm{RB}}(n, t_k) \leq (1 - D)u_{\mathrm{RB}}\},
\end{aligned}$$

where `SC-ABLE` is the event that the SC has enough energy to route the packet,

RB-ABLE is the event that the RB has enough energy to route the packet without going below its specified depth of discharge, and RB-RECHARGE is the event that the RB has exceeded its depth of discharge and cannot accept further route requests until it has recharged. We note that RB-RECHARGE is not the complement to RB-ABLE; our model assumes that the act of relaying a packet never takes the RB below its discharge depth- an RB can only cross the threshold by leaking. RELAY=true represents that the node has been chosen by the CHESS routing protocol to relay. Otherwise, RELAY=false. $\widehat{E}_{\mathrm{SC}}(n, t_k)$ denotes the residual energy (in Joules) on the n-th node SC at time t_k, $l(j)$ is the length of the j-th packet in units of bits, $R(j)$ is the route for the j-th packet, $E(\cdot)$ is the energy per bit required to fulfill the route, $R(j)$, $\widehat{E}_{\mathrm{RB}}(n, t_k)$ denotes the residual energy on the n-th node RB at time t_k, and u_{RB} denotes the maximum capacity in Joules of the RB.

We shall next define the switch states, S_1 and S_2, for the n-th node at time t_k in terms of the above events. We shall use the indicator function, $I(A)$, which is 1 if the condition A is true, and 0 when A is false. We observe that $\mathrm{S}_1 = 1$ only if the node is selected to relay the packet. Therefore,

$$\mathrm{S}_1(n, t_k) = I\{\texttt{RELAY} \cap (\texttt{SC-ABLE} \cup \texttt{RB-ABLE})\}. \tag{36}$$

$\mathrm{S}_2 = 0$ under different conditions depending on if the node is harvesting or transmitting.

$$\begin{aligned} \mathrm{S}_2(n, t_k) = 1 - I(&\overline{\texttt{SC-ABLE}} \cap \texttt{RB-ABLE} \cap \\ &\texttt{RELAY}) - I(\texttt{RB-ABLE} \cap \overline{\texttt{RELAY}}), \end{aligned} \tag{37}$$

The first indicator function can be 1 only if the node is chosen to relay, in which case, the second indicator function must be zero.

Next, we present the update equations for the residual energies stored on the SC and RB. The change in SC energy from time t_{k-1} to time t_k, because of leaking,

harvesting, and loading is modeled as follows:

$$\begin{aligned}\widehat{E}_{\mathrm{SC}}(n,t_k) = \min\Big[&(1-\alpha(t_{k-1},t_k))E_{\mathrm{SC}}(n,t_{k-1}^+)\\ &+\mathrm{S}_2(n,t_{k-1}^+)\gamma_n(t_{k-1}^+,t_k),u_{\mathrm{SC}}\Big],\end{aligned} \tag{38}$$

$$\widehat{E}_{\text{load, SC}}(n,t_k,R(j)) = l(j)E(n,R(j))\mathrm{S}_1(n,t_k)\mathrm{S}_2(n,t_k), \tag{39}$$

$$E_{\mathrm{SC}}(n,t_k^+) = \beta(n,D,t_k)\Big[\widehat{E}_{\mathrm{SC}}(n,t_k) - \widehat{E}_{\text{load, SC}}(n,t_k,R(j))\Big], \tag{40}$$

where $\alpha(t_{k-1},t_k)$ denotes the time-invariant fraction of energy leaked in the SC over a time slot, $\widehat{E}_{\text{load, SC}}(n,t_k,R(j))$ is the energy consumed by a packet if the SC is used,u_{SC} denotes the maximum capacity in Joules of the SC, and $\gamma_n(t_{k-1}^+,t_k)$ denotes the energy (in Joules) harvested at the n-th node during time slot $k-1$. We assume all the nodes in the network harvest the same amount of energy in a time slot, so we drop the subscript n. Further, for this first treatment of CHESS, we assume that the harvesting rate is time-invariant over the daily harvesting period. $E_{\mathrm{SC}}(n,t_k^+)$ denotes the residual energy (in Joules) on the n-th node SC at t_k^+ and $\beta(n,D,t_k)$ is an indicator function for the event that the RB on node n has not exceeded its finite cycle life at the beginning of time slot k. We note that $\beta(n,D,t_k)$ is a non-increasing function of t_k, and for a fixed t_k, is a strictly decreasing function of D, the depth of discharge on the RB.

We note that the "min" function in Equation (38) ensures that the SC is not charged beyond its maximum capacity.

Similarly, the change in RB energy from time t_{k-1} to time t_k, because of leaking, harvesting, and loading is modeled as follows:

$$\begin{aligned}\widehat{E}_{\mathrm{RB}}(n,t_k) = \min\Big\{&\big[(1-\psi)E_{\mathrm{RB}}(n,t_{k-1}^+)\big]\\ &+\big[1-\mathrm{S}_2(n,t_{k-1}^+)\big]\gamma_n(t_{k-1}^+,t_k),u_{\mathrm{RB}}\Big\},\end{aligned} \tag{41}$$

$$\begin{aligned}\widehat{E}_{\text{load, RB}}(n,t_k,R(j)) = &\,l(j)E(n,R(j))\mathrm{S}_1(n,t_k)\\ &\cdot\big[1-\mathrm{S}_2(n,t_k)\big],\end{aligned} \tag{42}$$

$$E_{\mathrm{RB}}(n, t_k^+) = \beta(n, D, t_k)\Big[\widehat{E}_{\mathrm{RB}}(n, t_k) - \widehat{E}_{\mathrm{load,\ RB}}(n, t_k, R(j))\Big], \tag{43}$$

where ψ denotes the time-invariant fraction of energy leaked in the RB in one time slot (zero, in case of an ideal RB), $\widehat{E}_{\mathrm{load,\ RB}}(n, t_k, R(j))$ is the energy consumed by a packet if the RB is used, and $E_{\mathrm{RB}}(n, t_k^+)$ denotes the residual energy on the n-th node RB at t_k^+.

7.2 CHESS Routing

The CHESS routing protocol chooses the route that has the smallest sum of CHESS metrics for each node along the route. The CHESS metric is zero for a node that has sufficient energy on its SC to route a packet. If the SC has insufficient energy, then a non-zero value will be calculated, based on the energy state of the RB. The CHESS metric is based on the cost function of [58], which treats RBs with infinite cycle life and 100% depth of discharge. The metric of [58] , which is claimed in [58] to be asymptotically optimal in terms of the competitive ratio, increases exponentially with energy depletion and thus, discourages use of a node if its harvesting rate is low. We can use this approach to assign cost of discharge within one cycle as in [58]. However, we need to also have a component of cost associated with using up the RB cycle life; for this, we can view the cycle life of a RB similarly to the life of a non-rechargeable battery. Therefore, we define two energy depletion functions for the RB – one to discourage selection of a node (within a single discharge cycle) that is near its specified depth of discharge, and another to discourage use of a node that is near the end of it's battery cycle life. The overall cost function should increase if either one of these cost components increases. This can be achieved by multiplying the components.

Let us first consider the cost component for discharge within one cycle. Following [58], let the within-cycle energy depletion exponent be defined as $\lambda_{\mathrm{RB}}(n, t_k) = \frac{u_{\mathrm{RB}} - \widehat{E}_{\mathrm{RB}}(n, t_k)}{D u_{\mathrm{RB}}}$. In words, this will be zero when the battery is fully charged, and

one when it is discharged down to it's specified level of discharge. Next, the "cost component" for the within-cycle discharge is defined as

$$\begin{aligned} &C_{\text{CHESS}}(n, t_k, R(j)) \\ &= \frac{D u_{\text{RB}}}{(\gamma_n + \epsilon) \log \mu} \cdot \Big(\mu^{\lambda_{\text{RB}}(n, t_k^+)} - 1\Big) l(j) E(n, R(j)). \end{aligned} \tag{44}$$

We note that the use of the SC is reflected in the S_2 term in (41).

We denote L_c as the cycle life in units of time slots, which can be known under our assumption that the batteries are charged only when they have been discharged to depth D. Following similarly to the non-rechargeable battery cost function in [58], a cycle-life cost component that penalizes the use of a RB with a shorter cycle life, can be multiplied to the within-cycle cost (in (44) to get an overall cost function. In the results section, however, we only consider the within-cycle cost because of the topology that was assumed. The CHESS metric could be modified to include a revenue function as in [58]. We note that in the absence of modification, the CHESS protocol will attempt to find a route, however circuitous, that uses SC energy only. The CHESS algorithm and the decision-loop for charging an RB are illustrated in Figs. 30 and 31, respectively.

7.3 Results For The Two-Relay Network

For this preliminary analysis of the CHESS metric, we consider the small network model, shown in Fig. 32, which consists of a source, and destination, and two relays. The objective of the CHESS routing algorithm in this particular network is to choose (for each packet) the relay to maximize the time until the first relay comes to the end of its cycle life. We will show simulation results for a very simple daily periodic solar energy model of 12 hours of uninterrupted sun, with constant intensity, and 12 hours of total darkness. We assume a traffic model of periodic packets for as long as there is energy to route them. When the sunlight stops, the protocol will use up the SCs first, and then it will use the RBs until they both reach their specified depth of

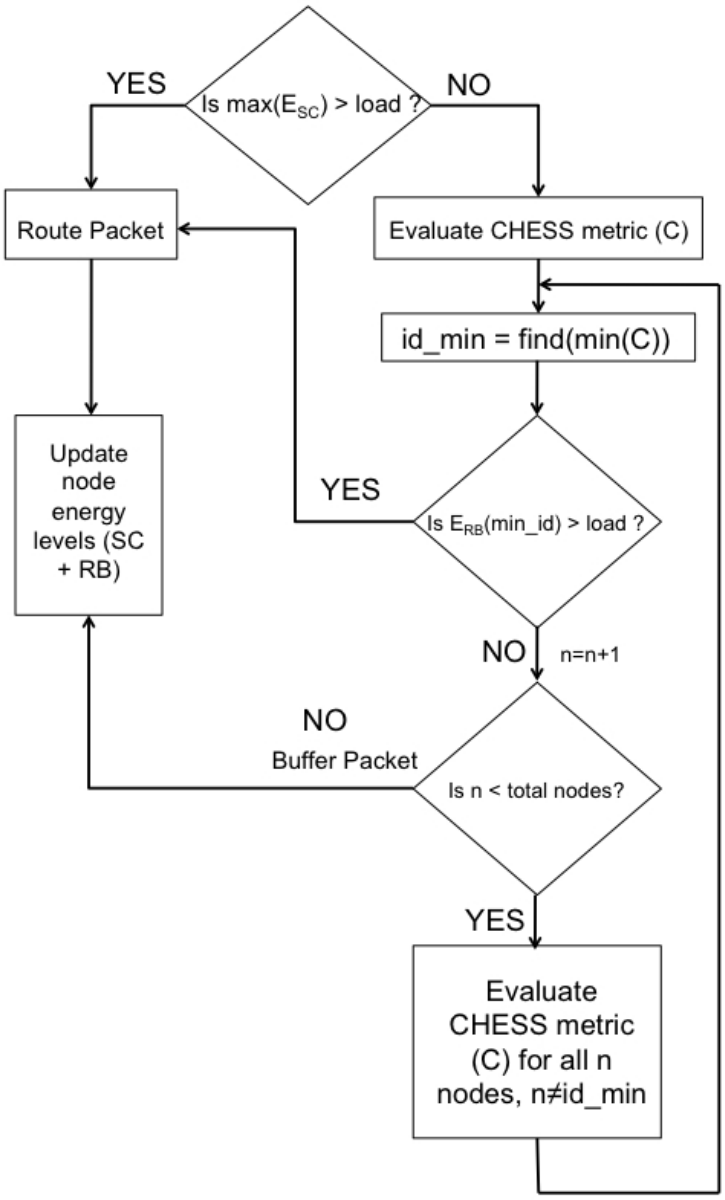

Figure 30: The basic CHESS algorithm.

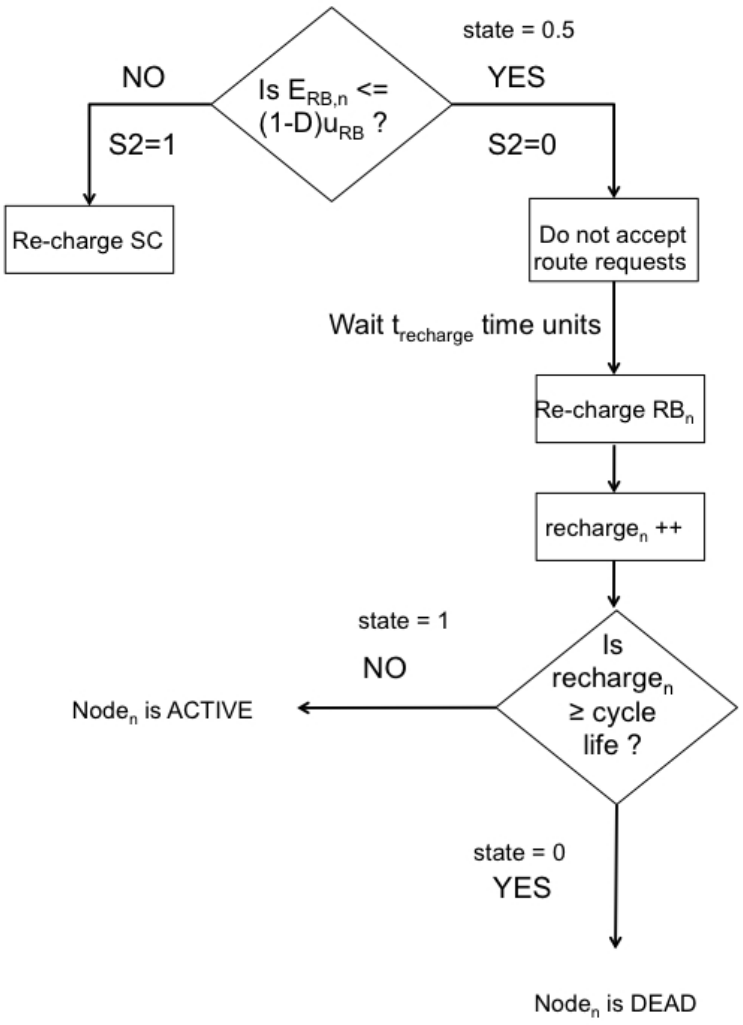

Figure 31: The recharging algorithm.

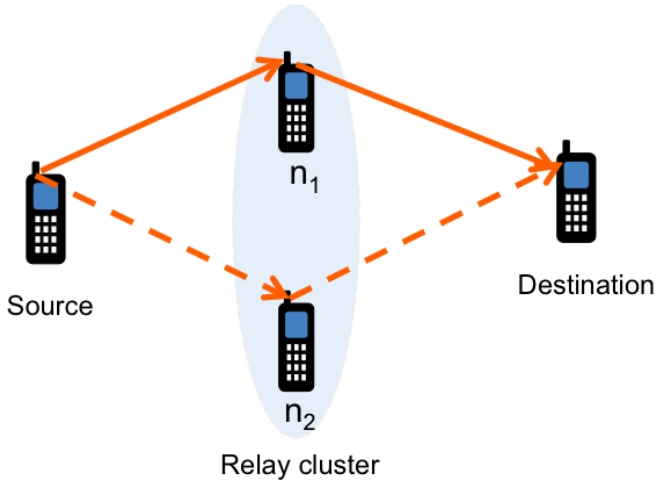

Figure 32: Network topology for evaluating routing performance using CHESS metric.

discharge. After that point, we assume no more packets are routed.

Table 7: Parameters used for evaluating CHESS.

Physical parameter	Symbol	Value	Citation
Energy harvested per unit time	γ_n	0.015 mW/cm^2	[92]
Fraction of energy leaked in the SC over a second	$\tilde{\alpha}$	0.8	[52]
Fraction of energy leaked in the RB over a month	$\tilde{\psi}$	5%	[93]
Depth of discharge	D	0.3	[94], [95]
Max. energy of RB	u_{RB}	130 J	[96]
Max. energy of SC	u_{SC}	12.5 J	[97]
Energy per bit	E_{rad}	100 nJ	[98]
Circuit Energy per bit	E_{elec}	300 nJ	[99]
Maximum Data rate	$R_{\text{b, max}}$	256 kbps	[99]
Packet transmission period	t_p	0.8 seconds	-
Harvesting period	t_h	0.2 seconds	-

In this simulation, the cycle-life part of the CHESS metric is ignored, and only the within-cycle part is used. This is done for two reasons, (1) to facilitate debugging and understanding of the results, and (2) because for this small "cluster" of just two nodes, the within-cycle cost alone is sufficient to balance the load. However, for a larger network with many more options for routing, and if the CHESS metric is

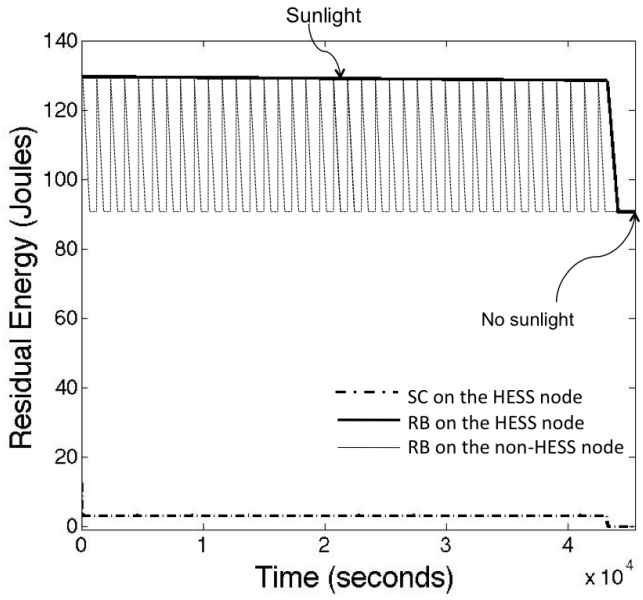

Figure 33: Comparison of the residual energies for the CHESS and non-CHESS cases over a single harvesting period.

combined with a penalty for number of hops, it is expected that the cycle-life part of the CHESS metric will play a role.

The HESS parameters used for the simulation are listed in Table 7. The leakage parameters $\tilde{\alpha}$ and $\tilde{\psi}$ and the leakage parameters α and ψ in Equations (38) and (41), are related in the following way: $\tilde{\alpha} = 1 - \alpha$ and $\tilde{\psi} = 1 - \psi$. For our simulation, the duration of each time slot is $t_h + t_p = 1$ second. The values of α and ψ per time slot are $1 - 0.8 = 0.2$ Joules and $1 - \frac{5 \cdot 130}{100 \cdot 30 \cdot 24 \cdot 3600} = 0.0000002$ Joules, respectively.

Figure 33 is a plot of the residual energies in Joules on the SCs and RBs for both nodes versus time for the HESS and non-HESS node architectures. Every packet is routed using the CHESS algorithm. For the node equipped with a HESS, when there is sunlight, the packet is routed using the SCs, and the RBs on both the nodes simply leak. Once the sunlight stops, the nodes use the SCs to route the packets until their residual energies are no longer enough to route a packet. Subsequent routing of packets involves computation of the CHESS metrics for the relay nodes, and the node with lowest cost function is selected as the relay node. Since there are only

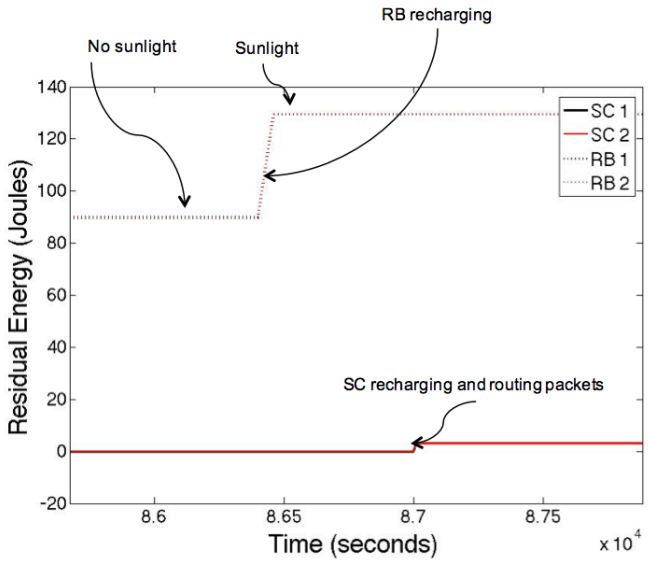

Figure 34: The residual energies on the nodes versus network lifetime.

two relay nodes, the CHESS routing metric, in this case, merely alternates between the nodes. Route requests are accepted until the residual energies on the nodes go below the specified depth of discharge. Since there is no sunlight, the nodes cannot recharge the RB, and further packets are simply buffered at the source. The batteries on both the nodes leak during the rest of the non-harvesting period. When there is sunlight, for the non-CHESS scenario, the RBs on both nodes route packets and have several charge-discharge cycles. It was found that one charge-discharge cycle for the CHESS case corresponded to 40 charge-discharge cycles for the non-CHESS case, which implies a network life extension of approximately 40 times by CHESS relative to non-CHESS.

Once sunlight returns (after 12 hours), the RB starts recharging. Our model assumes that a node does not accept route requests when the RB is charging. The charge-time for the RB for the specified DoD was assumed to be 10 minutes. Further, our model assumes that the SC charging does not start until the RB has been fully charged. This explains the 600 second time gap in Fig. 34 between the rise in RB energy and the rise in SC energy. Immediately after the charging of the RB is

complete, the RB energy is used to route a packet before the SC energy is used, since the SC still does not have enough energy to route a packet. Since we have assumed that charging of the SC is not instantaneous, when packet transmission resumes, the CHESS metric selects the node with the least cost function to route the packet. Another observation we can make from Figs. 33 and 34 is that at the data rate and harvesting rate given in Table 7, the RB contributes only a small percentage to the total number of routed packets. Yet the cost is high, because the RB uses up one cycle of its life in each dark period. A better strategy is to simply not use the RBs for routine reporting scenarios.

Finally, communication using hybrid energy storage systems (CHESS), the novel routing metric proposed and analyzed in [100], can be used with any routing protocol for networks that use HESSs. The HESS proposed in the dissertation consisted of a combination of a rechargeable battery (RB) and a supercapacitor (SC). The RB has a finite number of charge-discharge cycles, or cycle life, and low leakage. The SC has a relatively unlimited cycle life, but high leakage. SC energy is essentially free, while RB energy always has a cost. The CHESS metric assigns different costs to the energy in the SC and the energy in the RB; therefore CHESS favors routes with more SC energy. For the two-relay network with periodic solar-energy harvesting model considered in this dissertation, CHESS offered a network life extension of about 40 times relative to non-CHESS or until the energy storage device fails from aging during that time frame.

CHAPTER VIII

CONCLUSIONS

Widespread use of complex communication techniques with high demands on the analog front-end, and more recently the use of multiple antenna techniques for bolstering reliability increases the power consumption not only of the transceiver but of the complete wireless network. The growing popularity of wireless applications has increased the share of wireless in the global carbon footprint, which, in turn, has imposed another optimization criterion on the research agenda – **energy efficiency**. The prevailing theme of this doctoral research work has been to advance this agenda with the design of novel decentralized cooperative protocols and intelligent exploitation of energy scavenging using hybrid energy storage systems (HESSs).

The opportunistic large array (OLA) is a simple strategy that provides a signal-to-noise ratio (SNR) advantage from the spatial diversity of distributed single-antenna radios. The OLA-based broadcast schemes resulting from this doctoral work, namely, OLA with transmission threshold (OLA-T) and alternating OLA-T (A-OLA-T) are simple cooperative diversity-based protocols that solve the fundamental problems of **load-balancing** and **energy-deficit** in wireless networks. While OLA-T saves energy by limiting node participation within a broadcast, A-OLA-T optimizes over multiple broadcasts and drains the nodes in an equitable fashion. The introduction of the user-defined transmission threshold enables the network designer to craft network levels (in terms of distances from the source/sink) and hop sizes prior to node deployment depending on the application. Both OLA-T and A-OLA-T have the advantages that they are independent of node density and robust against mobility.

As the battery-operated sensor networks increase in number and the devices decrease in size, the replacement of depleted batteries is not practical. Therefore, another objective of this doctoral research was to explore routing by networks that do energy scavenging to enable **perpetual operation** without human intervention or servicing. For this purpose, a hybrid energy storage system (HESS) that comprises the traditional rechargeable battery (RB) and a supercapacitor (SC) was considered, and the routing strategy extended the RB-life by relaying exclusively with SC energy. The advantage of using a HESS is as a follows. Even though the SC with harvested energy may be sufficient for routine monitoring, if there is an alert, the "limited" energy from the RB will be a back-up and be used only as necessary to support the heavier reporting requirements.

Going forward, it is envisioned that deployment of these self-synchronizing protocols for network range extension would result in considerable energy savings, especially in highly attenuating environments. The marriage of energy- or harvest-awareness with the aforementioned cooperative strategies is a **novel** concept, and is a step toward designing the next-generation of self-powered sensing platforms.

CHAPTER IX

SUGGESTED FUTURE WORKS

The following is a list of possible directions for future research:

1. Existing analytical models for the supercapacitor (SC), which is an integral part of a HESS, may not be adequate to support network analysis. There are a few works that measure and characterize the leakage power in an SC, however, there are no available models that capture the energy dynamics (leakage and harvesting) in an SC. Simple voltage and energy-based models for the harvesting and leakage in an SC to support network analysis need to be explored.

2. The OLA-based protocols that have resulted from this Ph.D. work, namely, OLA-T, A-OLA-T, and their variants, have been analyzed using a deterministic path loss models. Subsequent research directions include a detailed analysis of the protocol for finite node density, under fading and shadowing wireless environments, a consideration of issues such as collisions and other hand-shaking mechanisms, and multiple flows (source-destination pairs) in a wireless network.

3. Future research directions include extending the development of the CHESS metric to capture the cycle life penalty, building a rigorous theoretical framework for analysis, and analyzing the performance of CHESS for practical network topologies and harvesting scenarios.

4. Finally, routing and medium access control (MAC) schemes have been proposed that are energy-and harvesting-aware, and also schemes exist that exploit cooperative transmission (CT) strategies (such as OLA), however, to our knowledge, no schemes exist that combine energy- or harvest-awareness with CT. Therefore,

exploring synergistically combining cooperative transmission with energy harvesting offers great potential and is the next step towards designing sustainable wireless sensor networks.

CHAPTER X

PUBLICATIONS

Journal Papers

1. L. Thanayankizil, **A. Kailas**, and M. A. Ingram, "Opportunistic large array concentric routing algorithm (OLACRA) for upstream routing in wireless sensor networks," *Ad Hoc Networks (Elsevier) Journal*, submitted, Nov. 2009.

2. **A. Kailas** and M. A. Ingram, "Simple cooperator recruiting using a received power threshold," *IEEE Transactions on Wireless Communications*, accepted pending revisions, Oct. 2009.

3. L. Thanayankizil, **A. Kailas**, and M. A. Ingram, "Routing protocols for wireless sensor networks that have an opportunistic large array (OLA) physical layer," *Ad-Hoc & Sensor Wireless Networks*, vol. 8, pp. 79–117, 2009.

4. **A. Kailas** and M. A. Ingram, "Alternating opportunistic large arrays in broadcasting for network lifetime extension," *IEEE Transactions on Wireless Communications*, vol. 6, no. 8, pp. 2831–2835, June 2009.

5. **A. Kailas**, L. Thanayankizil, and M. A. Ingram, "A simple cooperative transmission protocol for energy-efficient broadcasting over multi-hop wireless networks," *KICS/IEEE Journal of Communications and Networks*, vol. 10, no. 2, pp. 213–220, June 2008.

Conference Papers

1. **A. Kailas** and M. A. Ingram,"Alternating cooperative transmissions for a strip-shaped sensor network," *Proc. 44th Annual Conference on Information Sciences*

and Systems (CISS), Mar. 2010.

2. M. A. Ingram, J. W. Jung, Y. J. Chang, **A. Kailas**, and Y. Zhang, "On cooperative transmission in energy harvesting wireless sensor networks," *Proc. Energy Harvesting & Storage USA*, Oct. 2009.

3. **A. Kailas** and M. A. Ingram, "OLA with transmission threshold for strip networks," *Proc. 28th Annual IEEE Military Communications Conference (MILCOM)*, Boston, MA, Oct. 18–21, 2009, pp. 1–7.

4. **A. Kailas** and M. A. Ingram, "Investigating multiple alternating cooperative broadcasts to enhance network longevity," *Proc. IEEE International Conference on Communications (ICC)*, Dresden, Germany, June 14–18, 2009, pp. 1–5.

5. **A. Kailas**, M. A. Ingram, and Y. Zhang, "A novel routing metric for environmentally-powered sensors with hybrid energy storage systems," *Proc. First International Conference on Wireless VITAE*, Aalborg, Denmark, May 2009, pp. 42–46.

6. **A. Kailas** and M. A. Ingram, "Alternating cooperative transmission for energy-efficient broadcasting," *Proc. 51st Annual IEEE Global Telecommunications Conference (GLOBECOM)*, New Orleans, LA, Nov. 30–Dec. 4, 2008, pp. 1–5.

7. **(Invited)** J. W. Jung, **A. Kailas**, M. A. Ingram, and E. Popovici, "An evaluation of cooperation transmission considering practical energy models and passive reception," *Proc.First International Symposium on Applied Sciences in Bio-Medical and Communication Technologies (ISABEL)*, Aalborg, Denmark, Oct. 25–28, 2008, pp. 1–5.

8. R. Scott Frazier, **A. Kailas**, and M. A. Ingram, "Numerical evaluation of the energy for upstream opportunistic large array-based transmissions," *Proc. 10th International Symposium on Wireless Personal Multimedia Communications (WPMC)*, Jaipur, India, Dec. 3–6, 2007.

9. L. Thanayankizil, **A. Kailas**, and M. A. Ingram, "Two energy-saving schemes for cooperative transmission with opportunistic large arrays," *Proc. 50th Annual IEEE Global Telecommunications Conference (GLOBECOM)*, Washington, DC, Nov. 26–30, 2007, pp. 1038–1042.

10. **A. Kailas**, L. Thanayankizil, and M. A. Ingram, "Power allocation and self-scheduling for cooperative transmission using opportunistic large arrays," *Proc. 26th Annual IEEE Military Communications Conference (MILCOM)*, Orlando, FL, Oct. 29–31, 2007, pp. 1–7.

11. L. Thanayankizil, **A. Kailas**, and M. A. Ingram, "Energy-efficient strategies for cooperative communications in wireless sensor networks," *Proc. First IEEE International Conference on Sensor Technologies and Applications (SENSORCOMM)*, Valencia, Spain, Oct. 14–20, 2007, pp. 541–546.

APPENDIX A

CLOSED-FORM EXPRESSIONS FOR THE OLA-T RADII

For the constant RTT, the OLA boundaries can be found iteratively using

$$\overline{P_r}\left[f(r_{o,k}, r_{j,k+1}) - f(r_{i,k}, r_{j,k+1})\right] = \tau,\ j \in \{o, i\},$$

where $r_{o,k}$ and $r_{i,k}$ are the outer and inner boundary radii for the k-th OLA ring, respectively. The parameter τ takes the value τ_l (or τ_u) when computing outer (or inner) boundary radii for each OLA ring. Applying (1) yields $\frac{\tau}{\overline{P_r}} = \pi \ln \frac{|r_{j,k+1}^2 - r_{i,k}^2|}{|r_{j,k+1}^2 - r_{o,k}^2|}$. Using the initial conditions $r_{o,1} = \sqrt{\frac{P_s}{\tau_l}}$ and $r_{i,1} = \sqrt{\frac{P_s}{\tau_u}}$, recursive formulae for the k-th OLA are given by

$$r_{o,k}^2 = \frac{\beta(\tau_l) r_{o,k-1}^2 - r_{i,k-1}^2}{\beta(\tau_l) - 1},\ r_{i,k}^2 = \frac{\beta(\tau_u) r_{o,k-1}^2 - r_{i,k-1}^2}{\beta(\tau_u) - 1}, \tag{45}$$

where $\beta(\tau) = \exp\left[\tau/(\pi\overline{P_r})\right]$.

Next, the recursive problem is cast as a matrix difference equation as follows:

$$\begin{bmatrix} r_{o,k+1}^2 \\ r_{i,k+1}^2 \end{bmatrix} = \begin{bmatrix} \alpha(\tau_l) + 1 & -\alpha(\tau_l) \\ \alpha(\tau_u) + 1 & -\alpha(\tau_u) \end{bmatrix} \begin{bmatrix} r_{o,k}^2 \\ r_{i,k}^2 \end{bmatrix},$$

where $\alpha(\tau) = [\beta(\tau) - 1]^{-1}$.

The closed-form expressions for (45) were found to be

$$r_{o,k}^2 = \frac{\eta_1 A_1^{k-1} - \eta_2 A_2^{k-1}}{A_1 - A_2},\ r_{i,k}^2 = \frac{\zeta_1 A_1^{k-1} - \zeta_2 A_2^{k-1}}{A_1 - A_2}, \tag{46}$$

where

$$A_1 = \alpha(\tau_l) - \alpha(\tau_u),\quad A_2 = 1,\quad A_1 - A_2 \neq 0, \tag{47}$$

$$\eta_i = \left\{ \left[A_i + \alpha(\tau_u)\right] \frac{P_s}{\tau_l} - \alpha(\tau_l) \frac{P_s}{\tau_u} \right\}, \tag{48}$$

$$\zeta_i = \left\{ \left[1 + \alpha(\tau_u)\right] \frac{P_s}{\tau_l} + \left[A_i - \alpha(\tau_l) - 1\right] \frac{P_s}{\tau_u} \right\},\quad i \in \{1, 2\}, \tag{49}$$

$$\alpha(\tau) = \left[\beta(\tau) - 1\right]^{-1},\quad \beta(\tau) = \exp\left[\tau/(\pi\overline{P_r})\right]. \tag{50}$$

APPENDIX B

NECESSARY AND SUFFICIENT CONDITION FOR OLA-T BROADCAST

For a fixed $\overline{P_r}$ and τ_l, energy is reduced for OLA-T by minimizing τ_u (and hence, $\mathcal{R}$). Next an expression for $\mathcal{R}_{\text{lower bound}}$ is derived for a fixed $\mathcal{K}$. First, (46) is rewritten as shown below.

$$\mathbf{z_{k+1}} = \mathbf{A}\mathbf{z_k},$$

where $\mathbf{z_k} = \left(r_{o,k}^2, r_{i,k}^2\right)^T$, and $\mathbf{A} = \left(\alpha(\tau_l)+1, -\alpha(\tau_l); \alpha(\tau_u)+1, -\alpha(\tau_u)\right)^T$. It can be seen that A_1 and A_2 are the eigenvalues of $\mathbf{A}$. For infinite network broadcast, the OLA rings must continue to grow implying that the system described by (46) must be "unstable," i.e., $|A_1| > 1$ [101]. Since, radii are always positive and $\alpha(\tau_l) > \alpha(\tau_u) > 0$ by design, $A_1 > 1$ becomes a necessary and sufficient condition for infinite network broadcast. Setting $A_1 = 1$ would give us an expression for $\mathcal{R}_{\text{lower bound}}$.

$$\begin{aligned}
A_1 &= 1, \\
\Rightarrow \alpha(\tau_l) - \alpha(\tau_u) &= 1, \\
\Rightarrow \frac{1}{\left[\exp\left(\frac{\tau_l}{\overline{P_r}\pi}\right) - 1\right]} - 1 &= \frac{1}{\left[\exp\left(\frac{\tau_u}{\overline{P_r}\pi}\right) - 1\right]}, \\
\Rightarrow \frac{1}{\left[\exp\left(\frac{1}{\mathcal{K}}\right) - 1\right]} - 1 &= \frac{1}{\left[\exp\left(\frac{\mathcal{R}}{\mathcal{K}}\right) - 1\right]}.
\end{aligned}$$

Collecting the τ_l terms and solving for $\mathcal{R}$ results in

$$\mathcal{R}_{\text{lower bound}} = -\mathcal{K}\ln\left[2 - \exp\left(\frac{1}{\mathcal{K}}\right)\right].$$

and the following necessary and sufficient condition:

$$2 \geq \exp\left(\frac{1}{\mathcal{K}}\right) + \exp\left(\frac{-\mathcal{R}}{\mathcal{K}}\right).$$

APPENDIX C

PROOF OF THE PROPERTIES OF g

The properties listed in Section 4.3.1 are proved below, using the same list indices.

1. In [17], it was shown that $\lim_{x\to 0} h_\Omega(x) = 0$, $\Omega \in \{i, o\}$. Since, $g(x) = h_o(x) - h_i(x)$, it follows that $\lim_{x\to 0}(h_o(x) - h_i(x)) = \lim_{x\to 0} g(x) = 0$.

2. In order to show $g'(\cdot) > 0$, we differentiate with respect to x, to get $g'(x) = h'_o(x) - h'_i(x)$. From [17], we know that

$$h'_\Omega(x) = \frac{U(h_\Omega(x) + x)}{U(h_\Omega(x)) - U(h_\Omega(x) + x)},$$

where $\Omega = \{i, o\}$ and $U(x) = \frac{1}{x}\arctan\left(\frac{1}{2x}\right)$. Since $U(\cdot)$ is a decreasing function for $x > 0$, we also know that $h_o(x)$ and $h_i(x)$ are increasing functions in x. We use h_o and h_i instead of $h_o(x)$ and $h_i(x)$, respectively, for the sake of brevity. Further simplification results in the following closed-form expression for $g'(x)$:

$$g'(x) = \frac{U(h_i)U(h_o + x) - U(h_o)U(h_i + x)}{[U(h_o) - U(h_o + x)] \cdot [U(h_i) - U(h_i + x)]}.$$

The denominator is a product of *positive* terms, and so in order to complete the proof, it suffices to show that

$$U(h_i)U(h_o + x) - U(h_o)U(h_i + x) > 0 \Rightarrow \frac{U(h_i)}{U(h_i + x)} > \frac{U(h_o)}{U(h_o + x)}.$$

In other words, we need to show that $q(h, x) := \frac{U(h)}{U(h+x)}$ is decreasing in 'h'. However, because h_i and h_o are difficult to obtain, we computed them using iterative numerical methods. Thus, $U(h_i)$, $U(h_o)$, $\frac{U(h_i)}{U(h_i+x)}$, and $\frac{U(h_o)}{U(h_o+x)}$ are also computed numerically, upon which it can be verified that $q(h, x)$ is decreasing in h $\forall x > 0$. So, the inequality holds proving that g is a monotonically increasing function.

3. Numerically, it is found that $h_o(x)$ and $h_i(x)$ are concave downward functions, ie., $h_o^{''}(x) < 0$ and $h_i^{''}(x) < 0$. Using the results from [17],

$$h_\Omega^{''}(x) = \underbrace{\frac{U^2(h_\Omega + x)U^2(h_\Omega)}{[U(h_\Omega) - U(h_\Omega + x)]^3}}_{=:v(h_\Omega, x)} \cdot \underbrace{\left[\frac{U'(h_\Omega + x)}{U^2(h_\Omega + x)} - \frac{U'(h_\Omega)}{U^2(h_\Omega)}\right]}_{=:w(h_\Omega, x)},$$

where $\Gamma = u$ when $\Omega = i$ and $\Gamma = l$ when $\Omega = o$. Since closed-form expressions for h_i and h_o are very difficult to obtain, $v(h, x)$ and $w(h, x)$ were computed numerically. It can be verified that the product $v(h, x) \cdot w(h, x)$ is decreasing in h, i.e., $v(h_i, x) \cdot w(h_i, x) > v(h_o, x) \cdot w(h_o, x)\ \forall x > 0$. Thus, $g''(\cdot) < 0$, implying that g is concave downward.

4. Using the results from [17], $h_o^{'}(0) = \frac{1}{\exp\left(\frac{1}{\mathcal{K}}\right)-1}$ and $h_i^{'}(0) = \frac{1}{\exp\left(\frac{\mathcal{R}}{\mathcal{K}}\right)-1}$. Since $g'(0) = h_o'(0) - h_i'(0)$, (5) follows.

5. We know that $g'(x) = h_o'(x) - h_i'(x)$. Since $h_\Omega'(x) \xrightarrow{x\to\infty} 0,\ \Omega \in \{o, i\}$, it follows that $g'(x) \to 0$ as $x \to \infty$. If $g'(0) > 1$, then $g(x) > x$ for all $x > 0$ small enough. Since, $g(\cdot)$ is increasing and $g'(x) \to 0$, $g(x) < x$, for x large enough, i.e., the local attractor is away from the origin. On the other hand, when $g'(0) < 1$, $g(x) < x$ for sufficiently small $x > 0$. From the concavity of g, it follows that $g(x) = x$ can happen only at $x = 0$, i.e., the local attractor is the origin. Finally, in [17], it was shown that the solutions to (18) with respect to $h_\Omega(\cdot)$ exists, and are unique, for $\Omega \in \{o, i\}$. Using the property that $g(\cdot)$ is monotonically increasing, it follows that for $x_1 \neq x_2$, $g(x_1) \neq g(x_2)$, i.e., the solutions to $g(\cdot)$ are unique, and when $x_1 \neq x_2$, $g(x_1) = g(x_2)$, it just implies that the OLA propagation continues with fixed step sizes after the initial transient phase.

APPENDIX D

CLOSED-FORM EXPRESSION OF $\mathcal{R}_{\text{disc,upper bound}}$

The condition for *Broadcast 2* OLA formations to propagate throughout the network is given by

$$\Omega \geq 0,$$

where

$$\Omega = \Big(\alpha(\tau_l) + 1\Big)\zeta_1 - \alpha(\tau_l)\eta_1 A_1^{-1} - \zeta_1 A_1,$$

$$\eta_1 = \alpha(\tau_l)\left[\frac{P_s}{\tau_l} - \frac{P_s}{\tau_u}\right], \text{ and}$$

$$\zeta_1 = \Big(1 + \alpha(\tau_u)\Big)\left[\frac{P_s}{\tau_l} - \frac{P_s}{\tau_u}\right].$$

To determine the values that make $\Omega = 0$, substitute the expressions for η_1 and ζ_1 and get

$$0 = \Big(\alpha(\tau_l)+1\Big)\Big(1+\alpha(\tau_u)\Big)\left[\frac{P_s}{\tau_l}-\frac{P_s}{\tau_u}\right] - \alpha(\tau_l)\alpha(\tau_l)\left[\frac{P_s}{\tau_l}-\frac{P_s}{\tau_u}\right]A_1^{-1}\Big(1+\alpha(\tau_u)\Big)\left[\frac{P_s}{\tau_l}-\frac{P_s}{\tau_u}\right]A_1.$$

Next A_1 is substituted by the expression $\alpha(\tau_l) - \alpha(\tau_u)$. It is assumed that $\tau_l - \tau_u > 0$, and $P_s \neq 0$; therefore, the square bracketed term can be divided out. Making these changes, (51) reduces to

$$0 = \Big(\alpha(\tau_l) + 1\Big)\Big(1 + \alpha(\tau_u)\Big)\Big(\alpha(\tau_l) - \alpha(\tau_u)\Big) - \big[\alpha(\tau_l)\big]^2 - \Big(1 + \alpha(\tau_u)\Big)\Big(\alpha(\tau_l) - \alpha(\tau_u)\Big)^2.$$

Next, multiplying the terms and simplifying yields

$$0 = \Big(\alpha(\tau_l)\alpha(\tau_u) + \alpha(\tau_l) + \alpha(\tau_u) + 1\Big)\Big(\alpha(\tau_l) - \alpha(\tau_u)\Big) - \big[\alpha(\tau_l)\big]^2 - \Big(1 + \alpha(\tau_u)\Big)\Big(\big[\alpha(\tau_l)\big]^2 + \big[\alpha(\tau_u)\big]^2 - 2\alpha(\tau_l)\alpha(\tau_u)\Big).$$

Further simplification results in

$$0 \;=\; \Big(\big[\alpha(\tau_u)\big]^2+1\Big)\Big(\alpha(\tau_l)-\alpha(\tau_u)\Big)-\Big(\alpha(\tau_l)-\alpha(\tau_u)\Big)^2-\big[\alpha(\tau_u)\big]^2.$$

Replacing $\alpha(\tau_l)-\alpha(\tau_u)$ with A_1, multiplying on both sides by (-1), and rearranging yields

$$0 = A_1^2-\Big(\big[\alpha(\tau_u)\big]^2+1\Big)A_1+\big[\alpha(\tau_u)\big]^2.$$

The above equation is quadratic in A_1, and the roots are $A_1=\big[\alpha(\tau_u)\big]^2$ and $A_1=1$. Recall that A_1-A_2 is a factor in the denominator of the closed-form expressions for the OLA-T radii as given in (46). So, during the derivation for Ω, it was assumed that $A_1-A_2\neq 0$. Since $A_2=1$, only the root $A_1=\big[\alpha(\tau_u)\big]^2$ is considered and re-substituted into the expression for A_1 to get

$$\beta(\tau_l)-1 \;=\; \Big(\beta(\tau_u)-1\Big)\Big(1-\beta(\tau_u)^{-1}\Big),$$

which simplifies further to

$$\begin{aligned}\beta(\tau_u)+\beta(\tau_u)^{-1}-\beta(\tau_l) &= 1,\\ \Rightarrow \big[\beta(\tau_u)\big]^2-\Big(\beta(\tau_l)+1\Big)\beta(\tau_u)+1 &= 0. \qquad (51)\end{aligned}$$

(51) is quadratic in $\beta(\tau_u)$, with roots

$$r_{1,2}=\frac{\beta(\tau_l)+1\pm\sqrt{\Big(\beta(\tau_l)+1\Big)^2-4}}{2},$$

which can be rewritten as

$$r_{1,2}=\frac{1}{2}\left\{\exp\left(\frac{1}{\mathcal{K}}\right)+1\pm\sqrt{\left[\exp\left(\frac{1}{\mathcal{K}}\right)+1\right]^2-4}\right\}.$$

It can verified that for the choice of parameters, $r_1>r_2$. Finally, there are only two values of $\mathcal{R}$ where $\Omega=0$. The greater of the two values is the upper bound on $\mathcal{R}$. So, $\beta(\tau_u)=r_1\Rightarrow\tau_u=\overline{P_r}\pi\ln(r_1)$, and the upper bound is given by

$$\mathcal{R}_{\text{disc,upper bound}}=\frac{\mathcal{K}}{2}\cdot\ln(r_1).$$

APPENDIX E

RATIO OF AREAS

We first derive a simplified expression for the ratio of accumulated OLA areas in a OLA-T broadcast to the total network area, denoted as $\tilde{\Psi}$ in (28). Thus, the expression will apply to Broadcast 1 of A-OLA-T. For simplicity of analysis, consider the term

$$\frac{r_{o,k}^2 - r_{i,k}^2}{r_{o,k}^2 - r_{o,k-1}^2}, \tag{52}$$

which is the ratio of the k-th OLA in OLA-T to the k-th step-size. From [22], the closed-form expressions for OLA-T radii, which apply to Broadcast 1 in A-OLA-T, are given by $r_{o,k}^2 = \frac{\eta_1 A_1^{k-1} - \eta_2 A_2^{k-1}}{A_1 - A_2}$, and $r_{i,k}^2 = \frac{\zeta_1 A_1^{k-1} - \zeta_2 A_2^{k-1}}{A_1 - A_2}$, where

$$A_1 = \alpha(\tau_l) - \alpha(\tau_u), \quad A_2 = 1, \quad A_1 - A_2 \neq 0,$$

$$\eta_i = \left\{ \left[A_i + \alpha(\tau_u) \right] \frac{P_s}{\tau_l} - \alpha(\tau_l) \frac{P_s}{\tau_u} \right\},$$

$$\zeta_i = \left\{ \left[1 + \alpha(\tau_u) \right] \frac{P_s}{\tau_l} + \left[A_i - \alpha(\tau_l) - 1 \right] \frac{P_s}{\tau_u} \right\},$$

$$i \in \{1, 2\}, \ \alpha(\tau) = \left[\beta(\tau) - 1 \right]^{-1}, \ \beta(\tau) = \exp\left[\tau / (\pi \overline{P_r}) \right].$$

Substituting these closed-form expressions into (52), we get

$$\frac{r_{o,k}^2 - r_{i,k}^2}{r_{o,k}^2 - r_{o,k-1}^2} = 1 - \frac{\alpha(\tau_u)}{\alpha(\tau_l)}. \tag{53}$$

We observe that this ratio is independent of OLA index k. Solving (53) for $r_{o,k}^2 - r_{i,k}^2$ and substituting into (28), and noting that $\sum_{k=1}^{L} \left(r_{o,k}^2 - r_{o,k-1}^2 \right) = r_{o,L}^2$, yields $\tilde{\Psi} = 1 - \frac{\alpha(\tau_u)}{\alpha(\tau_l)}$. We observe that the ratio of areas is invariant to the network size L. When $\tilde{\Psi}$ is evaluated at $\overline{P_{r(\mathrm{A,min})}}$ for the A-OLA-T with two alternating sets [24], it is found that $\tilde{\Psi} \approx 0.5$.

APPENDIX F

DERIVATION OF $\mathcal{K}_{(\mathbf{A,min})}$ FOR m-SET A-OLA-T

Still focusing on Broadcast 1, which is an OLA-T broadcast, set $\tilde{\Psi} = \frac{1}{m}$. Substituting the definitions of $\alpha(\cdot)$ into the expression for $\tilde{\Psi}$ yields $\mathcal{R} = \mathcal{K} \ln \left[\frac{m \exp\left(\frac{1}{\mathcal{K}}\right) - 1}{m-1} \right]$. This expression tells us that for a given $\mathcal{K}$ (i.e., a given data rate and relay power density) there will be exactly one value of transmission threshold that will yield a ratio of areas of $1/m$. There is no guarantee, however, that the transmission threshold is sufficiently high to ensure sustained OLA propagation (i.e., that the step sizes do not approach zero). That guarantee is provided by the following bound for OLA-T [22]. From [22], the condition for a successful OLA-T broadcast takes the form of a lower bound on $\mathcal{R}$ given by $\mathcal{R}_{\text{lower bound}} = -\mathcal{K} \ln \left[2 - \exp\left(\frac{1}{\mathcal{K}}\right) \right]$.

Here is where we make our conjecture. In [24], we found for the $m = 2$ case that the upper and lower bounds for $\mathcal{R}$ converged at the minimum possible value of $\mathcal{K}$, denoted $\mathcal{K}_{(\text{A,min})}$. Therefore, the value of $\mathcal{K}$ that we get when we set $\mathcal{R}$ equal to $\mathcal{R}_{\text{lower bound}}$, is assumed to be the minimum $\mathcal{K}$ (corresponding to the lowest $\overline{P_r}$ and consequently the lowest energy, since eventually every node transmits in A-OLA-T).

$$\mathcal{R} = \mathcal{R}_{\text{lower bound}},$$

$$\left[\frac{m \exp\left(\frac{1}{\mathcal{K}}\right) - 1}{m - 1} \right] \cdot \left[2 - \exp\left(\frac{1}{\mathcal{K}}\right) \right] = 1.$$

Replacing $\exp\left(\frac{1}{\mathcal{K}}\right)$ with q, we can re-write the above as a quadratic equation in q as follows:

$$mq^2 - (2m+1)q + (m+1) = 0,$$

the roots of which are $q = \frac{m+1}{m}$. So, $\mathcal{K}_{(\text{A,min})} = \left[\ln\left(\frac{m+1}{m}\right) \right]^{-1}$.

APPENDIX G

CLOSED-FORM EXPRESSION OF $\mathcal{R}_{\text{strip,upper bound}}$ FOR STRIP-SHAPED ROUTES

Continuing to follow the analytical framework described in Section 5.2.1, we claim that as long as $\widetilde{d_k} \geq d_k$, $h_o(\widetilde{d_k}) \geq h_o(d_k)$ (because $h_o(\cdot)$ is monotonically increasing) and the inequality (31) will always be satisfied.

$$\begin{aligned} \widetilde{d_k} &\geq d_k, \\ \Rightarrow h_i(d_{k-1}) &\geq h_o(d_{k-1}) - h_i(d_{k-1}), \\ \Rightarrow 2h_i(d_{k-1}) &\geq h_o(d_{k-1}). \end{aligned}$$

Since $h_o(\cdot)$ and $h_i(\cdot)$ start from the origin [30],

$$2h_i^{'}(d_{k-1}) \geq h_o^{'}(d_{k-1}) \ \forall \ d_{k-1},$$

where $'$ denotes indicates the derivative. In particular,

$$\begin{aligned} 2h_i^{'}(0) &\geq h_o^{'}(0), \\ \Rightarrow \frac{2}{\exp\left(\frac{\mathcal{R}}{\mathcal{K}}\right) - 1} &\geq \frac{1}{\exp\left(\frac{1}{\mathcal{K}}\right) - 1}. \end{aligned}$$

Further simplification results in the upper bound for $\mathcal{R}$ that guarantees a successful Broadcast 2, and is given by

$$\mathcal{R}_{\text{strip,upper bound}} = \mathcal{K} \ln \left[2 \exp\left(\frac{1}{\mathcal{K}}\right) - 1 \right].$$

REFERENCES

[1] A. Sendonaris, E. Erkip, and B. Aazhang, "User cooperation – part i: System description, part ii: Implmentation aspects and performance analysis," *IEEE Trans. Commun.*, vol. 51, no. 11, pp. 1927–1948, Nov. 2003.

[2] J. N. Laneman, D. Tse, and G. W. Wornell, "Cooperative diversity in wireless networks: Efficient protocols and outage behaviour, " *IEEE Trans. Inf. Theory*, vol. 50, no. 12, pp. 3063–3080, Dec. 2004.

[3] J. N. Laneman and G. W. Wornell, "Distributed space-time coded protocols for exploiting cooperative diversity in wireless networks," *Proc. IEEE Global Telecommunications Conference (GLOBECOM)*, Taipei, Taiwan, Nov. 2002, pp. 77–81.

[4] A. Stefanov and E. Erkip, "Cooperative space-time coding for wireless networks," *IEEE Trans. Commun.*, vol. 53, no. 11, pp. 1804–1809, Nov. 2005.

[5] B. Zhao and M. C. Valenti, "Distributed turbo coded diversity for relay channel," *IEEE Commun. Lett.*, vol. 39, no. 10, pp. 786–787, May 2003.

[6] M. Janani, A. Hedayat, T. E. Hunter, and A. Nosratinia, "Coded cooperation in wireless communications: space-time transmission and iterative decoding," *IEEE Trans. Signal Process.*, vol. 52, no. 2, pp. 362–371, Feb. 2004.

[7] A. Nosratinia, T. E. Hunter, and A. Hedayat, T. E. Hunter, "Cooperative communication in wireless networks," *IEEE Commun. Magazine*, vol. 42, no. 10, pp. 74–80, Aug. 2004.

[8] S. -H. Chen, U. Mitra, and B. Krishnamachari, "Cooperative communication an routing over fading channels in wireless sensor networks, "*Proc. International Conf. on Wireless Networks Communications and Mobile Computing*, vol. 2, June 2005, pp. 1477–1482.

[9] A. Blestas, A. Khisti, D. P. Reed, A. Lippman, "A simple cooperative diversity method based on network path selection," *IEEE J. Sel. Areas Commun.*, vol. 24, no. 3, pp. 659–672, Mar. 2006.

[10] T. S. Quek, D. Dardari, and M. Z. Win, "Energy efficiency of dense wireless sensor networks: To cooperate or not to cooperate," *IEEE J. Sel. Areas Commun.*, vol. 25, no. 2, pp. 459–469, Feb. 2007.

[11] S. Biswas and R. Morris, "Opportunistic routing in multihop wireless networks," *Computer Commun. Review*, vol. 34, no. 1, pp. 69–74, 2004.

[12] M. C. Valenti and N. Correal, "Exploiting macrodiversity in dense multihop networks and relay channels," *Proc. 38th Asilomar Conference Signals, Systems and Computers*, Mar. 2003, pp. 1877–1882.

[13] A. Scaglione and Y. W. Hong, "Opportunistic large arrays: Cooperative transmission in wireless multihop ad hoc networks to reach far distances," *IEEE Trans. Signal Process.*, vol. 51, no. 8, pp. 2082–2092, Aug. 2003.

[14] Y. W. Hong and A. Scaglione, "Energy-efficient broadcasting with cooperative transmissions in wireless sensor networks," *IEEE Trans. Wireless Commun.*, vol. 5, no. 10, pp. 2844–2855, Oct. 2006.

[15] I. Maric and R. D. Yates, "Cooperative multi-hop broadcast for wireless networks," *IEEE J. Sel. Areas Commun.*, vol. 23, no. 1, pp. 1080–88, Aug. 2004.

[16] B. Sirkeci-Mergen and A. Scaglione, "On the power efficiency of cooperative broadcast in dense wireless networks," *IEEE J. Sel. Areas Commun.*, vol. 25, no. 2, pp. 497–507, Feb. 2007.

[17] B. Sirkeci-Mergen and A. Scaglione, "A continuum approach to dense wireless networks with cooperation," *Proc. IEEE Conference on Computer Communications (INFOCOM)*, Mar. 2005, pp. 2755–2763.

[18] B. Sirkeci-Mergen, A. Scaglione, G. Mergen, "Asymptotic analysis of multi-stage cooperative broadcast in wireless networks," *Joint special issue of the IEEE Trans. Inf. Theory and IEEE/ACM Trans. Netw.*, vol. 52, no. 6, pp. 2531–2350, June 2006.

[19] L. Thanayankizil, A. Kailas, and M. A. Ingram, "Two energy-saving schemes for cooperative transmission with opportunistic large arrays," *Proc. 50th Annual IEEE Global Telecommunications Conference (GLOBECOM)*, Washington, DC, Nov. 26–30, 2007, pp. 1038–1042.

[20] L. Thanayankizil, A. Kailas, and M. A. Ingram, "Energy-efficient strategies for cooperative communications in wireless sensor networks," *Proc. First IEEE International Conference on Sensor Technologies and Applications (SENSORCOMM)*, Valencia, Spain, Oct. 14–20, 2007, pp. 541–546.

[21] A. Kailas, L. Thanayankizil, and M. A. Ingram, "Power allocation and self-scheduling for cooperative transmission using opportunistic large arrays," *Proc. 26th Annual IEEE Military Communications Conference (MILCOM)*, Orlando, FL, Oct. 29–31, 2007, pp. 1–7.

[22] A. Kailas, L. Thanayankizil, and M. A. Ingram, "A Simple cooperative transmission protocol for energy-efficient broadcasting over multi-hop wireless networks," emph KICS/IEEE Journal of Communications and Networks (Special Issue on

Wireless Cooperative Transmission and Its Applications), vol. 10, no. 2, pp. 213–220, June 2008.

[23] A. Kailas and M. A. Ingram, "Alternating cooperative transmission for energy-efficient broadcasting," *Proc. 51st Annual IEEE Global Telecommunications Conference (GLOBECOM)*, New Orleans, LA, Nov. 30–Dec. 4, 2008, pp. 1–5.

[24] A. Kailas and M. A. Ingram, "Energy efficient broadcasting in multi-hop networks using alternating opportunistic large arrays," *IEEE Trans. Wireless Commun.*, vol. 6, no. 8, pp. 2831–2835, June 2009.

[25] A. Kailas and M. A. Ingram, "Investigating multiple alternating cooperative broadcasts to enhance network longevity," *Proc. IEEE International Conference on Communications (ICC)*, Dresden, Germany, June 14–18, 2009, pp. 1–5.

[26] L. Thanayankizil, A. Kailas, and M. A. Ingram, "Routing protocols for wireless sensor networks that have an opportunistic large array (OLA) physical layer," *Ad-Hoc & Sensor Wireless Networks: An International Journal*, vol. 8, pp. 79–117, 2009.

[27] L. Thanayankizil and M. A. Ingram, "Reactive robust routing with opportunistic large arrays," *Proc. IEEE International Conference on Communications (ICC) Workshop*, June 14–18, 2009, pp. 1–5.

[28] L. Thanayankizil, A. Kailas, and M. A. Ingram, "Opportunistic large array concentric routing algorithm (OLACRA) for upstream routing in wireless sensor networks," *Ad Hoc Networks (Elsevier) Journal*, submitted, Nov. 2009.

[29] A. Kailas and M. A. Ingram, "OLA with transmission threshold for strip networks," *Proc. 28th Annual IEEE Military Communications Conference (MILCOM)*, Boston, MA, Oct. 18–21, 2009, pp. 1–7.

[30] A. Kailas and M. A. Ingram, "Simple cooperator recruiting using a received power threshold," *IEEE Transactions on Wireless Communications*, accepted pending revisions, Oct. 2009.

[31] Y. J. Chang, M. A. Ingram, and R. .S. Frazier, "Cluster transmission time synchronization for cooperative transmission using software defined radio," *IEEE CoCoNet Workshop, International Communication Conference (ICC)*, accepted, May 2010.

[32] M. Luby, M. Watson, T. Gasiba, T. Stockhammer, and W. Xu,"Raptor codes for reliable download delivery in wireless broadcast systems," *Proc. Consumer and Communications Networking Conference (CCNC)*, Jan. 2006, pp. 192–197.

[33] P. Levis, N. Patel, D. Culler, S. Shenker, "Trickle: A self-regulating algorithm for code propagation and maintenance in wireless sensor networks," *Proc. First Symposium on Network Systems Design and Implementation (NSDI)*, Mar. 2004 (Available: `http://www.usenix.org/events/nsdi04/tech/levisTrickle/levisTrickle_html/`).

[34] I. F. Akyildiz, W. Su, Y. Sankarasubramaniam, and E. Cayirci, "A survey on sensor networks," *IEEE Commun.*, vol. 40 no. 8, pp. 102–115, 2002.

[35] S. Y. Ni, Y. C. Tseng, Y. S. Chen, and J. P. Sheu, "The broadcast storm problem in a mobile ad hoc network," *Proc. ACM Annual International Conference on Mobile Computing and Networking (MOBICOM)*, Aug. 1999, pp. 151–162.

[36] L. Gavrilovska and R. Prasad, "Ad hoc network towards seamless communications," Springer, 2006.

[37] J. E. Wieselthier, G. D. Nguyen, and A. Ephremides, "Energy-efficient broadcast and multicast trees in wireless networks," *Mobile Networks and Applications*, vol. 7, no. 6, pp. 481–492, Dec. 2002.

[38] I. Kang and R. Poovendran, "Maximizing static network lifetime of wireless broadcast ad hoc networks," *Proc. IEEE International Conference on Communications (ICC)*, May 2003, pp. 2256–2261.

[39] M. X. Cheng, J. Sun, M. Min, and D. Z. Du, "Energy-efficient broadcast and multicast routing in ad hoc wireless wetworks," *Proc. Performance, Computing, and Communications Conference*, Apr. 2003, pp. 87–94.

[40] I. Papadimitriou and L. Georgiadis, "Energy-aware broadcasting in wireless networks," *Mobile Networks and Applications*, vol. 9, no. 6, pp. 567–583, Dec. 2004.

[41] H. Lim and C. Kim, "Multicast tree structure construction and flooding in wireless ad hoc networks," *Proc. ACM International Conference on Modeling, Analysis and Simulation of Wireless and Mobile Systems (MSWiM)*, Aug. 2000, pp. 61–68.

[42] A. Qayyum, L. Viennot, and A. Laouiti, "Multipoint relaying for flooding broadcast messages in mobile wireless network," *Proc. Hawaii International Conference on System Sciences (HICSS)*, Jan. 2002, pp. 3866–3875.

[43] J. Cartigny and D. Simplot, "Border node retransmission-based probabilistic broadcast protocols in ad hoc networks," *Proc. Hawaii International Conference on System Sciences (HICSS)*, Jan. 2003.

[44] J. Cartigny, F. Ingelrest, and D. Simplot, "RNG relay subset flooding protocol in mobile ad hoc networks," *International Journal of Foundations of Computer Science*, vol. 14, no. 2, pp. 253–265, Apr. 2003.

[45] R. Wattenhofer, L. Li, V. Bahl, and Y. M. Wang, "Distributed topology control for power efficient operation in multihop wireless ad hoc networks," *Proc. IEEE Conference on Computer Communications (INFOCOM)*, Apr. 2001, pp. 1388–1397.

[46] N. Li, J. C. Hoy, and L. Sha,"Design and analysis of an MST-based topology control algorithm," *Proc. IEEE Conference on Computer Communications (INFOCOM)*, Apr. 2003, pp. 1702–1712.

[47] D. Dubhashi, O. Haggstrom, L. Orecchia, A. Panconesi, C. Petrioli, and A. Vitaletti, "Broadcasting in wireless sensor networks via sparse overlays," *Algorithmica*, vol. 49, no. 4, Dec. 2007.

[48] Battery life (and death). Available: `http://www.mpoweruk.com/life.htm#dod`. Date accessed: Jan. 2010.

[49] R. Somogye, "An aging model Of Ni-MH batteries for use in hybrid-electric vehicles," Master Thesis, Ohio State University, 2004.

[50] Perfect battery. Available: `http://www.buchmann.ca/Article4-Page1.asp`.

[51] Choosing a rechargeable battery, Electus Distribution, 2001. Available: `http://electusdistribution.com.au/images_uploaded/recharge.pdf`. Date accessed: Jan. 2010.

[52] Supercapacitors: Powerful mobile energy storage devices. Available: `http://www.csiro.au/science/Supercapacitors.html`. Date accessed: Jan. 2010.

[53] G. Merrett, A. S. Weddell, A. P. Lewis, N. R. Harris, B. M. Al-Hashimi, and N. M. White, "An empirical energy model for supercapacitor powered wireless sensor nodes," *Proc. 17th International IEEE Conference on Computer Communications and Networks*, Aug. 2008, pp. 1–6.

[54] Battery performance characteristics. `http://www.mpoweruk.com/performance.htm#life`. Date accessed: Jan. 2010.

[55] E. Decker and C. Millsaps, "Rechargeable battery cycle life issues," Motorola Energy Systems Group Testing Laboratories, Battery Power Products & Technology, March 2001. Available: `http://www.motorola.com/testservices/article1.htm`. Date accessed: Jan. 2010.

[56] I. Buchmann. Discharge Methods. Cadex Electronics Inc. Available: `http://www.batteryuniversity.com/partone-16.htm`. Date accessed: Jan. 2010.

[57] Voigt, H. Ritter, and J. Schiller, "Utilizing solar power in wireless sensor networks," *Proc. IEEE Conference on Local Computer Networks (LCN)*, Oct. 2003, pp. 416–422.

[58] L. Lin, N. Shroff and R. Srikant, "Asymptotically optimal power-aware routing for multihop wireless networks with renewable energy sources," *IEEE/ACM Trans. Netw.*, vol. 2, pp. 1262–1272, Oct. 2007.

[59] A. Kansal, J. Hsu, S. Zadehi, and M. Srivastava"Power management in energy harvesting sensor networks," *ACM Trans. on Embedded Computing Systems*, vol. 6, no. 4, Sep. 2007.

[60] T. A. Smith, J. P. Mars, and G. A. Turner, "Using supercapacitors to Improve battery performance," *Proc. IEEE 33rd Annual Power Electronics Specialists Conference (PESC)*, June 2002, pp. 124–128.

[61] P. Enjeti, J. W. Howze, and L. Palma, "An approach to improve battery run-time in mobile applications with supercapacitors," *Proc. IEEE 34th Annual Power Electronics Specialists Conference (PESC)*, June 2003, pp. 918–923.

[62] X. Jiang, J. Polastre, and D. Culler, "Perpetual environmentally powered sensor networks," *Proc. Fourth International Conference Information Processing in Sensor Networks (IPSN)*, Apr. 2005, pp. 463-468.

[63] R. Mudumbai, G. Barriac, and U. Madhow, "Spread-spectrum techniques for distributed space-time communication in sensor networks," *Proc. 38th Asilomar Conference Signals, Systems and Computers*, Nov. 2004, pp. 908–912.

[64] A. Bletsas, D. P. Reed, and A. Lippman, "A simple cooperative diversity method based on network path selection," *J. Sel. Areas Commun.*, vol. 24, no. 3, pp. 659–676, Mar. 2006.

[65] S. Lee, H. Myeongsu, and D. Hong, "Average SNR and ergodic capacity analysis for opportunistic DF relaying with outage over rayleigh fading channels," *IEEE Trans. Wireless Commun.*, vol. 8, no. 6, pp. 2807–2812, June 2009.

[66] F. A. Onat, A. Adinoyi, Yijia Fan, H. Yanikomeroglu, J. S. Thompson, and I. D. Marsland, "Threshold selection for SNR-based selective digital relaying in cooperative wireless networks," *IEEE Trans. Wireless Commun.*, vol. 7, no. 11, pp. 4226–4237, Nov. 2008.

[67] R. Madan, N. B. Mehta, A. F. Molisch, J. Zhang, "Energy-efficient cooperative relaying over fading channels with simple relay selection," *IEEE Trans. Wireless Commun.*, vol. 7, no. 8, pp. 3013–3025, Aug. 2008.

[68] A. Adinoyi and H. Yanikomeroglu, "Cooperative relaying in multiantenna fixed relay networks," *IEEE Trans. Wireless Commun.*, vol. 6, no. 2, pp. 533–544, Feb. 2007.

[69] H. S. Lichte, S. Valentin, H. Karl, I. Aad, L. Loyola, and J. Widmer, "Design and evaluation of a routing-informed cooperative MAC protocol for ad hoc networks," *Proc. IEEE Conference on Computer Communications (INFOCOM)*, Apr. 2008, pp. 1858–1866.

[70] Z. Zhou, S. Zhou, J. -H. Cui, and S. Cui, "Energy-efficient cooperative communication based on power control and selective relay in wireless sensor networks," *Proc. 26th Annual IEEE Military Communications Conference (MILCOM)*, Oct. 2007, pp. 1–7.

[71] E. Biagioni, "Algorithms for communication in wireless multi-hop ad hoc networks using broadcasts in opportunistic large arrays (OLA)," *Proc. International Conference on Computer Communications and Networks (ICCCN)*, Aug. 2007, pp. 1111–1116.

[72] J. -W. Jung, A. Kailas, M. A. Ingram, and E. M. Popovici, "Evaluation of cooperation transmission considering practical energy models and passive reception," *Proc. First International Symposium on Applied Sciences in Bio-Medical and Communication Technologies (ISABEL)*, Aalborg, Denmark, Oct. 2008, pp. 1–5.

[73] S. -L. Chen, H. -Y. Lee, C. A. Chen, C. -C. Lin, and C. -H. Luo, "A wireless body sensor network system for healthcare monitoring application," *IEEE Biomedical Circuits and Systems Conference (BIOCAS)*, Nov. 2007, pp. 243–46.

[74] B. Braem, B. Latre, I. Moerman, C. Blondia, and P. Demeester, "The wireless autonomous spanning tree protocol for multihop wireless body area networks," *Proc. Third Annual International Conference on Mobile and Ubiquitous Systems: Networking & Services*, Jul. 2006, pp. 1–8.

[75] H. Ren, M. Meng, and X. Chen, "Cross-layer optimization schemes for wireless biosensor networks," *Proc. Sixth World Congress on Intelligent Control and Automation (WCICA*, 2006.

[76] H. Ren, M. Meng, and X. Chen, "Developing a bioeffect metric for wireless biomedical sensor networks," *Proc. Sixth World Congress on Intelligent Control and Automation (WCICA)*, 2006.

[77] H. Ren and Q.-H. M. Max, "Bioeffects control in wireless biomedical sensor networks," *Proc. Third Annual IEEE Communications Society Conference on Sensor, Mesh and Ad Hoc Communications and Networks (SECON)*, Sep. 2006, pp. 896–904

[78] E. Ruesens, W. Joseph, G. Vermeeren, and L. Martens, "On-body measurements and characterization of wireless communication channel for arm and torso of human," *Prof. International Workshop on Wearable and Implantable Body Sensor Networks (BSN)*, Aachen, Mar. 2–7, pp. 26–28.

[79] E. Ruesens, W. Joseph, G. Vermeeren, and L. Martens, "Path-loss models for wireless communication channel for arm and torso: Measurements and simulations," *IEEE AP-S International Symposium*, June 2007.

[80] A. Fort, J. Ryckaert, C. Desset, P. De Doncker, P. Wambacq, and L. Van Biesen, "Ultra-wideband channel model for communication around the human body," *IEEE J. Sel. Areas Commun.*, vol. 24, pp. 927–933, Apr. 2006.

[81] Available: `http://www.btnode.ethz.ch/pub/uploads/Projects/`. Date accessed: Sep. 2009.

[82] Available: `http://focus.ti.com/lit/ds/symlink/cc1021.pdf`. Date accessed: Sep. 2009.

[83] Available: `http://focus.ti.com/lit/ds/symlink/cc2420.pdf`. Date accessed: Sep. 2009.

[84] Available: `http://www.nordicsemi.com/index.cfm?obj=product\&act=display\&pro=83`. Date accessed: Sep. 2009.

[85] Available: `http://www.nordicsemi.com/index.cfm?obj=product\&act=display\&pro=64`. Date accessed: Sep. 2009.

[86] Y. Zhang and J. Li, "Wavelet-based sensor data compression technique for civil Infrastructure condition monitoring," *ASCE Journal of Computing in Civil Engineering*, vol. 20, no. 6, pp. 390–399, Dec. 2006.

[87] S. Savazzi and U. Spagnolini, "Energy aware power allocation strategies for multi-hop-cooperative transmission schemes," *IEEE J. Sel. Areas Commun.*, vol. 25, no. 2, pp. 318–327, Feb. 2007.

[88] B. Gui, L. Dai, and L. J. Cimini Jr., "Routing strategies in multi-hop cooperative networks," *IEEE Trans. Wireless Commun.*, vol. 8, no. 2, pp. 843–855, Feb. 2009.

[89] R. L. Davney, An introduction to chaotic dynamical systems, Second Ed. Perseus Publishing Co., a division of Harper/Collins, 1989.

[90] A. Y. Wang and C. G. Sodini, "On the energy efficiency of wireless transceivers," *Proc. IEEE International Conference on Communications (ICC)*, June 2006, pp. 3783–3788.

[91] R. A. Dougal, S. Li, and R. E. White, "Power and life extension of battery-ultracapacitor hybrids," *IEEE Trans. Compon. Packag. Technol.*, vol. 25, No. 1, pp. 120–131, Mar. 2002.

[92] V. Ragunathan, A. Kansal, J. Hsu, J. Friedman, and M. Srivastava, "Design considerations for solar energy harvesting wireless embedded systems," *Proc. Fourth International symposium on Information Processing in Sensor Networks (IPSN)*, Apr. 2005, pp. 457–462 .

[93] Available: `http://www.allaboutbatteries.com/Battery-Energy.html`

[94] N. Picciano, "Battery aging and characterization of Nickel Metal Hydride and Lead Acid batteries," Ph.D. Dissertation, ME, Ohio State University, 2007.

[95] Available: http://www.rchelisite.com/lipo_battery_charging_and_safety_guide.php. Date accessed: Jan. 2010.

[96] Available: http://en.wikipedia.org/wiki/Lithium_polymer_battery. Date accessed: Jan. 2010.

[97] Available: http://hyperphysics.phy-astr.gsu.edu/hbase/electric/capeng.html. Date accessed: Jan. 2010.

[98] C. Pomalaza-Ráez, "Wireless sensor networks energy efficiency issues. Available: http://www.cwc.oulu.fi/~carlos/WSN_PPT/.Date accessed: Jan. 2010.

[99] Q. Wang, M. Hempstead, and W. Yang, "A realistic power consumption model for wireless sensor network devices," *Proc. Third Annual IEEE Communications Society Conference on Sensor, Mesh and Ad Hoc Communications and Networks (SECON)*, Sep. 2006, pp. 286–295.

[100] A. Kailas, M. A. Ingram, and Y. Zhang, "A novel routing metric for environmentally-powered sensors with hybrid energy storage systems," *Proc. First International Conference on Wireless VITAE*, Aalborg, Denmark, May 2009, pp. 42–46.

[101] S. Elaydi, "Differential equations: Stability and control," CRC Press, 1991.

VITA

Aravind Kailas's doctoral research work (as a Graduate Research Assistant in the Smart Antenna Research Laboratory (SARL) at the Georgia Institute of Technology) addressed the key issue of network sustainability with the design of novel, simple decentralized cooperative diversity-based protocols and intelligent exploitation of energy scavenging using hybrid energy storage systems. He received his M.Sc. in Applied Mathematics from Georgia Institute of Technology in 2010, M.S. in Electrical and Computer Engineering (ECE) from the University of Wisconsin-Madison, Madison in 2005, and B.E. in Electronics and Telecommunications from Mumbai University, India in 2002 with the highest honors.

Aravind is a recipient of the ECE Graduate Research Assistant Excellence Award (in 2010) and the Colonel Oscar P. Cleaver Award (in 2007) at the Georgia Institute of Technology. He has been a recipient of many other academic scholarships and awards for his Teaching throughout his undergraduate and graduate years. He was a Visiting Research Scientist at the DOCOMO USA Labs, Palo Alto, CA from Jan.–July, 2010, and a Visiting Researcher at the Center for TeleInfraStruktur (CTIF), Aalborg University, Aalborg, Denmark during the summers of 2007-2008. He has also held industry positions at QUALCOMM Inc. and General Electric (GE).